2005

Gas holdup in a gas-liquid-fiber semi-batch bubble column

Xuefeng Su
Iowa State University

Gas holdup in a gas-liquid-fiber semi-batch bubble column

by

Xuefeng Su

A dissertation submitted to the graduate faculty

in partial fulfillment of the requirements for the degree of

DOCTOR OF PHILOSOPHY

Major: Mechanical Engineering

Program of Study Committee:
Theodore J. Heindel, Major Professor
Francine Battaglia
Robert C. Brown
Ron M. Nelson
Brent H. Shanks

Iowa State University

Ames, Iowa

2005

Graduate College
Iowa State University

This is to certify that the doctoral dissertation of

Xuefeng Su

has met the dissertation requirements of Iowa State University

Signature was redacted for privacy.

Major Professor

Signature was redacted for privacy.

For the Major Program

TABLE OF CONTENTS

LIST OF TABLES

LIST OF FIGURES

NOMENCLATURE

a	coeficients in Eqs. (2.8), (2.9), (2.10), (5.12), and (5.17)
A	open area ratio, %
Ar	Archimedes number, (-)
b	constant in Eq. (2.8), (2.10)
BR	fiber bending ratio, (-)
c	constant in Eqs. (2.10) and (5.9)
C	fiber mass fraction, %
C_d	bubble drag coefficient in a swarm, (-)
C_o	drift flux model constant
C_v	fiber volume fraction
d	fiber diameter, μm
d_b	bubble diameter, mm
d_o	orifice diameter, mm
E	Young's modulus, Pa
EC	electrical conductivity, ms/cm
H	column height, m
j_g	drift flux, cm/s
k	constant in Eq. (2.12)
L	fiber length, mm
M_f	dry fiber mass, kg

M_t total mass of fiber-water mixture, kg

n_f number of fibers per gram of oven dry material, #/g

N_f number of fibers per unit volume, $\#/m^3$

N crowding factor, (-)

N_{ss} number of fiber contact points per unit shearing surface, $\#/m^2$

P pressure of the air-water-fiber suspension, Pa

P_o pressure of the water-fiber suspension, Pa

$\dot{Q}$ volumetric gas flow rate, l/min

r fiber aspect ratio, (-)

S^{eff} effective stiffness, (-)

t_f time of bubble formation

t time for a bubble, growing to a diameter equal to the hole separation distance, to begin bubble-bubble interaction

t_s time to drain the liquid film between bubbles to a critical thickness for rupture

TDS total dissolved solids, ppm

U absolute uncertainty

U_s slip velocity, cm/s

U_∞ terminal bubble rise velocity, cm/s

U_g superficial gas velocity, cm/s

U_l superficial liquid velocity, cm/s

V volume of the fiber-water mixture, m^3

V_{oj} average drift velocity or terminal bubble rise velocity, cm/s

v velocity of liquid carried by rising bubbles, cm/s

v_g gas velocity, cm/s

v_o orifice gas velocity, cm/s

v_r relative bubble rise velocity

We Weber number

Greek letters

ε gas holdup, (-)

ρ_{eff} effective density of the fiber-water mixture, kg/m^3

ρ_g gas density, kg/m^3

ρ_f dry fiber density, kg/m^3

ρ_m density of gas-liquid-fiber system, kg/m^3

ρ_w water density, kg/m^3

τ_y yield stress, Pa

$\dot{\gamma}$ shear rate, 1/s

ω fiber coarseness, kg/m

σ surface tension, mNm^{-1}

μ dynamic viscosity, kg/(m·s)

Δ difference

ACKNOWLEDGEMENTS

I would like to take this opportunity to thank various people for their contribution to this work. Above all of those whom I would like to thank is Dr. Ted Heindel, my major professor, for his commitment to education and willingness to lend his guidance and support throughout the entire graduate program. I would like to thank my committee members—Drs. Francine Battaglia, Robert C. Brown, Ron M. Nelson, and Brent H. Shanks for their constructive suggestions to this work. I also thank Iowa State University through a University Research Grant and the National Science Foundation under Grant Number CTS-0209928 for funding portions of this study. Thanks to Philip Hol, Ann Stardt, and Sarah Talcott for providing part of the data for this dissertation; to Chengzhi (Charles) Tang for thoughtful discussions concerning this research. Finally, my heartfelt appreciation goes to my family members, whose love and support made it possible to complete this journey.

ABSTRACT

A 4-m high, 15.24-cm diameter semi-batch bubble column connected to one of three perforated plate gas distributors with open area ratios A = 0.57%, 0.99%, and 2.14% is employed to study gas holdup and flow regime in Rayon and Nylon fiber suspensions. This study determines the effect of superficial gas velocity, fiber type, fiber mass fraction, fiber length, and aeration plate open area ratio on gas holdup and flow regime transition in various fiber suspensions.

Experimental results show that gas holdup increases with increasing superficial gas velocity, and the plot of gas holdup vs. superficial gas velocity depends on aeration plate open area. Gas holdup decreases with increasing fiber mass fraction and fiber length.

It is found that Nylon fiber is not an appropriate model system because gas holdup has been shown to vary with time. This phenomenon is mainly attributed to the fact that proprietary additives on the Nylon fiber surface modify the fiber suspension rheology and liquid surface tension with time.

Additional results show that gas holdup increases with aeration plate open area ratio when $A \leq 1\%$; when aeration open ratio was further increased (e.g., A = 2.14%), gas holdup decreases. Contributions to the decrease in gas holdup with increasing open area ratio are discussed.

Homogeneous, transitional, and heterogeneous flows are generated using three different aeration plates in air-water and low fiber mass fraction suspensions, and the superficial gas velocity at which the flow regime transition occurs depends on fiber length and aeration plate open area. The flow pattern changes to pure heterogeneous flow when the fiber mass fraction is high. The critical fiber mass fraction at which pure heterogeneous flow is observed depends on fiber length and aeration plate open area.

Finally, three gas holdup models are developed corresponding to different flow regimes by using data in this study (D = 15.2 cm). The models can reproduce most of the data within ± 15%. These models are also successfully extended to reproduce gas holdup within ± 15% in a similar bubble column with D = 32.1 cm.

CHAPTER 1: INTRODUCTION

1.1 Bubble Column Background

Bubble columns are devices used to affect gas-liquid (GL) or gas-liquid-solid (GLS) heat and/or mass transfer operations wherein a discontinuous gas phase in the form of bubbles moves relative to a continuous phase. In its simplest form, a bubble column is a vertical cylinder, as shown in Figure 1.1. (Figures are found at the end of the respective chapter in this document). Gas enters at the bottom through a gas distributor which may vary in design. The continuous phase may be supplied in batch form or it may move with or against the flow direction of the gas phase; the respective bubble columns are called semi-batch, cocurrent, and countercurrent bubble columns. Various modified bubble columns used in the chemical process industry are described by Shah et al. (1982). The continuous phase can be a liquid or a liquid-solid slurry, and the corresponding bubble column is called a GL bubble column and a GLS bubble column, respectively.

GL and GLS systems are encountered in many process industries such as petroleum-based fuel production, commodity and specialty chemical production, mineral processing, textile and pulp and paper processing, wastewater treatment, food processing, and biological organism production. The wide applications are partly a result of the many advantages of bubble columns including: absence of moving parts, high values of effective interfacial area and heat/mass transfer rate, no solid erosion, low relative cost, and slow reactions (Shah et al., 1982). Studies related to GL or GLS bubble columns have increased considerably in the

past 10-15 years because of their influence on the economic success of the above mentioned industries.

1.2 Motivation

One area of GLS bubble column research that has gained recent attention is gas-liquid-fiber (GLF) bubble columns, where the solid phase is a flexible fiber. GLF systems are found in the pulp and paper industry in many unit operations including paper recycling (i.e., flotation deinking), fiber bleaching, direct-contact steam heating, and deaeration.

Gas holdup, defined as the volumetric gas fraction in the two or three phase mixture, is one of the most important parameters in bubble column transport processes, and thus, has been extensively studied. A higher gas holdup generally implies an increase in the interfacial area between the gas and liquid (or solid), which enhances the heat and mass transfer rate (Lindsay et al., 1995). Maximizing gas holdup is desired to obtain high separation rates in flotation deinking and to create sufficient interfacial area for mass transfer in pulp bleaching.

The gas flow regime in GLF systems is also critical to system operation. For example, homogeneous flow generates uniform bubble sizes, which is important to improve flotation efficiency and provide uniform stock heating in direct-contact steam heating.

Gas flow in GLF bubble columns is more complex than typical GLS bubble columns. Unlike conventional solids used in gas-liquid-solid slurry systems, which are typically spherical, or slightly irregular, fibrous solids may be flexible and have a large aspect ratio, leading to fiber deformation and orientation as additional suspension characteristics (Schmid

et al., 2000; Joung et al., 2001). In addition, mechanical contacts result in fiber-fiber interaction, which make the fiber suspension effective viscosity increase significantly with fiber addition (Sundararajakumar and Koch, 1997). Fiber flocculation is an additional phenomenon in semi-concentrated and concentrated fiber suspensions, and is closely related to fiber shape, stiffness, mass fraction, aspect ratio, and interfiber friction (Schmid et al., 2000). This leads to a different suspension rheology for different fiber types and mass fractions, which in turn leads to different gas flow behavior in the resulting fiber suspension. Therefore, rheological characteristics of fiber suspensions are very complex and result in very complex gas flow behavior when a gas is bubbled through a fiber suspension. The complexity of this flow has led Reese et al. (1999) to conclude that gas flow in fiber suspensions is an area in need of further study.

The complex fiber suspension characteristics lead to a complex effect of fiber on gas holdup. Some researchers recorded gas holdup decreases with increasing fiber mass fraction (Went et al., 1993; Reese et al., 1996; Janse et al., 1999), but some others observed that gas holdup in a GLF suspension can be significantly higher than that recorded in a GL system operating under similar conditions (Lindsay et al., 1995; Schulz and Heindel, 2000). Hence, it is necessary to further study the effect of fiber addition (mass fraction) on gas holdup and determine factors that influence the results.

Fiber length also has a significant effect on fiber suspension rheology (Bennington et al., 1990; Sundararajakumar and Koch, 1997), thus, it is expected that fiber length influences gas holdup and flow regime as well.

Fibers with a uniform, fixed fiber length are necessary to determine fiber length effects on gas holdup. Rayon synthetic fiber is a good material to be employed for this intention. This is because: (i) Rayon fibers are formed from regenerated cellulose and (ii) synthetic fiber length, diameter, strength, and uniformity are easily controlled (Cruz, 1964). Thus, Rayon fiber will be used to study the effect of fiber mass fraction and length on gas holdup and flow regime transition in fiber suspensions. Nylon fiber, a non-cellulosic man-made fiber, is also employed to compare the Rayon fiber results.

The effect of gas distributor open area ratio on gas holdup and flow regime transition has been studied in gas-liquid systems (Shnip et al., 1992; Tsuchiya and Nakanishi, 1992; Zahradnik et al., 1997) and contradicted results were recorded. Tsuchiya and Nakanishi (1992) and Zahradnik et al. (1997) reported that gas holdup increases with increasing open area ratio and Shnip et al. (1992) claimed that gas holdup decreases with increasing open area ratio. Little study has been done on the effect of gas distributor on gas holdup in gas-liquid-solid systems. As both gas distributor (Miyahara and Takahashi, 1986; Solanki et al., 1992; Xie and Tan, 2003) and solid addition (De Swart et al., 1996; Heindel, 2002) affect bubble behavior and thus gas holdup, it is desired to study these effects in fiber suspensions while varying the fiber mass fraction and length. The information about the effect of gas distribution open area ratio in gas-liquid-fiber suspensions will be valuable when it is desired to optimize gas holdup behavior for selected pulp and paper industrial conditions and requirements.

1.3 Thesis Goals

Impelled by the needs of the pulp and paper industry for gas holdup conditions and the limited information about gas flow hydrodynamics in complex GLF systems, this thesis will investigate gas holdup behavior in fiber suspensions by employing Rayon and Nylon fibers. Specific thesis goals include:

1. Determine the effect of fiber type (Rayon and Nylon), length, and mass fraction on gas holdup and gas flow regime.

2. Determine the effect of aeration plate open area ratio on gas holdup and gas flow regime.

3. Determine the effect of bubble column diameter on gas holdup in cellulose fiber suspensions.

4. Identify the mechanism(s) behind the influences of fiber type, fiber geometry, fiber mass fraction, aeration plate open area ratio, and bubble column diameter, and interpret gas holdup behaviors in fiber suspensions.

5. Develop gas holdup correlations for GLF bubble column operations to predict performance and to control desired gas holdup characteristics when fibers are added to the process.

The knowledge gained in this study is expected to help control gas holdup conditions to improve transport rates in the pulp and paper industry and provides information on GLF bubble column design and scale-up. Also, it may provide information on the development of theoretical models enabling the mathematical simulation of GLF bubble columns.

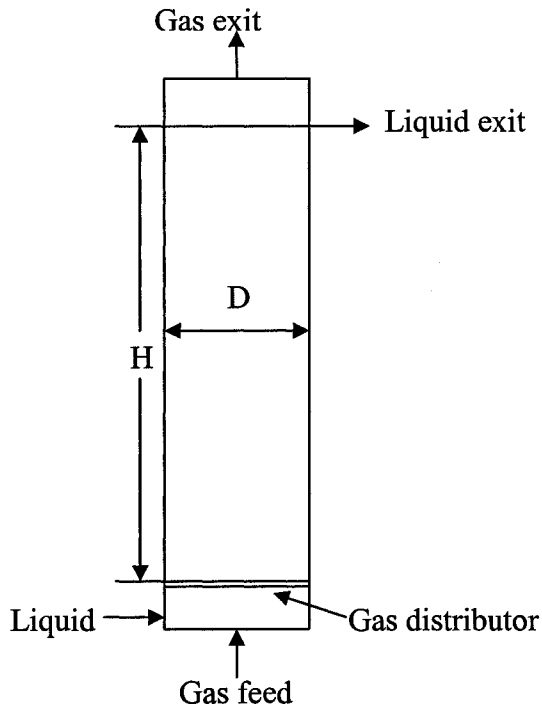

Figure 1.1: Schematic of a generic bubble column.

CHAPTER 2: LITERATURE SURVEY

This chapter includes six sections: the first two sections review gas holdup and flow regime and their influential factors, respectively, in gas-liquid and gas-liquid-solid systems, the third section reviews the characteristics in fiber suspensions and the effect of fiber on gas holdup, flow regime, and bubble behavior in a gas-liquid-fiber bubble column, the bubble behavior and the influencing factors are reviewed in the fourth section; the fifth part summarizes the gas holdup models in the literature, and the last section summarizes the literature review.

2.1 Gas-Liquid Bubble Columns

Extensive work has been completed addressing the hydrodynamics and characteristics of gas-liquid bubble columns. This section will summarize the main conclusions from this body of knowledge.

2.1.1 Introduction of Flow Regimes and Gas Holdup

Two main gas flow regimes occur in bubble columns: homogeneous flow and heterogeneous flow. These two flow regimes are separated by a transition regime (Zahradnik, et al., 1997; Chen et al., 1994). By using an appropriate gas distributor, the homogeneous and heterogeneous regimes can be obtained in the same facility by simply varying the gas flow rate. Homogeneous flow (Figure 2.1a) occurs when the gas flow rate is low. It is characterized by an almost uniform bubble size distribution and uniform radially gas holdup profile. Bubble coalescence and breakup are negligible. Bubbles rise virtually vertically or

with small scale transverse and axial oscillations. No large-scale liquid circulation exists in the system. When the gas flow rate is high, heterogeneous flow (Figure 2.1b) occurs and is characterized by a wide bubble size distribution and a radial gas holdup profile. The radial gas holdup profile causes a radial static pressure profile in which the central static pressure is lower than that near the wall, leading to macro-scale liquid circulation. Bubble coalescence and breakup are also common in heterogeneous flow. The transition regime between homogeneous and heterogeneous regimes is characterized by the onset and complete development of liquid circulation patterns (Zahradnik et al., 1997). The heterogeneous flow regime also can be produced by aeration plates with large holes at any gas flow rate and Ruzicka et al. (2001a) called this condition pure heterogeneous flow.

Gas holdup (or void fraction) is defined as the volumetric gas fraction. In a bubble column, gas holdup is easily recorded by measuring the liquid height or pressure drop with and without aeration. Gas holdup is related to the gas flow rate introduced into the bubble column. The relationship of gas holdup to gas flow rate depends on flow regime and the typical relationship is plotted in Figure 2.2. When homogeneous, transitional, and heterogeneous flow regimes are generated, there are two different relationships of gas holdup as a function of gas flow rate; one produces a local maximum gas holdup (line a) and another one does not (line b). These differences depend on aeration plate. For the former case, gas holdup increases with increasing gas flow rate until it reaches a local maximum value, then it decreases with increasing gas flow rate until it reaches a local minimum gas holdup, which indicates the end of transition flow regime and the onset of heterogeneous flow regime. Shnip et al. (1992) attributed the decrease in gas holdup with increasing superficial gas

velocity to liquid circulation within the column; for a given change in superficial gas velocity, the increase in liquid circulation causes bubbles to rise faster than the rate of bubble generation, leading to the reduction in gas holdup. In the heterogeneous flow regime, the effect of superficial gas velocity on liquid circulation lessens, and the rate of bubble generation is proportional to superficial gas velocity, therefore, gas holdup generally increases slightly with increasing gas flow rate. For the latter case, gas holdup monotonically increases with gas flow rate, but the slope is different between the homogeneous and heterogeneous flow regimes. A continuous but nonlinear increase in gas holdup with increasing gas flow rate is observed in pure heterogeneous flow regime (line c).

2.1.2 Gas Holdup

Gas holdup is strongly dependent on gas bubble behavior and liquid flow pattern within the bubble column. It has been shown that gas bubble behavior depends mainly on: (1) bubble column gas flow rate, (2) gas distributor design and column dimensions, and (3) physical properties of the liquid (liquid-solid) phase.

2.1.2.1 Influence of Column Diameter (D) on Gas Holdup

Numerous studies have been conducted to investigate the effect of bubble column diameter on gas holdup, and most of the studies focused on the heterogeneous flow regime. In general, gas holdup decreases with increasing bubble column diameter when D is below a critical value (Yoshida and Akita, 1965; Shah et al., 1982; Wilkinson, 1991; Deckwer, 1992; Zahradnik et al., 1997; Krishna et al., 2001). Zehner (1989) and Krishna et al. (2001) attributed the decrease in gas holdup with increasing bubble column diameter to the

increased liquid circulation intensity with increasing column diameter. The increased liquid circulation has the effect of accelerating the bubbles and results in a decreased gas holdup.

When the column diameter is beyond a critical value, the effect of D vanishes. Yoshida and Akita (1965), Shah et al. (1982), Deckwer (1992), Wilkinson (1991), and Zahradnik et al. (1997) reported that the critical diameter is between 0.1- 0.2 m. Zahradnik et al. (1997), however, claimed that the assumption of gas holdup independence on column diameter when D is greater than the critical value is only valid for heterogeneous flow. They used columns D = 0.14 m and 0.29 m with different aeration plate hole diameters of d_o = 0.5 and 1.6 mm. Two different flow patterns were generated for each column with different d_o: homogeneous, transitional, and heterogeneous flow for d_o = 0.5 mm and pure heterogeneous flow for d_o = 1.6 mm. They concluded that when homogeneous flow was observed, a higher gas holdup in the transitional flow regime was observed when D = 0.14 m. Similar gas holdup values were reported in the homogeneous and heterogeneous flow regimes when D = 0.29 and 0.14 m. The effect of column diameter diminished for pure heterogeneous flow. Krishna et al. (2001) numerically predicted that when $D \geq 0.15$ m, column diameter had an effect on gas holdup in the homogeneous flow regime and gas holdup decreased with increasing bubble column diameter. This observation supported the conclusions of Zahradnik et al. (1997) that the gas holdup dependence on column diameter is limited to the homogeneous and transitional flow regimes. The experimental results of Vandu and Krishna (2004) showed that column diameter affects gas holdup both in homogeneous and heterogeneous flow regimes even when $D \geq 0.15$ m.

The effect of bubble column diameter on gas holdup also relates to the liquid properties. Vatai and Tekic (1989) studied bubble columns with D = 5, 10, 15, and 20 cm and pointed out that the column diameter has no influence on gas holdup in an air-water system. However, the column diameter has an effect for a high liquid viscosity.

2.1.2.2 Influence of Gas Distributor on Gas Holdup

Gas holdup behavior is closely linked to gas distributor plate design, which is one of the reasons that different phenomena have been observed by different investigators. When using a perforated aeration plate, hole diameter (d_o) and area ratio (R, column cross-sectional area to total plate hole area) or open area ratio (A = 1/R) are two important parameters for gas distributor plate design.

Wilkinson (1991) showed that the effect of hole diameter on gas holdup was negligible when d_o was larger than 1-2 mm. This observation corresponds well with the studies of Zahradnik et al. (1997) who concluded that gas holdup was independent of hole diameter when $d_o \geq 1.6$mm. In contrast, Wilkinson (1991) pointed out that when d_o was less than 1 mm, small bubbles were formed leading to a higher gas holdup, which was in full agreement with the prediction of Shnip et al. (1992) who numerically showed that small hole diameters tend to increase gas holdup, as well as the experimental results of Zahradnik et al. (1997) and Tsuchiya and Nakanishi (1992). Wilkinson (1991) also acknowledged that the relatively high gas holdup for small hole diameters was more pronounced for short bubble columns, and this effect may diminish for very tall bubble columns due to the ongoing process of bubble coalescence.

Contradictory results have been obtained for the effect of open area ratio. Ohki and Inoue (1970), Zahradnik and Kastanek (1979), Tsuchiya and Nakanishi (1992), and Zahradnik et al. (1997) concluded that the local maximum gas holdup increased with increasing open area ratio. In these studies, the increase in open area was obtained by increasing the number of holes with a constant hole diameter. On the contrary, Shnip et al. (1992) numerically predicted that the critical gas holdup value at which transition from homogeneous to heterogeneous flow was observed increased with decreasing open area. Zahradnik et al. (1997) pointed out that this discrepancy was attributed to the assumption made by Shnip et al. (1992) that decreasing open area ratio means a reduction in the hole diameter at constant number of holes rather than a reduction in the number of holes at constant hole diameter. Shnip et al. (1992) insisted that decreasing the number of holes tended to produce non-uniform flow leading to the decrease in the stability of the homogeneous flow regime.

Zahradnik and Kastanek (1979) demonstrated that open area had no effect on gas holdup in the heterogeneous flow regime, and this phenomenon was not influenced by bubble column diameter. Similar phenomenon was observed by Zahradnik et al. (1997). They believed that in fully developed heterogeneous flow, the character of the gas flow was primarily determined by the bulk liquid circulation, with little effect of primary gas dispersion. Camarasa et al. (1999) also reported that the effect of gas distributor was insignificant at high superficial gas velocities because the bubble size tended to reach a common value which was determined only by coalescence, breakup, and bulk liquid circulation.

The effect of gas distributor is also dependent on the liquid properties. Kuncova and Zahradnik (1995) demonstrated that in moderately viscous liquids, the gas distributor had little effect on gas holdup.

2.1.2.3 Influence of Liquid Height (H) on Gas Holdup

In general, gas holdup is not uniform along the bubble column height. Wilkinson et al. (1992) claimed that the three gas holdup regions exist: (i) at the top of column, where gas holdup is always high resulting from the foam structure; (ii) near the sparger, where gas holdup is lower for a single-nozzle sparger and higher for a porous plate sparger when compared to that of bulk liquid; and (iii) the bulk region. However, when the column is tall enough ($H \geq$ 1-3 m or height to diameter ratios ≥ 5), the influence of the foam region at the column top and near the sparger region on overall gas holdup was negligible (Wilkinson et al., 1992; Zahradnik et al.,1997; Veera and Joshi, 1999).

Zahradnik et al. (1997) found a significant increase in gas holdup with decreasing column aspect ratio (liquid height-to-diameter ratio) for various plates generating homogeneous flow, which indicates that it is preferable to generate homogeneous flow in short bubble columns. Veera and Joshi (1999) showed that the effect of aspect ratio on gas holdup was influenced by aeration hole number, where a multipoint sparger led to a decrease in gas holdup with increasing aspect ratio and a single sparger led to the reverse effect.

2.1.2.4 Influence of Liquid Properties on Gas Holdup

Liquid viscosity: Zahradnik et al. (1997) showed that gas holdup decreased with increasing liquid viscosity. The negative effect of viscosity on gas holdup can be attributed to

the promotion of bubble coalescence and the suppression of bubble breakup, leading to the formation of large bubbles with a large rise velocity. Kuncova and Zahradnik (1995) found that the gas holdup exhibits a maximum value followed by a sustained decrease in gas holdup with increasing viscosity when plotted as a function of liquid viscosity. Similar observations were made by Eissa and Schugerl (1975) and Zahradnik et al. (1987). Eissa and Schugerl (1975) attributed the maximum gas holdup to the hindered bubble motion in low viscosity liquids, and enhanced bubble coalescence in high viscosity liquids.

Surface tension: Surface tension forces oppose bubble deformation and breakup (Walter and Blanch, 1986), which play an important role in bubble size and the resulting gas holdup. A low surface tension leads to a more stable gas-liquid interface and a smaller bubble size, resulting in a higher gas holdup (Kluytmans et al., 2001). Numerous studies varied liquid surface tension by adding surfactants. Zahradnik et al. (1997) added various surfactants and salts to distilled water and observed that the presence of surface active compounds consistently increased gas holdup. The effect of different surface active compounds had no difference for pure heterogeneous flow, but differed when three flow regimes (homogeneous, transitional, and heterogeneous) were observed. They also showed that surface active agents were more influential in the homogeneous and transitional flow regime. The increase in gas holdup with surfactant addition was also observed by Krishna et al. (2000) and Kluytmans et al. (2001). However, Krishna et al. (2000) observed that the influence of surfactant addition was more significant in the heterogeneous flow regime.

Zahradnik et al. (1999) used aliphatic alcohols to modify the gas flow behavior in viscous liquids. The results showed that gas holdup increased with increasing surfactant

concentrations, and when surfactant concentration was beyond a specified value, bubble coalescence was completely suppressed in viscous liquids and gas holdup was independent of the additional surfactant addition. The effect of surfactants was also more pronounced as liquid viscosity increased.

2.1.3 Flow Regimes

From the gas holdup review, the effects of parameters such as bubble column diameter, aspect ratio, and gas distributor on gas holdup are different in various flow regimes. Therefore, it is important to know the characteristics of the various flow regimes, the range of parameters over which a particular flow regime prevails, and the effects of factors on flow regime transition.

2.1.3.1 Macroscopic Flow Structure

Tzeng et al. (1993) studied macroscopic flow structures of gas-liquid and gas-liquid-solid fluidization systems through visualization using a two-dimensional semi-batch bubble column. It was observed that a gross circulation occurred at high gas velocities, which was interpreted based on two simplified flow conditions involving a single bubble rising in a stationary liquid and a single bubble chain injected in a batch liquid. In general, gross liquid circulation was initiated by bubble lateral migration. When gross circulation occurred, four flow regions were identified: (i) descending flow, (ii) vortical flow, (iii) fast bubble flow, and (iv) central plume, as shown in Figure 2.3.

Chen et al. (1994) studied macroscopic flow structures in 3-D gas-liquid and gas-liquid-solid semi-batch bubble columns using particle image velocimetry. The bubble column

diameter in this study was 10.2 cm. Three flow regimes were identified and are schematically represented in Figure 2.4. The dispersed bubble flow regime was observed at low superficial gas velocities and was characterized by negligible bubble coalescence, liquid transport by bubble-driven motion in the vicinity of ascending bubble streams, and liquid recirculated between the rising bubble streams. As the superficial gas velocity was increased, the vortical-spiral flow regime was observed, where bubbles may coalesce and liquid was carried upward by the rising spiral motion of the central bubble stream and flowed downward in the same spiral manner between the central bubble stream and column wall. At high superficial gas velocities, the turbulent regime was identified, where the central bubble stream was a spiral flow pattern and the liquid flow pattern was more chaotic and dynamic than that in the vortical-spiral flow regime. They further identified four flow regions (descending flow, vortical-spiral flow, fast bubble flow, and central plume) in the vortical-spiral flow regime where the gross circulation patterns occur (see Figure 2.5).

Reese and Fan (1994) employed two different gas distributors (porous plate and perforated plate) to investigate the hydrodynamic behavior in the entrance region of a cylindrical bubble column. In the dispersed bubble regime, the liquid phase was more turbulent in the entrance region than the flow occurring in the bulk region. The average liquid velocity and the flow in the entrance and bulk regions consisted of a single circulation cell in the axial direction, with the liquid ascending in the center of the column and descending along the column wall. The strength of this circulation decreased as the flow developed throughout the entrance region and into the bulk region. In the coalesced bubble region (including vortical-spiral and turbulent flow), the flow development was observed to be

faster and the entrance effects were found to diminish. Flow conditions in the bulk and the entrance regions were found to be independent of distributor design in the coalesced bubble region.

2.1.3.2 The Drift Flux Model

The drift flux model is a separated-flow model in which attention is focused on the relative motion rather than on the motion of the individual phases (Wallis, 1969). The drift flux model is widely used in flow regime identification for gas-liquid two phase flow because it is applicable to various flow patterns over a wide range of gas holdups (Zuber and Findlay, 1965).

Zuber and Findlay (1965) presented an exhaustive derivation of the drift flux model. The model is usually presented in the form

$$\frac{U_g}{\varepsilon} = C_o\left(U_g + U_l\right) + V_{oj} \tag{2.1}$$

where C_o is a distribution parameter which depends on the gas holdup profile and reflects the gas holdup uniformity, U_g is the superficial gas velocity, U_l is the superficial liquid velocity, V_{oj} is the weighted mean drift velocity. For fully established flow with a constant profile, C_o is constant and ranges from 1.0 for a uniform gas holdup profile to 1.5 for a parabolic gas holdup profile. The simplest expression for this drift velocity is to assume each bubble moves independently and is not affected by the presence of other bubbles. The average drift velocity of the gas is given by the following expressions (Zuber and Findlay, 1965):

$$V_{oj} = 0.35\left(\frac{g\Delta\rho\sigma}{\rho_L^2}\right)^{0.5} \tag{2.2}$$

for slug flow regime and

$$V_{oj} = 1.53\left(\frac{g\Delta\rho\sigma}{\rho_L^2}\right)^{0.25} \tag{2.3}$$

for churn-turbulent flow. V_{oj} is independent of gas holdup and is assumed to be equal to the terminal velocity of a rising bubble in an infinite medium. However, when a bubble is affected by the presence of other bubbles, V_{oj} depends on gas holdup, and is given by

$$V_{oj} = u_\infty (1-\varepsilon)^k \tag{2.4}$$

where k is a measure of the bubble interference and u_∞, the terminal rise velocity of a single bubble in an infinite medium; this value depends on the bubble size.

The Zuber and Findlay drift flux model is widely used when discussing two-phase and three-phase flow. However, Clark et al. (1990) warned that it should be used with caution when applied to low velocity bubble flows or large diameter pipes, where C_o was not constant and varied with gas holdup. They attributed this to the fact that under the conditions of low velocity flows or large diameter pipes, buoyancy played a significant role. In this case, C_o had a high value and varied with column diameter, gas holdup, fluid properties, and bubble rise velocity. Therefore, under these situations, the drift flux model should be modified. Recently, Hibiki and Ishii (2003) verified that the distribution parameter and drift velocity increased for large diameter pipes at low velocity compared to those of smaller diameter pipes.

Extensive studies have been completed using the drift flux model for two-phase flow where the liquid velocity is nonzero. However, limited citations are available using the drift flux model when the superficial liquid velocity is zero, which appears in semi-batch bubble

columns. Kataoka et al. (1987) pointed out that either the distribution parameter or drift velocity must be larger in semi-batch systems to get good agreement between the drift flux correlations and gas holdup data. They applied a two-region model, where a channel was divided into the inner region of cocurrent upflow and the outer region of single-phase liquid downflow. In doing so, the distribution parameters in semi-batch systems were larger than those when the liquid velocity was nonzero and high, and the drift velocities were almost the same for both liquid velocity conditions.

2.1.3.3 Flow Regime Identification

Flow regime identification is an important topic that has attracted various investigators. Flow regimes have been determined by interpretation of the gas holdup evolution, drift flux analysis, and pressure fluctuation analysis.

One way of determining flow regimes is by interpreting the behavior of gas holdup with superficial gas velocity (Figure 2.2). In the homogeneous flow regime, gas holdup increases almost linearly with increasing superficial gas velocity (Krishna et al., 1993; Krishna and Ellenberger, 1996). When the superficial gas velocity is further increased, the increase is no longer linear and the transition flow regime occurs. In the transition flow regime, gas holdup reaches a local maximum value (with an appropriate gas distributor) and then decreases with superficial gas velocity to a local minimum value, indicating the onset of the heterogeneous flow regime. In the heterogeneous flow regime, gas holdup increases slightly with superficial gas velocity.

The drift flux analysis of Wallis (1969) has been recommended to identify flow regimes (Vial et al., 2000). In a semi-batch bubble column, the drift flux, j_g is defined as

$$j_g = U_g(1-\varepsilon) \tag{2.5}$$

A plot of j_g vs. ε reveals the flow regime transitions, and a change in the slope of the j_g vs. ε indicates a change in flow pattern, as shown in Figure 2.6a.

The Zuber and Findlay drift flux model (Eq. (2.1)) is also used to distinguish the the various flow regimes by plotting $\frac{U_g}{\varepsilon}$ as a function of U_g (Zahradnik et al., 1997; Vial et al., 2000; Camarasa et al., 2001), as shown in Figure 2.6b. This model has also been successfully used to demarcate flow regimes in gas-liquid-solid systems (Gandhi et al., 1999).

Krishna et al. (1999a) combined the Wallis plot, i.e., drift flux, $U_g(1-\varepsilon)$ vs ε, and the Richardson and Zaki (1954) formula, i.e., $j_g = u_\infty \varepsilon (1-\varepsilon)^2$, which is valid for the homogeneous regime, to determine the regime transition point. They proposed that the point of deviation of the experimental values from the Richardson-Zaki curve indicated the regime transition point.

Sarrafi et al. (1999) adopted the conception of slip velocity (U_s) and drift flux (j_g) and extracted an experimental relationship to determine the flow regime transition. They found that flow regime transition always occurred when the difference in slip velocity and drift flux ($U_s - j_g$) was a minimum value.

Recently, pressure fluctuation analysis was used by Vial et al. (2000), Camarasa et al. (1999), and Lin et al. (2001) to identify flow regimes. Vial et al. (2000) applied statistical

analysis, spectral analysis, fractal analysis, and chaos analysis to the varying pressure signals, and concluded that statistical analysis was not superior to the drift flux model analysis, and spectral analysis could identify a particular regime but could not precisely determine flow regime transition. Fractal and chaos analysis was shown to accurately identify regime limits.

2.1.3.4 Factors Affecting Flow Regime

The formation and stability of bubble column flow regimes, and their associated limits depend on the gas flow rate, the kind of gas distributor, bubble column geometry, and the liquid physical properties.

2.1.3.4.1 Influence of Gas Distributors

The gas distributor has a significant effect on the gas flow pattern in a semi-batch bubble column. Ruzicka et al. (2001a) used two perforated plate gas distributors and generated two different of flow patterns: (i) a plate with small closely spaced holes, which generated homogeneous, transitional, and heterogeneous flow; and (ii) a plate with large holes, which generated pure heterogeneous flow. Zahradnik et al. (1997) showed that the open area ratio had an effect on flow regime transition and an increase in open area ratio tended to stabilize the homogeneous flow regime. They also reported that when the hole diameter was large (d_o > 1 mm), no homogeneous flow was generated and heterogeneous flow existed at all superficial gas velocities.

2.1.3.4.2 Influence of Bubble Column Diameter

Zahradnik et al. (1997) reported that increasing the bubble column diameter tended to destabilize homogeneous flow. This phenomenon was caused by an increase in the liquid circulation with increasing column diameter. This observation was verified by Ruzicka et al. (2001b) using semi-batch bubble columns with diameters of 14 cm, 29 cm, and 40 cm. Zahradnik et al. (1997) demonstrated that the effect of bubble column diameter depended on aeration plate hole diameter. When the hole diameter was greater than 1 mm, no effect of bubble column diameter was observed, and only heterogeneous flow existed over the entire range of superficial gas velocities in their study with bubble column diameters of 14 cm and 29 cm.

2.1.3.4.3 Influence of Liquid Properties

Liquid properties such as viscosity and surface tension have an effect on flow regime transition. A higher viscosity promotes bubble coalescence and suppresses bubble breakup, which promotes flow regime transition. Kuncova and Zahradnik (1995) and Zahradnik et al. (1997) reported that a high viscosity liquid had an unfavorable effect on the formation of homogeneous flow. When the viscosity was greater than 8 mPa s, no homogeneous flow was observed and the flow was pure heterogeneous.

Reducing surface tension forces stabilize the gas-liquid interface so that coalescence is suppressed, which promotes homogeneous flow at high superficial gas velocities. Zahradnik et al. (1999) demonstrated that the addition of a surfactant to a viscous liquid outweighed the negative effect of the high viscosity on the formation and stability of the homogeneous flow

regime. Krishna et al. (2000) also showed that the addition of alcohol delayed the flow regime transition, which was attributed to the suppression of bubble coalescence.

2.2 Gas-Liquid-Solid Bubble Columns

When a solid is added to a gas-liquid bubble column, additional complications result; these observations will now be discussed.

2.2.1 Gas Holdup

2.2.1.1 Effect of Solid Mass Fraction and Size

Gas holdup behavior in gas-liquid-solid (GLS) bubble columns, in which the solid material is spherical or irregular like glass beads, sand, or coal particles, has been extensively studied by various investigators (Kara et al., 1982; Kelkar et al., 1984; Koide et al., 1984; Banisi et al., 1995b; De Swart et al., 1996; Krishna et al., 1997; Li and Prakash, 1997; Gandhi et al., 1999). These studies show that the presence of a solid particle in a bubble column decreased gas holdup from that observed in simple gas-liquid (GL) systems. Kara et al. (1982) and Gandhi et al. (1999) found that the gas holdup decreased with increasing solid concentration, but the effect was less significant at higher solid concentrations. Koide et al. (1984) reported that the effect of solid concentration on gas holdup was larger in the transition flow regime.

De Swart and Krishna (1995) studied the effect of solid mass fraction on gas holdup in a 50-mm diameter bubble column using 40-μm diameter glass beads, and showed that increasing the solid mass fraction resulted in a pronounced decrease in the total gas holdup. They identified the mixure portion comprised primarily of large bubbles as dilute; the effect

of solid mass fraction on this phase was negligible. Hence, the dense gas phase, which was comprised of small bubbles, suffered a significant decrease in gas holdup due to enhanced small bubble coalescence.

Krishna et al. (1997) used a dynamic gas disengagement method to study the effect of solid volume fraction on gas holdup in the dense phase (small bubbles) and dilute phase (large bubbles) of a semi-batch bubble column. The results agreed with those of De Swart and Krishna (1995) that the dense phase gas holdup decreased with increasing solid volume fraction, especially when the solid volume fraction was low. The dilute phase gas holdup was independent of solid volume fraction when the solid volume fraction was greater than 16%. Similar phenomena have been observed by Li and Prakash (1997). These observations indicated that the decrease in total gas holdup with increasing solid volume fraction resulted from the decrease in the dense phase gas holdup because solid addition reduced the small bubble population.

Li and Prakash (1997), Zahradnik et al. (1997), and Gandhi et al. (1999) attributed the decrease in gas holdup with increasing solid mass fraction to fine particles enhancing the bubble coalescence rate and/or reducing the bubble breakup rate because the apparent suspension viscosity was higher than that of a similar GL system. Banisi et al. (1995b) also proposed two mechanisms for the decrease in gas holdup with solid addition: (i) an increase in the rise bubble velocity due to wake stabilization, leading to a decreased residence time and gas holdup, and (ii) a change in the radial gas holdup and flow profiles from nearly flat to parabolic with upward flow near the center and downward flow near the wall, reducing the average gas holdup.

Particle size is another factor concerned in gas-liquid-solid bubble columns. Kara et al. (1982) and Kelkar et al. (1984) stated that increasing particle size tended to reduce gas holdup at low gas velocities. Kara et al. (1982) reported that the effect of particle size was less significant for larger solid particles.

2.2.1.2 Effect of Solid Surface Wettability

It is well known that the presence of particles affects the hydrodynamics of slurry bubble columns through the apparent viscosity. However, Chen and Fan (1989), Jamialahmadi and Muller-Steinhagen (1991), Banisi et al. (1995a), and Van der Zon et al. (2002) investigated slurry bubble columns using hydrophilic and hydrophobic particles, and found that gas holdup for hydrophobic particles was lower than that of hydrophilic particles. This difference was not attributed to the apparent viscosity. An alternative explanation may be that hydrophobic particles enhanced bubble coalescence (Racz et al., 1996; Wang et al., 1999; Kluytmans et al., 2001). Van der Zon et al. (2002) explained that hydrophobic particles promoted bubble coalescence by enhancing film rupture or increased the critical film thickness when two bubbles approach. In contrast, wettable particles tend to repel the gas interface, acting as a buffer between two adjacent gas bubbles and result in a decrease in bubble-bubble interaction and reduced bubble coalescence. Kluytmans et al. (2001) and Chen and Fan (1989) also showed that hydrophobic particles suppress bubble breakup.

2.2.2 Flow Regimes

Tzeng et al. (1993) pointed out that the macroscopic flow structure of gas-liquid-solid systems could be represented by that of gas-liquid systems, although the vortex size and

descending velocities in three phase systems deviated from those of a GL system under similar operating conditions, which was due to the change in the rheological properties of the slurries when the solid particles were present.

The Zuber and Findlay drift flux model (Eq. (2.1)) has been successfully applied to demarcate flow regime transitions in gas-liquid-solid systems (Gandhi et al., 1999). Douek et al. (1997) extended the Zuber and Findlay drift flux model to three-phase flow. The model includes phase interaction terms which appear in the drift velocity correlation, and was given by

$$\frac{U_g}{\varepsilon} = C_0\left(U_g + U_L\right) + u_\infty\left(1-\varepsilon\right)^n \tag{2.6}$$

It was found that the use of a single representative bubble drift velocity was not suitable for describing gas phase hydrodynamics. Also, the gas drift velocity did not vary with increasing solid concentration, but was strongly affected by gas holdup due to bubble coalescence.

2.3 Gas-Liquid-Fiber Bubble Columns

Unlike conventional solids used in gas-liquid-solid slurry systems, which are typically rigid and spherical or slightly irregular, fibers are flexible and have a large aspect ratio, which leads to the unique complex rheology of fiber slurries.

2.3.1 Fiber Suspension Characteristics

2.3.1.1 Fiber-Fiber Interaction

Fiber-fiber interaction plays an important role in the characteristics of fiber suspensions (i.e., flocculation, yield stress, suspension viscosity, etc.), which is a function of the fiber mass fraction, fiber aspect ratio, and, to some extent, fiber type. In very dilute suspensions, little interaction between fibers is observed and individual fibers are free to flip, translate, and bend in simple shear flows. When fiber concentration increases, the fiber-fiber collision frequency increases, resulting in fibers flipping more frequently (Sundararajakumar and Koch, 1997). Further increasing fiber concentration leads to continuous fiber-fiber contact, and the relative fiber motion is suppressed, eventually immobilizing the fiber suspension. This is called flocculation (Kerekes and Schell, 1992).

Based on the fiber-fiber interaction conditions, Soszynski (1987) classified a fiber suspension into three different regimes: dilute, semi-concentrated, and concentrated. Correspondingly, the fiber contact was classified into three types: occasional collision, forced collision, and continuous collision. In terms of the number of fiber contacts, Kerekes and Schell (1992) used a crowding factor, N, which is a dimensionless number describing the number of fibers in a spherical volume of diameter equal to the fiber length, to demarcate the suspension regimes. The crowding factor is a function of fiber concentration (either mass fraction or volume fraction) and fiber aspect ratio, and is defined as

$$N = \frac{2}{3} C_v \left(\frac{L}{d}\right)^2 \approx 5\frac{CL^2}{\omega} \tag{2.7}$$

where C_v is the fiber volume fraction, C is the fiber mass fraction, L is the fiber length, and ω is the fiber coarseness. As indicated by Kerekes and Schell (1992), the terms in the approximate expression have specific units; they are C (%), L (m), and ω (kg/m). When $N < 1$, the fiber regime is dilute; $1 < N < 60$, it is semi-concentrated; and $N > 60$ corresponds to concentrated.

Another parameter to describe fiber suspensions, including information related to the fiber mass fraction and fiber dimensions, $N_f L^2 d$, has also been used, where N_f is the number of fibers per unit volume, L is the fiber length, and d is the fiber diameter (Sundararajakumar and Koch, 1997; Chaouche and Koch, 2001). In this case, when $N_f L^2 d << 1$, a dilute or semi-dilute regime is defined; when $N_f L^2 d \sim 1$, a semi-concentrated regime is defined; and when $N_f L^2 d > 1$, a concentrated regime is defined.

Hydrodynamic interaction and mechanical contact are two modes that control fiber-fiber behavior. Which one of these two modes plays a more important role is related to the fiber suspension regime, which has a significant impact on fiber suspension rheological characteristics. The relative importance of hydrodynamic interaction and mechanical contacts has been studied by Sundararajakumar and Koch (1997). They confirmed that hydrodynamic interaction was more important in controlling fiber motion in dilute or semi-dilute fiber suspensions ($N_f L^2 d << 1$), but in semi-concentrated and concentrated fiber suspensions ($N_f L^2 d \gtrsim 1$), mechanical contact was the main factor that determined fiber suspension structure. In dilute or semi-dilute fiber suspensions, fibers rotate occasionally, and spend most of their time aligned along the flow direction. In this case, the fiber contribution to the suspension rheology was small, and the rheological characteristics of the suspension were

identical to the suspending medium. In semi-concentrated and concentrated fiber suspensions, mechanical contacts increase fiber-fiber interaction, which increased the frequency of fiber flipping and the orientation distribution. However, Petrich et al. (2000) insisted that the contacts first enhance flipping due to collision, as Sundararajakumar and Koch (1997) simulations indicated, but then decrease flipping when fiber concentration was further increased. When mechanical contacts dominate, the fiber contribution to the rheological characteristics of the suspension became very important. Sundararajakumar and Koch (1997) found that the increase in suspension viscosity with fiber concentration was enhanced when $N_f L^2 d > 1$. Chaouche and Koch (2001) proposed that in the concentrated regime, mechanical contacts gave rise to shear thinning flow below a certain shear rate. They interpreted this phenomenon to the formation and breakage of fiber flocs due to the competition between the hydrodynamic and colloidal forces. Also, in the concentrated regime, coherent fiber networks were formed due to fiber-fiber interaction; as a result, a yield stress at low shear stress must be overcome before fiber flocs are dispersed (Bennington et al., 1990).

2.3.1.2 Flocculation

Fibers form networks when each fiber is in contact with other fibers. Fiber distribution within the network is never uniform, giving local mass concentration variations. Regions in which the local mass density is higher than the network average are called flocs. Flocculation is the term used to describe both the state of unevenness of fiber network, as well as the process by which all fiber networks form (Kerekes et al., 1985).

Mason (1950) proposed that flocculation is a dynamic equilibrium process, with fibers continuously entering and leaving flocs, both rates being equal at steady state. Flocculation can occur through various mechanisms, such as colliodal forces like London-van der waals and electrostatic, mechanical forces like friction and cohesion, or a combination of forces. In fiber suspensions, flocculation is primarily due to mechanical entanglement (i.e., friction or cohesion) (Mason, 1950). Fiber mass (volume) fraction, fiber aspect ratio (the ratio of fiber length to diameter), fiber flexibility, and fiber frictional force have a close relationship to floc formation, size, and strength.

Kerekes and Schell (1992) emphasized the importance of fiber contact number in flocculation and believed that inter-fiber contact was the key requirement in fiber flocculation, and the formation of coherent fiber flocs required a minimum number of fiber-fiber contacts. They characterized this requirement by the crowding factor (N). When $N \leq 1$, fiber-fiber contact only happens occasionally, and fibers are free to move; when $1 < N < 150$, flocs may appear in the suspension and fiber mobility decreases. The effectiveness of the crowding factor to describe fiber flocculation behavior has been verified by experiments (Kerekes and Schell, 1992). However, the crowding factor is merely an indicator of the number of inter-fiber contacts, and only reflects the effects of fiber concentration and fiber aspect ratio, which led Kerekes (1996) to point out that the critical crowding factor was only a necessary condition for floc formation, not a sufficient one. Other factors like fiber shape, flexibility, and friction force also have an impact on fiber flocculation behavior.

Schmid et al. (2000) believed that fiber flocculation is not only affected by fiber volume fraction and aspect ratio, but it is also affected by fiber properties and inter-fiber friction.

Using a particle-level simulation and neglecting hydrodynamic forces, they studied the effect of the fiber friction coefficient, stiffness, shape, and concentration on fiber flocculation. Friction force played an important role in fiber flocculation. Friction induced mechanical interlocking and prevented sliding between contacting fibers. Increasing the friction coefficient increased the fiber retention by the flocs. Friction also enhanced fiber deformation in shear flow, which assisted fiber flocculation. Soszynski and Kerekes (1988a; 1988b) also proposed that flocculation was caused by interfiber contact forces.

Chaouche and Koch (2001) suggested that adhesive mechanical forces existed between the fibers and they were the source of fiber flocculation. When shear stress is not high enough to overcome the adhesive forces, fibers adhere to each other and form flocs. The adhesive force is independent of the suspending medium viscosity, but is a function of the particle wettability in the liquid medium. Experimental results showed that the adhesive force of Nylon fiber in 15%/85% glycerin/water by volume is about 20 times larger than in silicone oil, and the authors attributed this phenomenon to the hydrophobicity of Nylon fiber. Thus, fiber surface characteristics also have an effect on fiber flocculation.

Fiber stiffness is also an important factor in the formation and persistence of flocs. Schmid et al. (2000) argued that decreasing fiber stiffness led to the reduction in the inter-particle force magnitudes and elastic energy storage; both factors encourage floc breakup and dispersion under shear flow. Switzer and Klingenberg (2004) confirmed this result and showed that a suspension of fibers that is too flexible would not flocculate under shear flow. They suggested that stiffness has an impact and tends to increase the normal force between contacting fibers, which increases the strength of the friction force. This mechanism was

observed by Soszynski and Kerekes (1988a); Nylon fiber flocs readily dispersed when the fiber stiffness was reduced by heating them above the glass transition temperature of Nylon. Switzer and Klingenberg (2004) used an effective stiffness ($S^{eff} = EI/\mu\dot{\gamma}L^4$) to describe the effect of fiber flexibility on flocculation, where E is Young's modulus, μ is the liquid dynamic viscosity, $\dot{\gamma}$ is shear rate, and L is fiber length. They determined that flocculation was encouraged when the effective stiffness was large. This conclusion was true when the effective stiffness was varied by varying E, which varied the inter-fiber force, and μ, which varied the viscous force and allowed the fiber to follow the fluid motion and assisted fiber dispersion. However, when S^{eff} is reduced by increasing fiber length, flocculation should be difficult; on the contrary, fiber flocculation is enhanced because the number of fiber-fiber contacts is increased.

Schmid et al. (2000) and Switzer and Klingenberg (2004) claimed that the fiber equilibrium shape significantly impacts the rheology of the fiber suspension. An irregular fiber shape increases fiber-fiber interactions and faster aggregation of the fiber suspension. They also simulated the effect of fiber concentration (N_fL^3) and determined that fiber concentration had an effect on fiber flocculation behavior, and the critical concentration was related to fiber equilibrium shape; a deformed fiber was more likely to flocculation than a straight fiber.

Beghello and Eklund (1999) studied the effect of the chemical environment on fiber flocculation. They disclosed that electrolytes and pH have an insignificant effect on fiber flocculation. Although electrolytes added to the fiber system changed the fiber surface

chemistry, leading to repulsive forces in the fiber network, they were not strong enough to break coherent flocs under turbulent and dynamic conditions.

Kerekes et al. (1985) pointed out the presence of air also affects fiber flocculation. As gas holdup increases, the nature of fiber flocculation changes from that of mass concentrations of fiber in water to that of water-fiber aggregates surrounded by gas voids. Fiber networks will rupture at their weak points, i.e. water-fiber flocs surrounded by gas voids. They reasoned that flocs should disperse in a large volume of gas flow.

2.3.1.3 Yield Stress

Yield stress is an important characteristic to fiber suspension rheology. It results from fiber-fiber interaction. When stress generated by a suspension falls below the suspension yield stress, the fiber suspension acts as an elastic solid, and above the yield stress, it behaves as a liquid. Suspension yield stress may produce a significant effect on gas flow behavior in a fiber suspension, assist fiber flocs in trapping bubbles, and produce channeling phenomenon at high fiber mass fractions. Fiber concentration, aspect ratio, length distribution, stiffness, friction coefficient, and type have an impact on the suspension yield stress.

Kerekes et al. (1985) reviewed the literature about network strength and summarized a simple empirical equation to predict yield stress in fiber suspensions

$$\tau_y = aC^b \tag{2.8}$$

where C is the fiber mass fraction, and a and b are constants that depend on fiber type and range 1.18~24.5 and 1.26 ~3.02, respectively.

Bennington et al. (1990) extended Eq. (2.8) by considering the effects of elastic modulus and aspect ratio, and expressed the yield stress as

$$\tau_y = kEr^2C_v^{\ 3} \tag{2.9}$$

where k is a constant, E is Young's modulus, r is the fiber aspect ratio, and C_v is the fiber volume fraction. They assumed that network strength is proportional to the frictional force. In the expression, yield stress is proportional to elasticity modulus; this was supported by the findings of Thalen and Wahren (1964) for synthetic fiber suspensions. However, this relation is not always valid. The experimental results of Bennington et al. (1990) showed that fiber suspension network strength did not vary linearly with the elasticity modulus. They attributed the lack of agreement to more complex surface interactions than that accounted for in the model. Wikstrom et al. (1998) attributed this deviation to the omittion of the effect of the fiber length distribution. They found that fiber length distribution had a greater influence on the network strength than the mean fiber length. Switzer and Klingenberg (2004) attributed the inconsistency to the fact that besides fiber modulus, the fiber shape, the type and amount of additives also have an effect on yield stress.

The network strength of non-flocculated fiber suspensions, in which the fiber network is evenly distributed and no flocs are observed, was studied by Andersson et al. (1999) who emphasized the effect of the fiber-fiber friction force. A new model for yield stress was proposed as a product of the number of contact points per unit shearing surface (N_{ss}) and the average friction force per contact point. Effects of both fiber length distribution and fiber volume fraction are reflected in N_{ss}, and N_{ss} is roughly proportional to C_v^2. The frictional force comprises two parts: (i) the part when the normal force is zero and (ii) the part related

to the normal force that results from fiber bending. The fiber with a higher elasticity modulus would produce a larger normal force, resulting in a larger friction force. The advantage of this model is that it accounts for the effect of fiber length distribution. The shortcoming of this model is that it is only applicable to non-flocculated suspensions. Measurements in flocculated suspensions showed that the network strength was much lower compared to non-flocculated suspensions.

The yield stress should be modified when gas flows through a fiber suspension. Bennington et al. (1995) studied the yield stress in fiber suspensions including a gas phase and incorporated gas volume fraction into the yield stress correlation. According to Bennington et al. (1990), the influence of fiber aspect ratio is not significant for fiber suspensions, thus the yield stress correlation did not include the aspect ratio term and was only a function of fiber mass fraction (C) and volumetric gas fraction (ε), which was expressed as:

$$\tau_y = aC^b(1-\varepsilon)^c \tag{2.10}$$

The coefficients a, b, and c depend on fiber type. However, this model was not appropriate for synthetic fibers. Bennington et al. (1995) experimentally determined that yield stress in Nylon fiber suspensions was dependent on fiber aspect ratio to the power 1.5.

2.3.1.4 Suspension Viscosity

Suspension microstructure is very important to the effective fiber suspension viscosity. Hydrodynamic interaction and mechanical contacts control fiber-fiber interaction. Sundararajakumar and Koch (1997) showed that in dilute or semi-dilute fiber suspensions, in

which hydrodynamic interaction dominated, the presence of fiber contributed little, and the suspension viscosity was close to that of the suspending medium. In semi-concentrated and concentrated fiber suspensions, in which mechanical contact was the main factor that determined the fiber suspension structure, the suspension viscosity dramatically changed and it increased non-linearly with the term $N_f L^3$. They attributed the suspension behavior to mechanical contact. In dilute or semi-dilute fiber suspensions, fibers rotate occasionally, and spend most of their time aligned along the flow direction; thus, the fiber influence on the suspension viscosity was small. When the fiber concentration was high, mechanical contacts increased fiber-fiber interaction, which increased the frequency of fiber rotation and produced a broad fiber orientation distribution. A wide fiber orientation distribution led to an increased shear viscosity, which was enhanced further by the transmission of stress by mechanical contacts, and the shear viscosity showed an abrupt increase with increasing fiber concentration for $N_f L^2 d > 1$.

The experimental results of Petrich et al. (2000) showed that although shear stress increased considerably with fiber concentration, the fiber orientation distribution broadened and then became more uniform, approaching the dilute value at high fiber concentrations, which indicated that the contribution of fiber orientation to shear viscosity was small. They attributed the increase in shear viscosity with increasing fiber concentration to the transmission of stress due to the presence of fiber-fiber contacts.

Fiber flexibility also has an effect on viscosity. Fibers, particularly some synthetic and natural fibers, are far from rigid straight rods like glass fibers. Simulations using flexible fiber have shown good agreement with experimental results (Schmid et al., 2000). Fibers

may be flexible and tend to deform in the flow direction, which can significantly influence the rheological characteristics of the fiber suspension. Joung et al. (2001) reviewed the effect of fiber flexibility on fiber suspension apparent viscosity. Only accounting for hydrodynamic interaction, their simulation showed that the viscosity of semi-concentrated flexible fiber suspensions was 7-10% greater than the equivalent rigid fiber suspension, and the viscosity was inversely dependent on the fiber stiffness.

Fiber flexibility depends on fiber aspect ratio, and it is more important when the fiber aspect ratio is large or Young's modulus is low. Forgas and Mason (1959) gave the critical shear stress beyond which fibers bend:

$$(\mu\dot{\gamma})_{critical} = \frac{E[\ln(2r) - 1.75]}{2r^4} \tag{2.11}$$

where μ is the fluid viscosity, $\dot{\gamma}$ is the shear rate, E is Young's modulus, and r is the fiber aspect ratio. When the fiber has a large aspect ratio, or Young's modulus is low, the fiber deforms under a relatively small shear stress.

Fiber shape also has an effect on the fiber suspension viscosity. A recent study on this relationship was conducted by Joung et al. (2002). They numerically studied the effect of curvature and suggested that small deformities in the fiber generated a large increase in the suspension viscosity. The greatest effect occurred when the curvature was between 5 and 10 degrees. They explained that curved fiber tends to misalign to the flow direction. The more curved a fiber, the larger the fiber profile in the flow direction, resulting in an increased viscosity compared to straight fiber suspensions. Yet this could not explain the finding that

viscosity decreased beyond a curvature of around 10 degrees. This numerical result has yet to be observed experimentally.

2.3.2 Gas Holdup

2.3.2.1 Effect of Fiber Mass Fraction

Gas holdup behavior in natural fiber suspensions has been investigated by several investigators. Walmsley (1992) used two and three dimensional semi-batch bubble columns and fiber suspensions derived from bleached kraft pine (BKP), bleach kraft eucalyptus (BKE), and recycled yellow paper (RYP). It was recorded that in BKP and BKE, gas holdup increased above that of an air-water system when the fiber mass fraction (C) was low; when $C > 0.6\%$, gas holdup decreased with increasing fiber mass fraction. However, no gas holdup enhancement was observed in RYP, instead, gas holdup monotonically decreased with increasing fiber mass fraction. Gas holdup was not significantly affected by further fiber addition when $C > 2\%$. Went et al. (1993) observed that in a semi-batch bubble column, gas holdup decreased with increasing fiber mass fraction, and when $C \geq 1\%$, the effect of fiber mass fraction leveled off; this was attributed to fibers agglomerating in a large mat near the bottom of the column, lowering the effective fiber mass fraction in the upper column region. Lindsay et al. (1995) showed that in a semi-batch bubble column, gas holdup was lower in fiber systems with fiber mass fractions of 1% and 2% than in an air-water system because gas channeling resulted in a lower gas residency time. Reese et al. (1996) recorded a consistent gas holdup decrease with increasing fiber mass fractions from 0.1 to 1%. They also observed that the fiber distributed uniformly in the axial direction when the fiber mass fraction was low; however, fiber tended to build up at the bottom of the column when the fiber mass

fraction was high. A decrease in gas holdup caused by fiber addition was also observed by Janse et al. (1999), and they pointed out the effect of fiber addition was more pronounced at higher superficial gas velocities.

Gas holdup in a cocurrent fiber slurry bubble column has also been studied. Using unprinted old newspaper (ONP), Lindsay et al. (1995) observed that in a cocurrent bubble column, the gas holdup was greater than that of an air-water system when C = 1%. Extending this study, Schulz and Heindel (2000) recorded that at low liquid flow rates, gas holdup decreased with increasing fiber mass fraction; at high liquid flow rates, the presence of fibers increased the gas holdup above that of a similar gas-liquid system, and a maximum gas holdup was reached at C = 0.8%. Recently, Xie et al. (2003) used kraft softwood cellulose fiber and applied gamma-ray densitometry to measure gas holdup, and showed that gas holdup reached a maximum value at C = 1% for most of the liquid flow rates in their study.

It has been widely accepted that gas holdup decreases with increasing fiber mass fraction because fiber addition increases the apparent viscosity of the fiber suspension, which enhances bubble coalescence. Fibers also tend to trap bubbles and hinder bubble rise, resulting in enhanced bubble coalescence (Walmsley, 1992; Went et al., 1993; Lindsay et al., 1995; Reese et al., 1996; Janse et al., 1999).

2.3.3 Flow Regimes

Heindel (2000) observed that gas flow regimes in a fiber suspension changed from vortical to heterogeneous (also called churn-turbulent) as the fiber mass fraction increased from 0.5% to 5%. Two new flow regimes were identified at higher fiber mass fractions:

surge churn-turbulent flow where churn-turbulent flow existed as surges because of large bubbles trapped in the fiber suspension, and discrete channel flow, where individual air channels form at the highest fiber mass fraction.

Reese et al. (1996) observed flow regimes in fiber suspensions over a range of fiber mass fractions from 0.1% to 1.0% in a 10.2 cm diameter semi-batch bubble column. Two flow regimes were observed: the dispersed bubble regime and the coalesced bubble regime. These observations agreed with those of Chen et al. (1994). According to the observation of Chen et al. (1994), the coalesced bubble regime was further divided into vortical-spiral flow and turbulent flow. It was observed that at lower fiber mass fractions (0.1% and 0.25%), there were three flow patterns: dispersed flow, vortical-spiral flow, and turbulent flow. At higher fiber mass fractions ($C > 0.5\%$), no vortical-spiral flow was observed, and flow transitioned directly from dispersed flow to turbulent flow.

In a 5.08-cm diameter cocurrent slurry bubble column, Xie et al. (2003) explored various flow regimes for fiber mass fractions up to 1.5% by using visual observation, flash X-ray radiography and gamma-ray densitometry. Five flow regimes were visually identified in the small diameter bubble column: dispersed bubbly, layered bubbly, plug, churn-turbulent, and slug. Flow regime transitions were sensitive to fiber mass fraction, and increasing the fiber mass fractions tended to increase the superficial gas velocity at which flow regime transition occurred. These phenomena were attributed to the fact that fiber addition retarded bubble coalescence in the cocurrent system. Additionally, flow regime maps were constructed for different fiber mass fractions using phasic superficial velocities as coordinates.

2.3.4 Bubble Behavior in Fiber Suspensions

Pelton and Piette (1992) studied air bubble behavior in quiescent cellulose fiber suspensions. They found that individual bubble holdup in the fiber bed was mainly due to mechanical entrapment of bubbles in the fiber network (Figure 2.7). Bubbles escaped when the buoyant force was strong enough to disrupt the fiber network. The higher the fiber mass fraction, the larger the required bubble diameter to escape from the fiber network.

Walmsley (1992) concluded that fibers act as barriers to upward bubble motion. When flocs exist in the fiber suspension, rising bubbles become trapped beneath the flocs or rise between flocs in regions of low fiber concentration. Bubbles are more likely to become trapped in the fiber network at high fiber mass fraction, and remain there until additional bubbles coalesce with the trapped bubble until a critical bubble size is reached, which provides a sufficient buoyant force to break through the fiber network. As the large bubbles escape from the network, they create a channel through which small bubbles pass; this phenomenon is called channeling.

Ajersch and Pelton (1999) extended the work of Pelton and Piette (1992) and studied the migration of air bubbles in flowing and quiescent cellulose fiber suspensions. They reported that small bubbles on the order of 10-50 μm in diameter are small enough to penetrate inside fiber flocs without disrupting the floc's fiber network. Larger bubbles may penetrate inside fiber flocs but do so by disrupting the flocs. When the bubble buoyant force was not strong enough to overcome the floc yield stress, the bubble becomes trapped in or under the floc. They insisted that mechanical entrapment in the flocs was the main mechanism for bubble

holdup, and bubble-fiber adhesion can be neglected for most wetted cellulose fiber suspensions. Trapped bubbles in agitated fiber suspensions was less significant than in quiescence cellulose fiber suspensions because of the presence of shear forces, which disperse the transient fiber flocs and/or detached trapped bubbles from coherent fiber flocs. They also gave four mechanisms of bubble escape from flocs in agitated fiber suspensions: (i) small bubble escape by slipping through the void space between individual fibers, (ii) bubble escape by fiber network disruption, (iii) bubble release through floc deformation, stretching, breaking, and fragmentation under turbulent flow conditions, and (iv) bubble detachment is shear forces acting at the bubble-floc interface which was due to the relative velocity gradients between the floc and the surrounding fluid medium in the presence of large-scale turbulence. These mechanisms are schematically represented in Figure 2.8.

Reese et al. (1996) found that in fiber suspensions, bubbles became flatter compared to a pure water system and bubbles tended to be flatter at the bottom of the column. The flatter the bubble, the lower the bubble rise velocity. Flatter bubbles were also more likely to interact with each other, which led to an increased probability of bubble coalescence.

Heindel (1999) measured bubble size using flash X-ray radiography in a quiescent fiber suspension with fiber mass fractions of 0.1%, 0.5%, and 1.0%. The results showed that bubbles became larger and less dispersed, and followed preferential rise paths with increasing fiber mass fractions. Using the same measurement method, Heindel (2002) studied bubble size in a cocurrent fiber slurry and reported that bubbles can be categorized as either small ($d_B \leq 10$ mm) or large ($d_B > 10$ mm). Small bubble diameter distributions were characterized by log-normal distributions. It was also found that the large bubble size and

population increased with increasing bubble column height, superficial velocity, and fiber mass fraction. However, fiber addition hindered small bubble coalescence in the cocurrent flow. In a semi-batch bubble column, Heindel (2000) observed that the number of small bubbles decreased and large bubbles increased with increasing fiber mass fraction. Bubbles rose upward in a serpentine flow pattern at low fiber mass fractions and this changed to a near vertical path at high fiber mass fractions.

Heindel and Omberg (2001) studied the effect of Rayon fiber lengths on bubble size in C = 1% fiber suspensions and found that at this fiber mass fraction, the effect of fiber length on bubble size was negligible. However, the limited data from this study can not be extended to low fiber mass fraction systems, where the effect of fiber length may be significant.

2.4 Bubble Behavior

Bubble size and distribution play an important role in gas flow hydrodynamics in bubble columns. They govern overall gas holdup, gas holdup distribution, interfacial area, and the resulting transport rate. Bubble behavior in bubble columns also has a close relationship to the resulting gas flow regimes.

2.4.1 Bubble Coalescence and Breakup

Bubble coalescence and breakup are basic processes that take place in bubble columns. They are important because they not only govern the bubble size distribution, but also directly affect interfacial mass transfer through bubble surface renewal.

It is well accepted that bubble coalescence occurs in three steps: (i) two bubbles collide, trapping a small amount of liquid between them; (ii) the liquid drains as the bubbles move closer together; and (iii) the liquid film between the two bubbles rupture after it is reduced to a critical thickness, resulting in bubble coalescence (Otake et al., 1977).

Crabtree and Bridgwat (1971) studied the manner in which bubbles draw together and demonstrated that the bubble wake plays an important role, through which following bubbles were accelerated in the wake of leading bubbles. The following bubble may catch the leading bubble, resulting in the possibility of bubble coalescence. The role of the wake was clearly shown from the fact that one leading bubble was caught by a following bubble with the same volume. Colella et al. (1999) also proposed that bubble-bubble interaction was caused by bubble wake effects, and bubble shape had an effect on both bubble coalescence and breakup. Prince and Blanch (1990) pointed out that bubble collision also arises due to other mechanisms such as turbulence, buoyancy, and the presence of liquid temperature and/or concentration gradients. They also stated that bubble coalescence resulting from bubble-bubble collision was determined by the contact time of the coalescing bubble, which should be longer than the time needed to drain the liquid film between the two bubbles.

Prince and Blanch (1990) insisted that bubble breakup occured through bubble interactions with turbulent eddies. Bubble breakup took place when eddies were equal to or marginally smaller than the bubble size. Larger turbulent eddies resulted in bubble transport without causing breakup, and smaller eddies did not contain sufficient energy to affect breakup. Therefore, any factor that affects turbulent intensity and bubble size will have an effect on bubble breakup.

Tsuchiya et al. (1996) provided five mechanisms through visual analysis that contribute to large cap bubble breakup: (i) inherent instability of the cap itself, (ii) bubble attachment to the cap bubble base resulting in the indentation on the underside of the bubble and initiating bubble breakup, (iii) impact of an intermediate bubble on the cap bubble base through the bubble wake action, (iv) "lifting" enhancement of the cap bubble by the wakes of two adjacent bubbles, and (v) suction of part of the top of the cap bubble into the wake of an intermediate bubble.

2.4.2 Effect of Superficial Gas Velocity

Prince and Blanch (1990) showed that both bubble coalescence and breakup rate increased with increasing superficial gas velocity; the resultant bubble size was determined by the competition of these two processes. The tendency to increase the bubble breakup rate with increasing superficial gas velocity was also identified by Colella et al. (1999). Otake et al. (1977) showed that bubble breakup occurred more readily rather than bubble coalescence as superficial gas velocity increased.

2.4.3 Effect of Liquid Properties

Otake et al. (1977) believed that liquid properties influence bubble coalescence and breakup through affecting bubble wake volume and vortex shedding from the rising bubble. In a viscous liquid, the bubble wake tends to be stable, which provides enough time for a second bubble to approach and the liquid film to drain. This process favors bubble coalescence. In an inviscid liquid, the bubble wake is small and unstable, thus, the probability of bubble coalescence is reduced, and instead, bubble breakup is more favorable. Schafer et

al. (2002) reported that increasing the liquid viscosity reduced the liquid phase turbulence and bubble collision frequency. As a result, both bubble breakup and coalescence were suppressed.

Walter and Blanch (1986) studied bubble breakup mechanisms in a turbulent flow field and found that bubble breakup was caused by fluctuating turbulent eddies and breakup occurred through bubble elongation. Both liquid viscosity and surface tension increased the resistance to bubble elongation, thus decreasing the bubble breakup frequency and increasing the maximum stable bubble size.

Prince and Blanch (1990) studied the effect of electrolyte solutions on bubble coalescence and found that the addition of NaCl and Na_2SO_4 tended to reduce bubble coalescence. They attributed this to the fact that NaCl and Na_2SO_4 decreased the surface tension.

2.4.4 Bubble Formation in Perforated Plates

Miyahara et al. (1983a) and Miyahara and Hayashino (1995) studied the bubble size generated from perforated plates in water and a non-Newtonian liquid, respectively. In both liquids, the bubble size distribution followed a log-normal distribution. However, the standard deviation of the bubble diameter was approximately 1 mm in water and 1.5 mm in the non-Newtonian liquid, indicating that more uniform bubbles are generated in water and bubble coalescence was favored in the non-Newtonian liquid.

Miyahara et al. (1983a) reported that the aeration plate hole spacing had an effect on the resulting bubble size. The effect was not significant for small hole spacing, but bubble size

tended to decrease when the ratio of the hole pitch to hole diameter was greater than 8. They attributed this phenomenon to the coalescence of adjacent bubbles when the hole spacing was small. Visual observations supported their conclusion.

Titomanlio et al. (1976) concluded that the gas chamber volume affects the bubble size formed through a perforated plate. However, Kumar et al. (1976) suggested that bubble size was independent of the gas chamber volume. Miyahara et al. (1983a) reported that if the gas chamber volume had an effect on bubble size, it depends on the number of holes in the perforated plate. When the number of the holes was fewer than 17, the bubble size increased with increasing gas chamber volume, but the effect of the gas chamber volume disappeared when the number of holes was greater than 17.

2.5 Gas Holdup Models

Various gas holdup correlations and models are found in the literature. They may be classified into two broad categories, empirical ones which are based on experimental data (Akita and Yoshida, 1973; Gestrich and Rahse, 1975; Hikita et al., 1980; Sotelo et al., 1994; Jordan and Schumpe, 2001) and those having a theoretical or semi-theoretical basis, e.g., the correlations based on the slip velocity concept (Inga and Morsi, 1999; Sarrafi et al., 1999; Ruzicka et al., 2001a). A large scatter is obtained by using these correlations. Possible reasons for the scatter include the range of operating conditions and applicability, reactor geometry (size of the reactor and gas distribution plate), and liquid properties. Also, the presence of trace impurities may change the coalescing behavior of the liquid (Krishna et al., 1999a).

For some operating conditions, under which no maximum gas holdup is observed, the gas holdup is expressed by

$$\varepsilon = kU_g^n \tag{2.12}$$

where k is constant and the exponent n depends on the flow regime. For homogeneous flow, n varies from 0.7 to 1.2, and for the heterogeneous flow, n varies from 0.4-0.7 (Shah et al., 1982).

In the homogeneous flow regime, the slip velocity concept is used to predict gas holdup (Shah and Deckwer, 1983; Zahradnik et al., 1997). The slip velocity U_s is defined for semi-batch flow to be

$$U_s = \frac{U_g}{\varepsilon} \tag{2.13}$$

Under homogeneous flow conditions, U_s is assumed to be independent of U_g and it is only a function of the terminal bubble rise velocity U_∞ and gas holdup, and is represented by

$$U_s = U_\infty \varphi(\varepsilon) \tag{2.14}$$

In general, the slip velocity is smaller than the terminal bubble rise velocity due to the hindrance effect by neighboring bubbles; this effect increases with an increase in gas holdup (Shnip et al., 1992). Several functional forms of $\varphi(\varepsilon)$ are available in the literature and are summarized by many researchers (Shah et al., 1982; Zahradnik et al., 1997; Sarrafi et al., 1999); they are generally expressed as

$$\varphi(\varepsilon) = (1-\varepsilon)^{n-1} \tag{2.15}$$

In the heterogeneous flow regime, the drift flux analysis has been recommended by many investigators to estimate gas holdup (Saxena et al., 1991; Thorat et al., 1998; Zahradnik et al., 1999) due to its simplicity.

According to different features of various flow regimes (homogeneous, transitional, and heterogeneous), Ruzicka et al. (2001a) developed a gas holdup model for each flow regime in a semi-batch bubble column. Homogeneous flow was characterized by a finite amount of liquid that was carried along with the rising bubbles, and then recirculated which caused a hindrance to bubble rise. The recirculating liquid velocity was calculated by assuming the net liquid flux was zero. Thus, the actual bubble rise velocity (i.e., the slip velocity in a stagnant liquid) was obtained by

$$v_g = U_\infty - v \tag{2.16}$$

Where v_g is the actual gas velocity (or mean bubble slip velocity with zero net liquid flux), U_∞ is the terminal bubble rise velocity, and v is the liquid velocity given by

$$v = \frac{aU_g}{(1-(1+a)\varepsilon)} \tag{2.17}$$

where a is the bubble drift coefficient, representing the ratio of liquid volume carried by the bubble to the bubble volume (i.e., the strength of the coupling between the gas and liquid phases) and accounts for information about the liquid velocity field, boundaries, bubble arrangement, and interactions. Both a and U_∞ were extracted from experiment data by Ruzicka et al. (2001a). Combining Eqs. (2.16), (2.17), and $U_g = v_g\varepsilon$ and linearizing, a bubble slip velocity was obtained:

$$v_g = \frac{U_g}{\varepsilon} = U_\infty - aU_\infty\left(\frac{\varepsilon}{1-\varepsilon}\right) \tag{2.18}$$

In the heterogeneous flow regime, Ruzicka et al. (2001a) believed that the bubble drove upward liquid movement, which enhanced bubble rise velocity, and liquid velocity was nearly proportional to the superficial gas velocity (i.e., $v = C_o U_g$). Thus, the slip velocity was given by

$$v_g = \frac{U_g}{\varepsilon} = U_\infty + C_o U_g \tag{2.19}$$

Equation (2.19) has the same form as that of the Zuber and Findlay drift flux model. They also considered the slip velocity model in the transitional flow regime based on the fact that both homogeneous and heterogeneous flow regimes coexist in the column. The model of Ruzicka et al. (2001a) agreed well with other models.

2.6 Literature Survey Summary

Gas holdup and flow regime are influenced by bubble column diameter, gas distributor plate design, and liquid properties in gas-liquid systems. In general, larger bubble column diameters tend to reduce gas holdup and enhance flow regime transition. Increasing hole diameter in a perforated plate gas distributor leads to a decrease in gas holdup and promotes flow regime transition. In a certain range, aeration plate open area enhances gas holdup and delays flow regime transition. Both increase in liquid surface tension and viscosity promotes bubble coalescence and suppresses bubble breakup, leading to a reduction in gas holdup and enhancement of flow regime transition. Thus, any operation that changes the liquid properties affects gas holdup and flow regime transition.

The addition of solid particles to air-liquid systems results in a decreases in gas holdup due to an increase in effective viscosity. The addition of a fibrous solid increases the

effective slurry viscosity, but even more so, leads to a very complex suspension rheology. Flocculation and yield stress occur in fiber suspensions, which have significant effects on bubble behavior and gas holdup. Fiber type, mass fraction, length, flexibility, and fiber shape control fiber suspension rheology, which influences gas holdup behavior and flow regimes in fiber suspensions.

Therefore, it is important to examine the factors influencing gas holdup and flow regime in gas-liquid systems and the influence fiber addition has on those factors. The available literature on bubble coalescence and breakup and bubble behavior in fiber suspensions, as well as fiber suspension characteristics, provide insight into how gas holdup and flow regime may be influenced by fiber addition.

The drift flux model has been successfully applied to both gas-liquid and gas-liquid-solid systems. It is worth examining its application to gas-liquid-fiber systems and determining if it can be extended and/or modified to describe gas holdup in these complex systems.

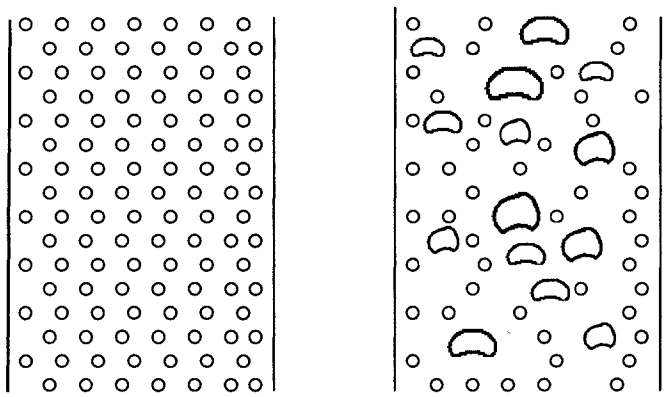

(a) Homogeneous regime (b) Heterogeneous regime

Figure 2.1: Schematic of features in the homogeneous (a) and heterogeneous (b) regimes.

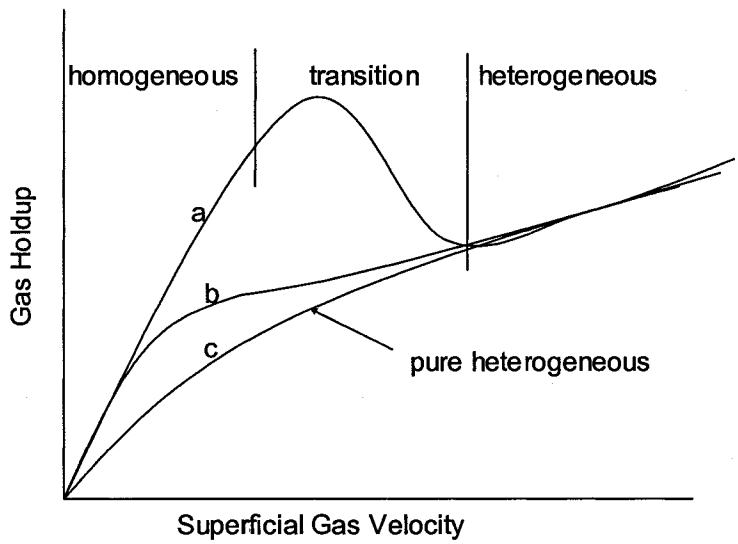

Figure 2.2: Schematic of the gas holdup behavior in the homogeneous, transitional, and heterogeneous flow regimes and the pure heterogeneous flow regime.

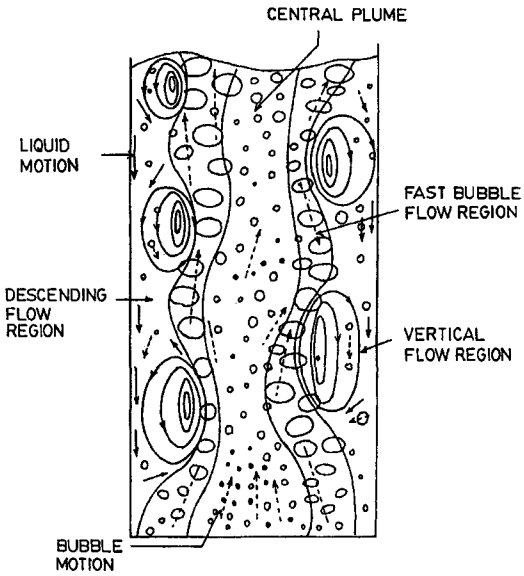

Figure 2.3: Four flow regions observed by Tzeng et al. (1993) in a two-dimensional bubble column.

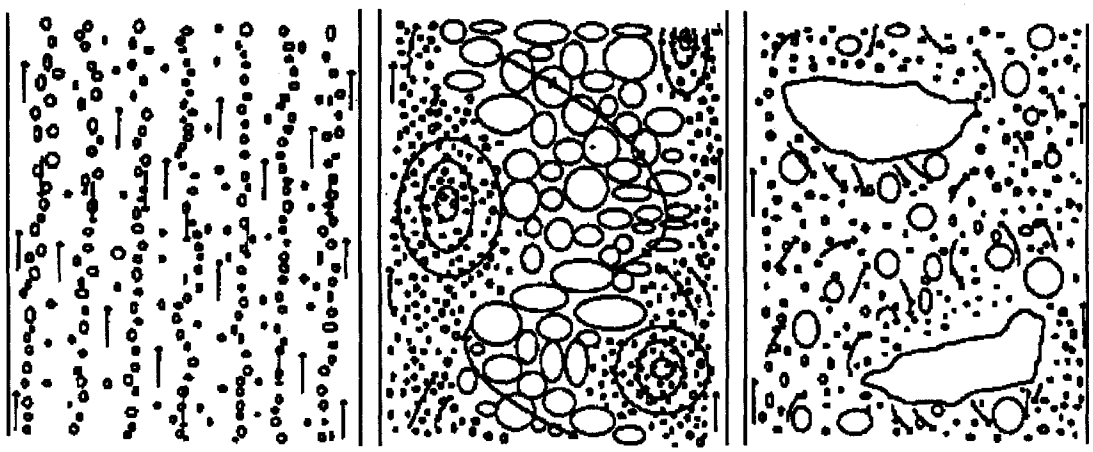

Dispersed bubble regime Vortical-spiral flow regime Turbulent flow regime

Figure 2.4: Flow regimes in a 3-D bubble column and gas-liquid-solid fluidization system (Chen et al., 1994).

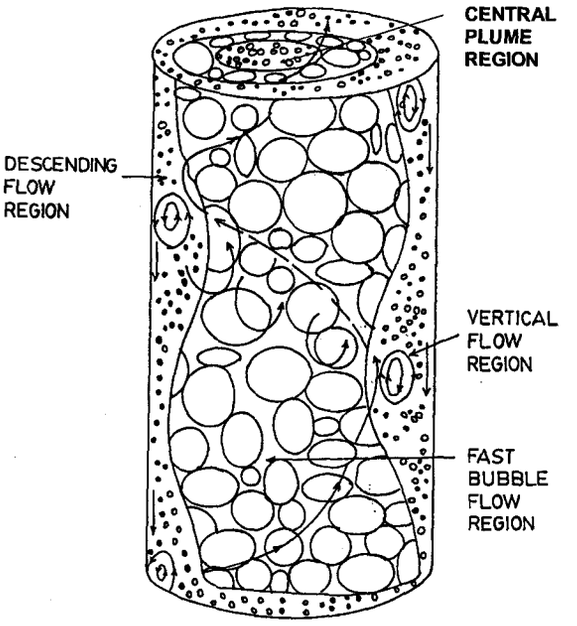

Figure 2.5: Flow patterns observed by Chen et al. (1994) in a three-dimensional bubble column.

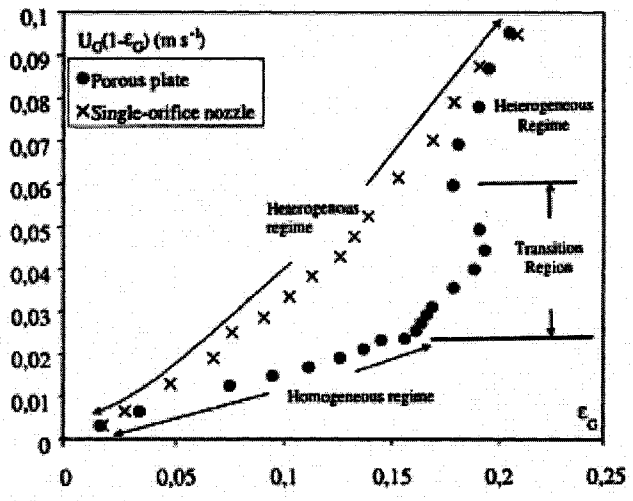

(a) Wallis (1969) drift flux model

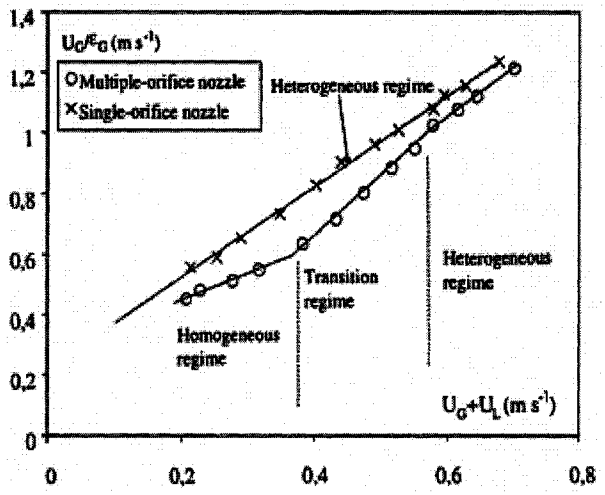

(b) Zuber-Findlay drift flux model

Figure 2.6: Demarcation of regime transitions with the drift flux models (air-water system); (a) Wallis (1969) drift flux plot, (b) Zuber-Findlay drift flux model (both figures are from Vial et al., 2000).

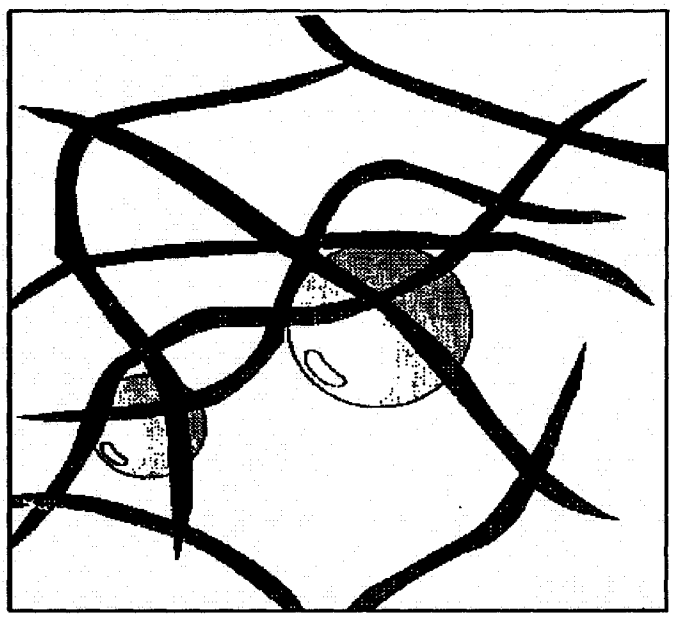

Figure 2.7: Illustration of bubbles physically trapped in a fiber network (Pelton and Piette, 1992).

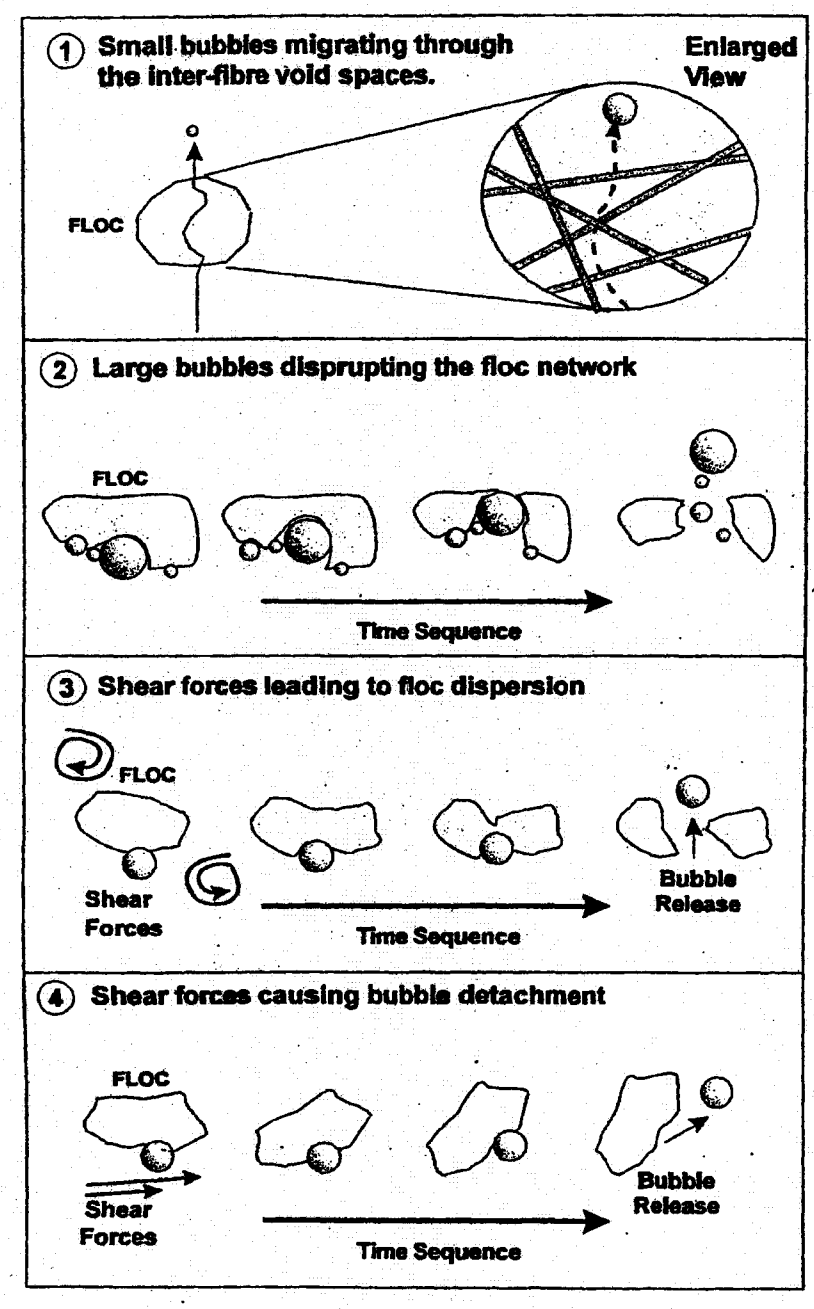

Figure 2.8: Mechanisms by which bubble escape from fiber flocs. Escape mechanisms (1) and (2) may occur in both quiescent and flowing fiber suspensions, while escape mechanisms (3) and (4) only occur in flowing fiber suspensions (Ajersch and Pelton, 1999).

CHAPTER 3: EXPERIMENTAL METHODS

This chapter provides a detailed description of experimental set up, experimental conditions, and procedures used for recording gas holdup.

3.1 Experiment Equipment

The bubble column experimental facility used in this study is schematically and pictorially represented in Figure 3.1. The bubble column consists of four 1-m sections of 15.24 cm ID cast acrylic, yielding a total column height of 4 m. Gas is injected at the base of the column through one of three stainless steel perforated plates. A gas plenum is located below the aeration plate and filled with glass beads to promote uniform gas distribution into the test facility. Three mass flow meters are used to measure the gas flow rate to encompass a low, medium, and high gas flow rate range. Three pressure transducers are installed along the column, one located at the column base, one at H = 1 m, and one at H = 2 m, where H is the column height from the aeration plate. The mass flow meters and pressure transducers are interfaced to a data acquisition system. Average gas flow rate and pressures are recorded from 4000 individual readings sampled at a frequency of 200 Hz.

Three perforated aeration plates with different open areas (A = 0.57%, 0.99%, and 2.14%), and shown in Figure 3.2, are used to introduce gas into the bubble column. The active plate area with a diameter equal to the column diameter (D = 15.24 cm) was used in calculating the open area ratio A. For each plate, 1-mm diameter holes are uniformly distributed over the entire plate, and the change in open area is produced by changing the

number of holes. The hole pattern is such that all holes are approximately equidistant from adjacent holes. This is accomplished using a MATLAB program that equated the radial hole pitch with the azimuthal hole pitch. Additional design criteria included open areas as close as possible to 0.5%, 1%, and 2% and aeration holes spanning the column diameter. Hence, the change in open area is produced by changing the number of uniformly distributed holes.

3.2 Experimental Conditions

The gas-liquid-fiber system used in this study is composed of air, water, and fiber. Synthetic fibers are used in this study and their types and nominal fiber lengths are shown in Table 3.1. Nylon powder with a diameter between 105 and 180 microns is also used to compare the results of Nylon fibers. For each type of fiber, various fiber mass fractions ($0 \leq C \leq 1.8\%$) and superficial gas velocities ($U_g \leq 18$ cm/s) are investigated. The superficial liquid velocity in this study is held constant at zero.

Table 3.1: Fiber types used in the gas-liquid-fiber bubble column.

Solid type	Fiber length (mm)	Fiber (particle) diameter (μm)	Aspect ratio (-)	Specific gravity (-)
Rayon fiber	0.38	20.6	18.4	1.5
	1	20.6	48.5	1.5
	3	20.6	145	1.5
	6	20.6	290	1.5
	12	20.6	580	1.5
Nylon fiber	2	27	74	1.14
	3	27	110	1.14
	6	27	220	1.14
Nylon Powder	NA	105~180	NA	1.14

3.3 Data Acquisition

A data acquisition system, based on LabVIEW data acquisition software, is used to collect the data from the gas flow meters and pressure transducers. The gas holdup (ε) is determined in the upper column section ($1 \leq H \leq 2$ m), where it is assumed bubble behavior is not influenced by the distributor region (near the column base). The gas holdup is calculated from the column pressure drop. It is assumed that fiber is uniformly distributed in bubble column and air density is negligible. Also, in a semi-batch system, the frictional pressure drop is negligible. Thus, the total pressure drop corresponds to the hydrostatic head; in this case,

$$\varepsilon = 1 - \frac{\Delta P}{\Delta P_o} \tag{3.1}$$

where ΔP is the difference between the average local pressure at any two pressure transducers with $U_g > 0$, and ΔP_o is the corresponding average value with $U_g = 0$. For the GL system, ΔP_o equals the liquid hydrostatic head; for the GLF system, ΔP_o corresponds to the fiber slurry hydrostatic head.

Experiments are performed at specified fiber mass fractions (C), where the actual fiber mass added to the system is determined from

$$M_f = CM_t \tag{3.2}$$

The total mass of the fiber-water mixture M_t is determined from $M_t = \rho_{eff} V$, where ρ_{eff} is the effective slurry density determined from

$$\frac{1}{\rho_{eff}} = \frac{C}{\rho_f} + \frac{1-C}{\rho_w} \tag{3.3}$$

and the moisture-free Rayon and Nylon fiber density is ρ_f = 1500 kg/m^3 and 1140 kg/m^3, respectively, and V is the volume of the fiber-water mixture.

Before an experiment is initiated, the dry fiber mass calculated from Eq. (3.2) is soaked in tap water for 2-3 days, and during this period, the fiber is washed with fresh water for 2-3 times to remove any residual contaminants and additives absorbed on the fiber surface. The soaked and washed fiber is then added to a small container of water and mixed at low speed using an electronic mixer equipped with a propeller blade. The resulting mixture is then added to the bubble column which is partially filled with water. Additional water is added to fill the column to a height of 2.13 m (14 column diameters). All experiments are initiated with this slurry volume. The column is then operated at a high gas flow rate for approximately 35 minutes to ensure the slurry was well mixed throughout the column. The gas flow rate is then reduced to the lowest value of interest to begin data collection and then incremented sequentially for additional data points. Note that data are collected approximately 15 minutes after each gas flow rate adjustment. The gas used in all experiments is filtered compressed air.

Although fiber settling did occur with no air injection, the mixing caused by air injection is generally sufficient to maintain a well mixed system when $C \lesssim 0.4\%$. At higher fiber mass fractions, some bulk fiber settling is observed, but only at the lowest superficial gas velocities, and once the air injection produces sufficient mixing, the fiber slurry is uniformly dispersed throughout the bubble column.

The percent uncertainty in the superficial gas velocity measurements is estimated to be ±2~4% of the reading, and the absolute uncertainty in the gas holdup is estimated to be $\Delta\varepsilon$ = ±0.006~0.008.

3.4 Additional Data

Additional data obtained by other researchers in our group are also used in this study. Gas holdup in cellulose (softwood, hardwood, BCTMP (bleached Chemithermomechanical Pulp) fiber suspensions was determined by Ann Stardt through a Professional Women in Science and Engineering (PWSE) internship. Relevant characteristics of the cellulose fiber are provided in Table 3.2.

Data of cellulose fiber suspensions are also used in the following analysis that were acquired in a 32.1 cm semi-batch bubble column. A detailed assessment of these data was provided by Hol (2005).

Table 3.2: Cellulose fiber properties.

Properties \ Fiber type	Hardwood	Softwood	BCTMP (Bleached Chemithermomechanical Pulp)
Wood species	Eucalyptus	65-75% Northern Black Spruce, 20-25% Jackpine, 5-10% Balsam Fir	Softwood (northern pine)
Length – PAFL (mm)	0.69	1.2	0.8
Length – LWAFL (mm)	0.78	2.31	1.91
Coarseness (mg/100m)	6.9	13.08	29.5
Number of fibers per gram (millions)	21.4	6.37	4.25

PAFL - particle average fiber length
LWAFL – length weighted average fiber length

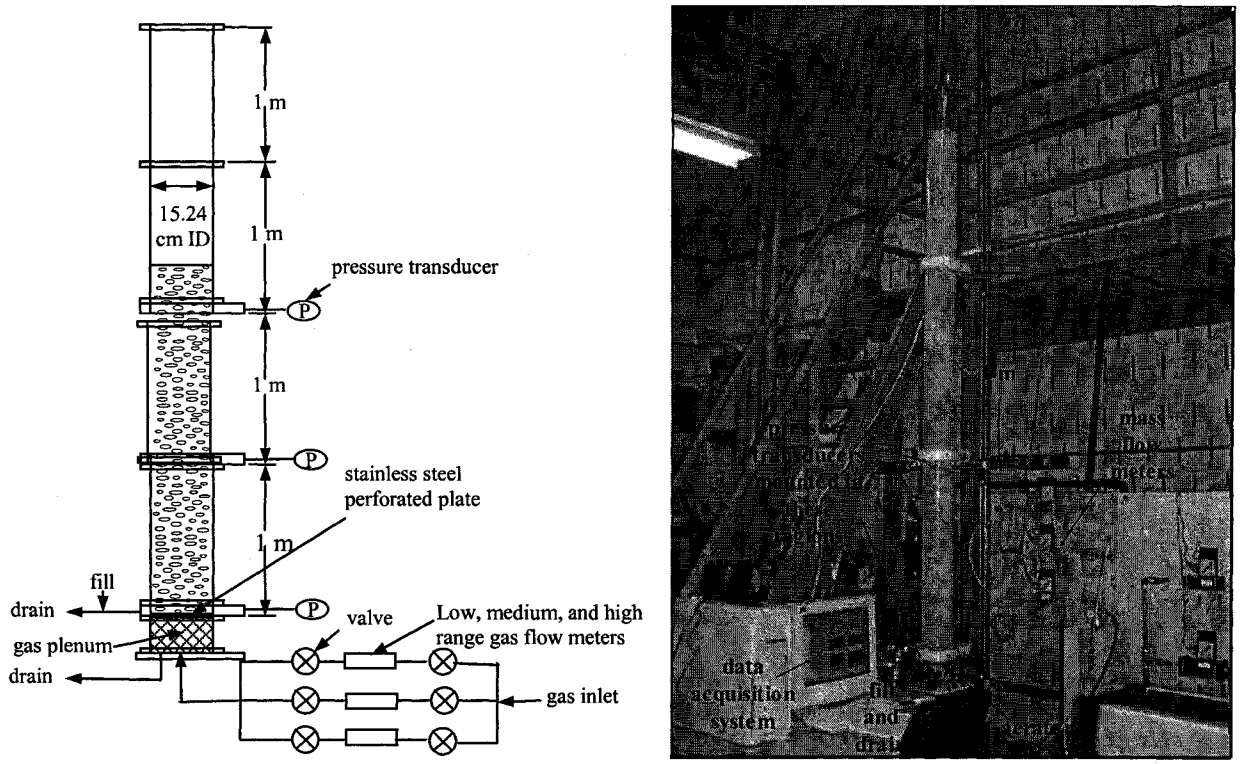

Figure 3.1: Experimental bubble column.

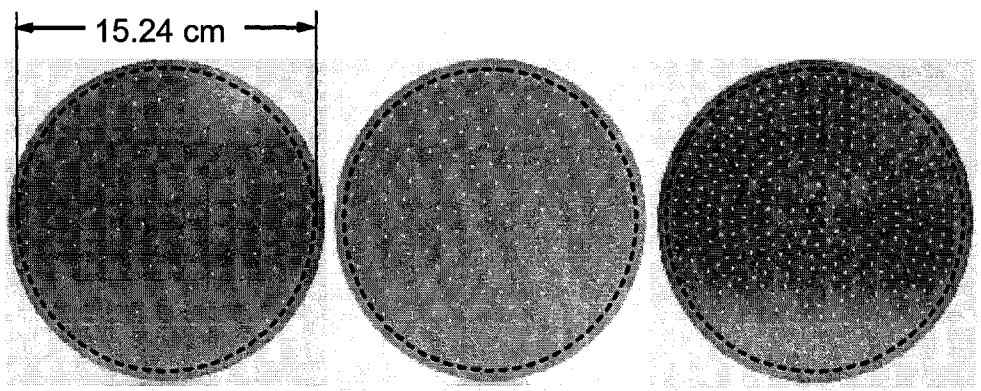

Figure 3.2: Aeration plates used in this study; (a) A = 0.57%, (b) A = 0.99%, and (c) A = 2.14%.

CHAPTER 4: RESULTS AND DISCUSSION

This Chapter is divided into five parts. The first section investigates the effects of superficial gas velocity, fiber mass fraction, and fiber length on gas holdup and flow regime transition by employing Rayon fiber with fiber lengths of 3, 6, and 12 mm and a single aeration plate with A = 0.57%. The effects of aeration plate on gas holdup and flow regime transitions are studied in the second section by using three open area ratios (A = 0.57%, 0.99%, and 2.14%) and three Rayon fiber lengths (3, 6, and 12 mm). The third section studies the effect of Nylon fiber on gas holdup with fiber lengths of 2, 3, and 6 mm and an aeration plate with A = 0.57%. The fourth section discusses the effect of fiber addition with short Rayon fiber (L = 0.38 and 1 mm), and thus small aspect ratio fiber, to approximate Rayon particle systems. The last section studies the effect of bubble column diameter on gas holdup in cellulose fiber (softwood and BCTMP) suspensions.

4.1 Gas Holdup in Rayon Fiber Suspensions

This study employs Rayon fibers as the solid phase to examine the effects of fiber mass fraction and length on gas holdup and flow regime transition in a 15.24 cm semi-batch GLF bubble column. The results and discussion are based on the aeration plate with A = 0.57%. Data are presented for three different Rayon fiber lengths (3, 6, and 12 mm), over a range of superficial gas velocities ($U_g \leq 18$ cm/s), and a range of fiber mass fractions ($0 \leq C \leq 1.8\%$). Results from this study have been presented in Su and Heindel (2003).

4.1.1 Gas Holdup

4.1.1.1 Air-Water

Baseline gas holdup measurements were completed in a fiber-free (air-water) system. As shown in Figure 4.1, a pronounced local maximum gas holdup is observed indicating the homogeneous, transitional, and heterogeneous flow regimes are observed over a range of gas velocity. When the superficial gas velocity is low, bubbles disperse uniformly in the bubble column and no bubble collisions occur. The bubble size is small and uniform, resulting in uniform bubble rise velocities; as a result, no bubble coalescence occurs. The gas holdup initially increases linearly with increasing superficial gas velocity. These are typical characteristics of the homogeneous regime.

As the superficial gas velocity increases further, bubbles begin to move laterally and a serpentine flow pattern is observed. The bubbles also rise in groups but do not coalesce. This flow has been characterized as vortical flow (Tzeng et al., 1993; Chen et al., 1994; Heindel, 2000). The serpentine flow pattern becomes more evident and bubbles begin to coalesce as the superficial gas velocity increases, indicating the onset of the transitional flow regime. Gas holdup continues to increase to a maximum value but becomes a nonlinear function of superficial gas velocity.

As the superficial gas velocity increases further, a net decrease in gas holdup is recorded. Two competing effects influence this decrease: (i) bubble coalescence increases due to a wider range of bubble rise velocities, caused by a wider bubble size distribution with increasing superficial gas velocity (De Swart et al., 1996; Heindel, 2002), and (ii) bubble

breakup is enhanced because larger bubbles increase turbulence, leading to bubble breakup. The drop in gas holdup implies that bubble coalescence is dominant in this regime. With superficial gas velocity continuing to increase, gas holdup begins to increase after undergoing a local minimum value, which indicates the flow regime enters the heterogeneous flow regime, also called churn-turbulent flow.

4.1.1.2 Effect of Fiber Mass Fraction

When a low mass fraction of fiber ($C \leq 0.4\%$) is added to the bubble column, the bubble column hydrodynamics are visually similar with those of $C = 0\%$. As can be seen from Figure 4.1 for a fiber length of $L = 3$ mm, the gas holdup results for $C \leq 0.4\%$ follow similar trends to those of $C = 0\%$, which implies that the flow regimes are equivalent (i.e., homogeneous, transition, and heterogeneous). For $C = 0.10\%$, it is observed that all three fiber lengths disperse uniformly in the bubble column. At $C = 0.25\%$, equi-size flocs and a heterogeneous fiber distribution are observed throughout the column for the fiber lengths of $L = 6$ and 12 mm. Flocculation is observed for $L = 3$ mm fibers at $C = 0.4\%$. These observations are similar to those of Went et al. (1993), Lindsay et al. (1995), and Reese et al. (1996) who recorded fiber flocculation at $C \approx 0.3\%$.

Fiber-fiber interaction changes between $C = 0.4\%$ and 0.6%. When the fiber fraction is greater than $C = 0.6\%$, distinct fiber networks are formed. The homogeneous flow regime is not observed, even at very low superficial gas velocities, and the flow regime is categorized as heterogeneous for all superficial gas velocities; Ruzicka et al. (2001) classified this regime

as pure heterogeneous flow. This trend was also observed by Went et al. (1993) who showed that a high cellulose fiber mass fraction led to a continuous heterogeneous regime.

When $C \geq 0.6\%$, the slurry phase recirculation is suppressed, this was also reported by Lindsay et al. (1995) and Heindel (2000, 2002), and is attributed to a decreased level of turbulence resulting from an increased slurry viscosity. This change in slurry flow characteristics results in fiber settling when $Ug \leq 0.9$ cm/s, causing a locally higher fiber mass fraction in the lower column region than in the upper column region. The fiber mass fraction at which fiber settling is observed is influenced by fiber length and decreases with increasing fiber length. This fiber mass fraction is, respectively, $C = 1.0$, 0.8, and 0.6%, corresponding to $L = 3$, 6, and 12 mm. The locally high fiber mass fractions in the lower column region result in channel formation, which dissipates when the superficial gas velocity increases beyond a certain value when $C \leq 1.0\%$, but exists through the entire range of superficial gas velocities when $C \geq 1.4\%$. Channeling increases bubble coalescence and results in large bubbles even at low superficial gas velocities.

It can be observed from Figure 4.1 that the gas holdup decreases with increasing fiber mass fraction. This trend has been observed by Went et al. (1993), Lindsay et al. (1995), and Janse et al. (1999) in GLF bubble columns. This decrease in gas holdup is characterized by a larger bubble size due to the increasing fiber mass fraction, which leads to faster bubble rise velocities and smaller bubble residence times. Increase in bubble size with the increasing fiber mass fraction has been observed by Reese et al. (1996) and Heindel (1999, 2002) in GLF systems. The larger bubble size can be ascribed to either an increase in the bubble

coalescence rate during bubble formation and growth stages or a decrease in the bubble break-up rate (Gandhi, 1999).

Prince and Blanch (1990) pointed out that bubble coalescence is the result of bubble collision, which is partially due to the difference in rise velocities of different size bubbles. The bubble collision rate and subsequent bubble coalescence can be enhanced by a wide range of bubble rise velocities resulting from a broad bubble size distribution. Broad bubble size distributions with increasing slurry concentrations have been confirmed by De Swart et al. (1996). Furthermore, in fibrous systems, the effect of fiber addition on bubble coalescence is also significant. Pelton and Piette (1992), Lindsay et al. (1995), and Heindel (1999, 2000) have observed that fibers tend to retard bubble ascension; small bubbles are trapped in the fiber network and coalesce with others to form larger bubbles, until the buoyant force is strong enough to break through the fiber network. Increasing the fiber mass fraction also results in higher yield stress of the fiber network (Bennington et al., 1995), implying a higher buoyant force is needed to disrupt the fiber network, which leads to a larger bubble size, and a drop in gas holdup. Lindsay et al. (1995) also reported that a high fiber mass fraction results in channeling which reduced the gas flow area, and thus increased the bubble rise velocity leading to enhanced bubble coalescence and formation of large bubbles. Finally, increasing the fiber mass fraction may also lead to a reduction in the bubble break-up rate. Bubble break-up is linked to bubble interaction with turbulent eddies that are of equivalent size to, or slightly smaller than, the bubble size (Prince and Blanch, 1990). For a given superficial gas velocity, the addition of fibers will suppress the turbulent intensity due to the increase in effective suspension viscosity. As a result, the turbulent eddies are small and

cannot provide enough energy to support bubble breakup, which leads to a significant decrease in the bubble break-up rate. Therefore, it can be summarized that the gas holdup decrease with increasing fiber mass fraction can be attributed to an increase in the bubble coalescence rate and/or a decrease in the bubble break-up rate.

As shown in Figure 4.2, the rate of decrease in gas holdup with increasing fiber mass fraction depends on fiber mass fraction. This trend is more noticeable at intermediate superficial gas velocities (U_g = 5 and 10 cm/s). For L = 3 mm fiber, when C ≥ 1.4%, no significant gas holdup decrease is observed. This phenomenon indicates that gas holdup is more sensitive at a relatively low fiber mass fraction than a relatively high mass fraction. The possible reason for the negligible influence at high fiber mass fraction on gas holdup is that although the nominal fiber mass fraction increases, the change in fiber mass fraction in the upper column region, where gas holdup is measured, is small, because of fiber settling and channeling at the high mass fraction.

Figure 4.2 also shows that the influence of fiber mass fraction on the rate of gas holdup reduction depends on the superficial gas velocity. There is a significant drop in gas holdup with an increase in relatively low fiber mass fractions at intermediate superficial gas velocities (U_g = 5 and 10 cm/s), and just a slight decrease at both low and high superficial gas velocities (U_g = 1 and 15 cm/s). It can be observed from Figure 4.1 that U_g = 15 cm/s is clearly heterogeneous for all fiber mass fractions, and U_g = 5 and 10 cm/s are in or near the transition flow regime at low fiber mass fractions, suggesting this regime is more sensitive to fiber addition.

4.1.1.3 Effect of Fiber Length

Figure 4.3 displays gas holdup as a function of fiber mass fraction for three different superficial gas velocities for the three fiber lengths addressed in this section. At low fiber mass fraction, longer fiber produces a steeper drop in gas holdup with increasing mass fraction. When the fiber mass fraction is greater than a specified value (i.e., C = 0.8, 1.2, and 1.4% corresponding to L = 12, 6, and 3 mm, respectively), gas holdup becomes nearly independent of fiber mass fraction. This trend may be influenced by the small change in actual fiber mass fraction in the upper column region, where gas holdup is measured, with increasing nominal fiber mass fraction because of fiber settling and channel formation in the lower column region. Different fiber lengths lead to different fiber mass fractions at which fiber begins to settle. Also, at a high fiber mass fraction, fibers tend to trap bubbles and retard bubble rise, both of which would increase gas holdup. This increase in gas holdup compensates for the decrease in gas holdup due to fiber addition.

Figure 4.3 also shows that the fiber length effect on gas holdup is a function of fiber mass fraction. The fiber length effects are more pronounced at lower fiber mass fractions and this influence decreases with increasing fiber mass fraction. When $C \geq 1.4\%$, fiber length has a negligible effect on gas holdup.

4.1.2 Flow Regime Transition

4.1.2.1 Flow Regime Identification

The drift flux model proposed by Zuber and Findlay (1965) was used to determine the superficial gas velocity at which flow regime transition occurs. The Zuber-Findlay drift flux

model has been assumed to be applicable in GL bubble columns. It has also been successfully applied to GLS systems by Gandhi et al. (1999). For a semi-batch bubble column, the drift flux model expressed in Eq. (2.1) is rewritten as:

$$\frac{U_g}{\varepsilon} = C_o U_g + V_{oj} \tag{4.1}$$

The drift flux model is applicable to heterogeneous flow conditions and has been used to identify the flow regime by plotting $\frac{U_g}{\varepsilon}$ as a function of U_g (Zahradnik et al., 1997). Using this method, two mass fractions (C = 0.25% and 0.6%), which represent two distinct flow characteristics, are selected to show how the analysis is completed (Figure 4.4). A similar analysis was completed for all other conditions. For C = 0.25%, the curve comprises four linear sections with different slopes. The first and last sections represent, respectively, the homogeneous and heterogeneous regime; because there is maximum gas holdup in the transitional flow regime, this regime is represented by two sections (the second and third sections). For C = 0.6%, the drift flux model fits the data well, indicating that only heterogeneous flow exists for all superficial gas velocities. This confirms that with increasing fiber mass fraction, the flow regime will undergo the change from three possible flow regimes (homogeneous, transition and heterogeneous) to pure heterogeneous flow. Figure 4.4 also suggests that the Zuber-Findlay drift flux model is applicable to GLF systems.

4.1.2.2 Effect of Fiber Mass Fraction and Length

Figure 4.5 shows the effects of fiber mass fraction and length on the superficial gas velocity beyond which the transition flow regime is observed. It is clear the transitional superficial gas velocity decreases with increasing fiber mass fraction; the critical fiber mass

fraction at which pure heterogeneous flow appears depends on fiber length, and is approximately 0.6%, 0.4% and 0.4% for L = 3, 6, and 12 mm, respectively. Figure 4.5 confirms that fiber addition will destabilize the homogeneous regime, where a relatively low mass fraction restricts the homogeneous flow regime to a narrow range of superficial gas velocities, and a high fiber mass fraction will completely suppress homogeneous flow. Figure 4.5 also shows that there is a slight decrease in the transitional superficial gas velocity with increasing fiber length; however, this difference depends on the fiber mass fraction. It is of interest to note that although the fiber length affects gas holdup, it has no significant effect on the observance of pure heterogeneous flow for long fibers (L = 6 and 12 mm); the critical fiber mass fraction at which pure heterogeneous flow is recorded is between 0.25% and 0.4% for both L = 6 and 12 mm. This suggests that for long fiber, the fiber mass fraction has more influence on bubble column hydrodynamics than fiber length, and the small effect of fiber length becomes negligible when $C \geq 0.4\%$.

4.1.3 Effect of Fiber Crowding Factor

The combined effect of fiber mass fraction and length on fiber flocs and network formation has been described in section 2.3.1.1 by a dimensionless number termed the crowding factor (N) (see Eq. (2.7)) (Kerekes and Schell, 1992). For Rayon fiber studied here, the fiber coarseness $\omega = 5\times10^{-7}$ kg/m.

The crowding factor is a useful tool for describing fiber flocculation regimes (Kerekes and Schell, 1992). Fibers tend to flocculate as N increasing. Therefore, it is hypothesized that N can also be used to describe gas flow characteristics in a fiber slurry; as the crowding factor increases, gas holdup tends to decrease and gas flow is more heterogeneous. For a

given fiber type, this hypothesis is applicable because, for N is only a function of fiber mass fraction (C). However, it is questionable when N is used for different fiber lengths. According to the hypothesis, the gas flow regimes for different fiber lengths should be equivalent at the same value of N; this, however, is not observed in our data. For example, when N = 72, the fiber mass fraction for L = 3 and 12 mm fibers is, respectively, 0.8% and 0.05%. The flow regime of the former is pure heterogeneous, but the hydrodynamic behavior of the latter is similar to the air-water system throughout the range of superficial gas velocities. This phenomenon may be attributed to the different effects of fiber length and mass fraction on the crowding factor and on gas flow behavior. From Eq. (2.7), N is dependent on L to the power 2 and C to the power 1, indicating fiber length has more influence on the crowding factor than mass fraction. The current study has demonstrated that gas flow behavior is more dependent on fiber mass fraction than on fiber length. Therefore, it can be concluded that although the crowding factor is a useful tool for describing fiber-fiber interaction, it is not appropriate to employ N to describe gas holdup behavior in fiber suspensions.

4.2 Effect of Gas Distributor Open Area on Gas Holdup

This study employed Rayon fibers as the solid phase to examine the effects of gas distributor open area ratio on gas holdup and flow regime transitions in a 15.24 cm, semi-batch GLF bubble column. For these studies, the aeration plate open area ratios are A = 0.57%, 0.99%, and 2.14%. Data are presented for three different Rayon fiber lengths (3, 6, and 12 mm) over a range of superficial gas velocities ($U_g \leq 18$ cm/s) and a range of fiber

mass fractions ($0 \leq C \leq 1.8\%$). Results from this phase of the thesis have been presented in Su and Heindel (2005)

4.2.1 Air-Water

The effect of aeration plate open area on gas holdup in an air-water system is shown in Figure 4.6 (open symbols). At low and high gas flow rates, where the corresponding flow regime is homogeneous and heterogeneous, respectively, the open area ratio has a negligible effect on gas holdup. This phenomenon agrees with the observations of Zahradnik et al. (1997) and Zahradnik and Kastanek (1979) who observed that gas holdup began to deviate among different open area ratio plates after a maximum value was recorded and then converged in the heterogeneous flow regime. In the heterogeneous flow regime, gas holdup is determined primarily by bulk liquid circulation, and is hardly affected by bubble formation modes (Zahradnik et al., 1997), leading to little gas holdup difference among the three plates in this regime. At medium gas flow rates, where the gas flow is in the transitional regime, gas holdup behavior deviates among the three plates. Gas holdup increases with increasing open area ratio from A = 0.57% to 0.99%; this agrees well with the results of Zahradnik et al. (1997), Ohki and Inou (1970), Tsuchiya and Nakanishi (1992), and Zahradnik and Kastanek (1979) in which A has a favorable effect on gas holdup. Note, however, that all of these studies were based on $A \leq 1\%$. When A is further increased to 2.14%, the gas holdup decreases dramatically. In the transitional flow regime for both A = 0.57% and 0.99%, gas holdup increases with increasing superficial gas velocity until a maximum gas holdup is reached, and then gas holdup decreases with increasing superficial gas velocity to a minimum value which indicates the end of the transitional flow regime. For A = 2.14%, no maximum

gas holdup is observed, and the gas holdup continuously increases with superficial gas velocity.

Combining the observations in this study and Zahradnik et al. (1997), Ohki and Inoue (1970), Tsuchiya and Nakanishi (1992), and Zahradnik and Kastanek (1979), we can conclude that the favorable effect of plate open area on gas holdup is valid only within a certain range ($A \lesssim 1\%$); when open area is beyond this range, gas holdup decreases. The following will provide possible explanations of the latter phenomenon.

For a given superficial gas velocity, the gas velocity through the aeration holes is reduced with increasing open area when the number of holes is increased with a constant hole diameter, leading to smaller bubble sizes (Miyahara et al., 1983b), lower bubble rise velocities, a lower degree of liquid circulation, and more bubbles, all of which result in a higher gas holdup and a delay in the flow regime transition. This causes gas holdup to be higher when $A = 0.99\%$ than when $A = 0.57\%$. However, further increasing open area beyond a critical value by increasing the number of holes with a constant hole diameter enhances bubble coalescence near the aeration plate due to a reduced hole spacing; this leads to a reduction in gas holdup. Solanki et al. (1992) proposed that coalescence of adjacent bubbles formed at closely spaced holes may occur and depends on three time factors: (i) time of bubble formation (t_f), (ii) time required for a bubble to grow to a diameter equal to the hole separation distance to begin bubble-bubble interaction (t_i), and (iii) time to drain the liquid film between bubbles to a critical thickness for rupture (t_s). For $t_f > t_i + t_s$, coalescence occurs. Smaller hole spacing leads to a smaller bubble size required for the occurrence of interaction with adjacent bubbles. Thus, provided the bubble growth rate is constant, smaller

hole spacing results in smaller t_i and $t_i + t_s$, which leads to a higher probability of bubble coalescence compared to a larger hole spacing. Enhanced bubble-bubble interaction with decreasing hole spacing was observed by Xie and Tan (2003). Additionally, when formed through holes, bubble diameter increases with increasing gas flow rate (Li, 1999); hence, the probability of bubble-bubble interaction increases with increasing gas flow rate. Therefore, when the superficial gas velocity is increased, the likelihood of bubble coalescence is higher for A = 2.14% than for A = 0.57% and 0.99%. As a result, the gas holdup for A = 2.14% is lower than that of A = 0.57% and 0.99%. This is not observed when A = 0.99% because the holes are not close enough to encourage bubble-bubble interaction.

A lower gas holdup for A = 2.14% when compared to A = 0.57% and 0.99% may also be ascribed to the fact that for A = 2.14%, the open area ratio is too large to produce a stable gas inlet for the range of superficial gas velocities addressed in this study. Zahradnik and Kastanek (1979) and Haug (1976) determined that when the plate pressure drop is less than a critical value, bubble formation is influenced by pressure fluctuations in the gas-liquid layer (i.e., bubbling bed), and the plate works in unstable operation. Unstable distributor operation leads to partial aeration, a non-uniform gas distribution, large scale liquid circulation, and an unstable flow pattern (Haug, 1976). The critical gas flow rate at which the plate works in stable operation is estimated by the Weber number, We. As suggested by Zahradnik and Kastanek (1979), stable plate operation occurs when

$$\mathrm{We} = \frac{v_o^2 d_o \rho_g}{\sigma} \geq 2 \tag{4.2}$$

where v_o is the aeration hole gas velocity, d_o is the aeration hole diameter, ρ_g is the gas density, and σ is the surface tension. To achieve the critical Weber number, a higher gas flow

rate is required for a larger open area. For example, if We = 2, d_o = 1 mm, ρ_g = 1.57 kg/m^3, and σ = 72.7 mNm^{-1}, the critical v_o is 9.62 m/s. Thus, the corresponding superficial gas velocities in our system are 5.4 cm/s, 9.4 cm/s, and 20.6 cm/s for A = 0.57%, 0.99%, and 2.14%, respectively. It is clear that the plate with A = 2.14% will not operate in stable operation for the entire superficial gas velocity range of this study, which may contribute to the lower gas holdup. The gas holdup of A = 0.99% is greater than that of A = 0.57% after U_g = 9.5 cm/s, verifying the importance of stable plate operation.

Hole spacing also changes with open area and this affects the bubble formation mode, thus influencing the inlet gas distribution and the resulting gas holdup and flow regime transition. In addition to bubble jetting, Ruzicka et al. (1999) and Xie and Tan (2003) identified two basic bubble formation modes for multi-hole aeration plates: (i) synchronous and (ii) asynchronous. The synchronous mode produces a uniform gas holdup profile and low liquid circulation. This is favorable for homogeneous flow regime in bubble column operations. In the asynchronous mode, bubble formation at adjacent holes is either out of phase, or they form at alternating holes. Some active holes tend to produce liquid circulation that makes the other holes passive, resulting in a non-uniform inlet gas distribution. This further enhances liquid circulation and leads to flow regime transition. They also observed that hole spacing plays an important role in the bubble formation modes. When the hole spacing is large, the synchronous mode occurs at gas flow rates below a critical value. When hole spacing is small, the close proximity prevents the gas flow through adjacent holes from being in phase and no synchronous mode is observed. The critical gas flow rate at which the transition from the synchronous to asynchronous mode occurs decreases with decreasing hole

spacing (i.e., increasing open area) (Ruzicka et al., 2000). Therefore, the critical gas flow rate for A = 2.14% is lower than that of A = 0.57% and 0.99%. It is possible that at the same superficial gas velocity, the tendency of the synchronous regime for A = 0.57% and 0.99% is higher than that of A = 2.14%. This would produce a more uniform gas distribution for A = 0.57% and 0.99% than 2.14%. Zahradnik and Kastanek (1978) demonstrated that a non-uniform gas distribution will induce liquid circulation and an unstable flow pattern; this results in enhanced bubble-bubble interaction and bubble coalescence, leading to a reduced gas holdup when compared to a uniform gas distribution at the same gas flow rate. From Figure 4.6, it is plausible that the aeration plates with A = 0.57% and 0.99% produce a more uniform inlet gas distribution than that from A = 2.14%.

Figure 4.6 also shows the flow regime transitions for A = 0.57%, 0.99%, and 2.14% by applying the Zuber-Findlay drift flux model (Zuber and Findlay, 1965) (solid symbols). In this model, U_g/ε represents the mean bubble rise velocity. All three plates produce homogeneous, transitional, and heterogeneous flow regimes. For the homogeneous flow regime, U_g/ε slightly decreases with increasing U_g and reaches a minimum value denoted as the critical superficial gas velocity at which transitional flow appears. Similar observations were obtained by Tsuchiya and Nakanishi (1992). The negative slope of the plot of U_g/ε vs. U_g in the homogeneous regime for all aeration plates may be the result of downward liquid flow between bubbles, compensating for the amount of liquid carried by the bubble wake to ensure conservation of mass (Chen et al., 1994). This downward liquid flow has a hindrance effect on the bubble rise velocity, leading to a bubble rise velocity less than the terminal rise

velocity. This reduction in bubble rise velocity increases with increasing gas holdup (i.e., increasing superficial gas velocity) (Shnip et al., 1992; Shen and Finch, 1996)).

When the superficial gas velocity is further increased, bubble-bubble interaction is enhanced, and bubble coalescence occurs, which indicates the flow regime transition. In the transitional flow regime, gross liquid circulation, increasing with increasing superficial gas velocity, changes the slope of U_g/ε vs. U_g to increase with increasing U_g.

The transitional superficial gas velocity, identified by the down arrows in Figure 4.6, is similar when A = 0.57% and 0.99%. This is because the two plates produce similar gas holdup results until a maximum gas holdup is reached for A = 0.57%. This observation indicates that increasing the open area ratio may increase the maximum gas holdup, but it may not delay the flow regime transition. The transitional superficial gas velocity is ~3.4 cm/s for A = 2.14%, which is less than ~5.7 cm/s for A = 0.57% and 0.99%. The lower superficial gas velocity at which transition occurs when A = 2.14% may be attributed to two affects. First, bubble coalescence is enhanced with closer hole spacing (large open area), and this induces liquid circulation and triggers flow regime transition. Second, a large open area (close hole spacing) results in a partially activated aeration plate (Ruzicka et al., 1999), leading to a non-uniform gas distribution and liquid circulation, promoting flow regime transition.

4.2.2 Fiber Suspensions

4.2.2.1 Effect of Fiber Mass Fraction

Typical trends of the effect of fiber mass fraction on gas holdup using the three different aeration plates (A = 0.57%, 0.99%, and 2.14%) are shown in Figure 4.7 for L = 3 mm Rayon fiber. For all three aeration plates, gas holdup decreases with increasing fiber mass fraction. This phenomenon is attributed to the promotion of bubble coalescence and/or reduction of bubble breakup due to the increase in the effective suspension viscosity with increasing fiber mass fraction, and the increasing large bubble sizes due to the increasing yield stress of the fiber suspension; this has been explained by in the section 4.1. The reduction in gas holdup with increasing fiber mass fraction is more pronounced at low fiber mass fractions. When fiber mass fraction is high ($C \geq 1.4\%$), fiber addition does not significantly affect gas holdup. The trends of gas holdup variation with fiber mass fraction of A = 0.57% and 0.99% are similar. At low fiber mass fractions ($C \leq 0.4\%$, Figure 4.7a,b), gas holdup behavior is similar to that of an air-water system: there is a maximum gas holdup, indicating homogeneous, transitional, and heterogeneous flow regimes exist over the range of superficial gas velocities. The effect of fiber mass fraction is more significant in the transitional flow regime, while little influence is observed in the homogeneous flow regime. At $C > 0.4\%$, gas holdup continuously increases with increasing superficial gas velocity and pure heterogeneous flow, as defined by (2001a), is observed.

For A = 2.14% (Figure 4.7c), gas holdup increases with increasing superficial gas velocity monotonically for all fiber mass fractions. At low fiber mass fractions ($C \leq 0.25\%$),

the homogeneous flow regime exists at low superficial gas velocities, and when C > 0.25%, pure heterogeneous flow appears over the range of superficial gas velocities. Similar to A = 0.57% and 0.99%, gas holdup is not influenced by fiber mass fraction in the homogeneous flow regime, whereas the transitional flow regime is affected by fiber addition. Similar trends are obtained for Rayon fiber with L = 6 mm and 12 mm for all three aeration plates.

4.2.2.2 Effect of Aeration Plate Open Area

Figure 4.8 depicts the effect of aeration plate open area on gas holdup in L = 3 mm Rayon fiber suspensions. At low superficial gas velocities ($U_g \leq 3$ cm/s), the open area ratio has a negligible effect on gas holdup. This phenomenon is similar to that of the air-water system. When $U_g > 3$ cm/s, the effect of aeration plate open area ratio on gas holdup is pronounced. At low fiber mass fractions (e.g., C = 0.1%), where homogeneous, transitional, and heterogeneous flow regimes exist, the aeration plate open area has a significant effect on gas holdup behavior in the transitional gas flow regime; a higher gas holdup is observed when A = 0.57% and 0.99% than that recorded with A = 2.14%. This was also observed in the air-water system (i.e., Figure 4.6). In the heterogeneous flow regime, open area influences gas holdup in fiber suspensions, which was not observed in the air-water system (see Figure 4.6). This may be due to the fact that for the air-water system, there is a significant amount of liquid turbulence at high superficial gas velocities, leading to a negligible effect of the aeration plate on bubble behavior. In contrast, fiber addition results in a decrease in turbulence intensity because the effective suspension viscosity increases with increasing fiber mass fraction, and the effect of bubble formation on gas holdup becomes important. The reasons that the aeration plate with A = 2.14% decreases the gas holdup in

fiber suspensions compared to that of A = 0.57% and 0.99% is ascribed to the same reasons as that of the air-water system.

The effect of aeration plate open area on gas holdup for A = 0.99% is influenced by fiber mass fraction. With increasing fiber mass fraction, the performance of A = 0.99% changes from that similar to A = 0.57% to that similar to A = 2.14%. At low fiber mass fraction (C = 0.1%), the gas holdup when A = 0.99% has similar behavior to that of the air-water system, i.e., it is higher than that of A = 0.57%. As the fiber mass fraction is further increased (C = 0.25%), the gas holdup of A = 0.99% drops faster than A = 0.57% and the two are very similar. At C = 0.60%, the gas holdup of A = 0.99% is lower than that of A = 0.57%, but almost the same as that of C = 2.14%. The larger decrease in gas holdup when A = 0.99% with increasing fiber mass fraction than that of A = 0.57% may be attributed to the increase in the bubble formation size with increasing fiber mass fraction; when the bubble formation size is large enough, adjacent bubbles near the aeration plate begin to coalesce, which is enhanced when A = 0.99% due to its smaller hole spacing compared to that A = 0.57%. This leads the performance of A = 0.99% to be closer to that of A = 2.14% with increasing fiber mass fraction.

Figure 4.8 also demonstrates that the effect of aeration plate open area is less significant with increasing fiber mass fraction when the fiber mass fraction is high. The difference of gas holdup of the three aeration plates disappears when the fiber mass fraction is $C \geq 1.2\%$. Similar trends are observed for L = 6 and 12 mm Rayon fiber. Consequently, the aeration plate open area has an effect on gas holdup in low fiber mass fraction suspensions, which

depend on the gas flow regime. However, in high fiber mass fraction suspensions, the aeration plate open area has a negligible effect on gas holdup.

It can be concluded that increasing aeration plate open area may enhance or reduce gas holdup in air-water and air-water-fiber systems, and the results are influenced by bubble formation size, hole diameter, superficial gas velocity, fiber mass fraction, and hole spacing. Increasing aeration plate open area tends to increase gas holdup when the hole spacing is large enough that a bubble formed at the inlet hole has no interaction with adjacent bubbles. Otherwise, increasing the open area tends to reduce gas holdup when bubble formation size is increased by either increasing hole diameter (Valencia et al., 2002), superficial gas velocity, or fiber mass fraction.

4.2.2.3 Effect of Fiber Length

The effect of fiber length on gas holdup behavior for the three open area ratios are shown in Figure 4.9. The trends of A = 0.57% and 0.99% are similar, and for low and medium fiber mass fractions, gas holdup decreases significantly when the fiber length is increased from L = 3 mm to L = 6 mm, but a negligible change is observed when the fiber length is further increased to L = 12 mm. In contrast, there is a negligible effect of fiber length on gas holdup when A = 2.14% at low fiber mass fractions (e.g., C = 0.1%). At medium fiber mass fractions (e.g., C = 0.8%), a decrease is observed between L = 3 mm and L = 6 mm which is similar to that of A = 0.57% and 0.99%.

In general, increasing fiber length tends to reduce gas holdup in fiber suspensions. However, for long fiber (e.g., L = 6 and 12 mm), the effect of fiber length on gas holdup is

not significant. This phenomenon is analogous to that of a viscous liquid. When liquid viscosity is high, a further increase in viscosity has little effect on gas holdup (Gandhi et al., 1999). This may be attributed to two competing effects: (i) bubble rise velocity of small bubbles is reduced in highly viscous liquids (Li and Prakash, 2000), leading to an increase in gas holdup; and (ii) bubble coalescence is enhanced, reducing gas holdup. In fiber suspensions, the longer the fiber, the larger the effective viscosity at the same fiber mass fraction. Therefore, long fiber suspensions tend to hinder bubble rise, and enhance bubble coalescence. In addition, the yield stress increases with fiber length (Bennington et al., 1990), which further reduces bubble rise velocity and traps more bubbles. These factors may be the reasons that gas holdup does not reduce significantly with increasing fiber length for long fibers.

Figure 4.9 also shows that at high fiber mass fractions (C = 1.4%), the three aeration plates produce similar gas holdup results for all three fiber lengths. To more clearly depict the effect of open area and fiber length at high fiber mass fractions, Figure 4.10 provides all results for C = 1.4%, which shows that when the fiber mass fraction is high, gas holdup has only a weak dependence on fiber length and aeration plate open area. It also implies that the gas holdup in a high fiber mass fraction suspension is mainly determined by slurry mixing.

4.2.2.4 Flow Regime Transition

Figure 4.11 shows the effect of fiber mass fraction, length, and open area on the superficial gas velocity at which transitional flow is observed for the three distributor plates. The superficial gas velocity at which transitional flow begins is determined by the Zuber-Findlay drift flux model (Zuber and Findlay, 1965) and shown by the arrows in Figure 4.6. In

general, fiber addition tends to destabilize the homogeneous flow regime, and when the fiber mass fraction is beyond a critical value, pure heterogeneous flow is observed over the entire range of superficial gas velocities. This phenomenon is ascribed to the increase in effective suspension viscosity with increasing fiber mass fraction. Zahradnik et al. (1997) have shown that the flow pattern will change from that of the existence of three flow regimes (homogeneous, transitional, and heterogeneous) to pure heterogeneous flow as the liquid viscosity increases. The fiber length has an effect on flow regime transition where the longer the fiber, the lower the superficial gas velocity at which transition begins. This effect is more significant when fiber length increases from 3 mm to 6 mm. There is not a pronounced difference between L = 6 and 12 mm in either the superficial gas velocity or the critical fiber mass fraction at which transitional flow begins. This is consistent with the trends shown in Figure 4.10 that the effect of fiber length on gas holdup is not significant when fiber length is increased from 6 mm to 12 mm for all three aeration plates.

It is apparent that in fiber suspensions, increasing aeration plate open area is not favorable to the homogeneous flow stabilization. The aeration plate with A = 2.14% obviously encourages the flow regime transition and the transitional superficial velocities for the three fiber lengths are lower than those of A = 0.57% and 0.99%. A = 0.99% produces very similar results to that of A = 0.57 for all three fiber lengths. The critical fiber mass fraction beyond which pure heterogeneous flow regime exists is also dependent on the aeration plate open area and decreases with increasing open area. When A = 0.57%, pure heterogeneous flow appears when $C \geq 0.6\%$, and the dependence of the critical fiber mass fraction on fiber length is negligible. For the other two plates, the critical fiber mass fraction

is affected by fiber length between L = 3 mm and 6 mm. A = 0.99% does not affect the critical fiber mass fraction for L = 3 mm and the homogeneous flow also can be observed when C < 0.6%. For L = 6 and 12 mm, the homogeneous flow exists when C < 0.4%. When A = 2.14%, the critical fiber mass fraction further decreases. For L = 3 mm, homogeneous flow is observed when C ≤ 0.25%, and for L = 6 and 12 mm, this critical value reduces to 0.16%.

4.3 Gas Holdup in Nylon Fiber Suspensions

This study employed Nylon fibers as the solid phase to examine the effects of fiber type, fiber mass fraction, and length on gas holdup and flow regime transition in a 15.24 cm, semi-batch GLF bubble column. The explanations for the gas holdup behavior in a Nylon fiber suspension are also provided. The distributor plate in this study has an open area ratio of 0.57%. Data are presented for three different Nylon fiber lengths (2, 3, and 6 mm) over a range of superficial gas velocities ($U_g \leq 18$ cm/s) and a range of fiber mass fractions ($0 \leq C \leq 1.8\%$). These data have been summarized in Su and Heindel (2004).

4.3.1 Effect of Nylon Fiber

4.3.1.1 Effect of Fiber Mass Fraction

The effect of fiber mass fraction on gas holdup with L = 6 mm is shown in Figure 4.12. Note that these data were taken on the same day that fiber was added to the bubble column. In Nylon fiber suspensions, the gas flow is in the pure heterogeneous regime for most fiber mass fractions (except C = 0.05%). Even at C = 0.05%, the gas holdup behavior deviates

from that of the air-water system, and no local maximum gas holdup behavior is observed over the entire range of superficial gas velocities. This behavior is different from Rayon fiber suspensions (see for example Figure 4.1 and section 4.1). Visual observations at C = 0.05% reveal that the flow conditions are not homogeneous and bubbles are not uniform in size, even when $U_g \leq 0.9$ cm/s. Under these conditions, two types of bubbles are observed: (i) relatively large ellipsoidal bubbles (~15 mm in diameter), and (ii) small spherical bubbles (~2 mm in diameter). At higher superficial gas velocities, large spherical-cap bubbles are also observed. Similar phenomena was observed by Philip et al. (1990) in highly viscous liquids. They suggested two mechanisms to explain the appearance of small spherical bubbles: (i) bubble coalescence occurred near the gas distributor plate, and during the coalescence process, smaller bubbles are generated by the breakup of the trailing bubble, and (ii) entrained small bubbles generated by the breakup of a large bubble at the liquid surface. Mechanism (i) contributes to the small bubble appearance when the gas flow rate is low. When the gas flow rate is high, the accumulation of small bubbles is attributed to both mechanisms. The presence of small spherical bubbles in a Nylon fiber suspension implies that even a small amount of Nylon fiber leads to suspension behaviors similar to highly viscous liquids. Tse et al. (2003) give another explanation of small bubble formation in that small bubbles may be generated by the coalescence-mediated breakup of bubbles, and state that this mechanism is very significant in systems that are coalescence-dominated. This mechanism could also contribute to the small bubbles observed in the heterogeneous gas flow regime found in the Nylon fiber suspensions of this study.

Experimental observations reveal that Nylon fibers tend to agglomerate with other fibers and bubbles. Visual observations made after shutting off the gas flow show that Nylon fibers form flocs which contain many small bubbles; these flocs float to the top of the column even though the fiber density is slightly greater than water. It is also observed that at very low superficial gas velocities, a single small bubble may rise with several fibers attached to it.

From the data shown in Figure 4.12, it is seen that gas holdup data taken on the first day fiber is added to the bubble column tends to decrease with increasing Nylon fiber mass fraction. The decrease in gas holdup is more pronounced at low fiber mass fractions ($C \leq 0.25\%$), and this effect diminishes when $C > 0.25\%$. These general fiber mass fraction trends qualitatively agree with those observed in Rayon fiber systems discussed in section 4.1, however, the influence of fiber mass fraction occurs up to $C = 1.2\%$ in a Rayon fiber suspension.

Similar trends are observed in Nylon fiber systems with $L = 3$ mm when the fiber is soaked for 3-5 days before experiments are initiated. When fiber is soaked for 2 weeks before it is added to the bubble column, different behavior is recorded and will be discussed below.

4.3.1.2 Effect of Fiber Length on Gas Holdup

Figure 4.13 shows the effect of Nylon fiber length on gas holdup, which reveals little influence. The gas holdup in shorter Nylon fiber suspensions ($L = 3$ mm) is no different from that of longer fiber suspensions ($L = 6$ mm) at all fiber mass fractions including low ($C = 0.05\%$) and high ($C = 1.6\%$) fiber mass fractions. These observations contradict those of section 4.1 and 4.2 where gas holdup decreases with increasing fiber length when $C \leq 1.4\%$

in Rayon fiber suspensions. The negligible dependence of gas holdup on Nylon fiber length may be because Nylon fiber is stiff leading to a small effect of fiber aspect ratio on suspension rheology.

4.3.2 Comparison of Gas Holdup with Rayon Fiber Suspension

Figure 4.14 compares gas holdup results in Nylon and Rayon fiber suspensions with L = 6 mm and various fiber mass fractions. At a low fiber mass fraction of C = 0.16%, gas holdup in the Nylon fiber suspension is much lower than that in the Rayon fiber suspension. Additionally, heterogeneous flow exists over the entire range of superficial gas velocities in the Nylon suspension; while three flow regimes (homogeneous, transitional, and heterogeneous) exist in the Rayon suspension. When C = 0.8%, only pure heterogeneous flow is observed for both the Nylon and Rayon suspension, but the gas holdup in the Nylon suspension is lower than that of the Rayon suspension. The gas holdup difference between Nylon and Rayon suspensions decreases with increasing fiber mass fraction, and at C = 1.8% (Figure 4.14c), there is negligible difference between the two systems.

The hydrophobic nature of the Nylon fiber surface is one possible mechanism to explain why the gas holdup in a Nylon fiber suspension is much lower than that in a Rayon fiber suspension at low fiber mass fractions. Many studies (Chen and Fan, 1989; Jamialahmadi and Muller-Steinhagen, 1991; Banisi et al., 1995a; Van der Zon et al., 2002) have been conducted on the effect of particle wettability on bubble behavior and gas holdup, and point out that gas holdup in a non-wettable particle slurry is lower than in a wettable particle slurry. They claim that an important characteristic observed for non-wettable particles is a high tendency for bubbles to attach to the particles, and the particles tend to form aggregates;

this is consistent with the phenomena observed in the Nylon fiber suspension of this study. In comparison, Rayon fiber disperses uniformly and individual fibers can be clearly seen when the gas is shut off. Also, no bubbles are observed on the Rayon fiber surface.

Studies have shown that particle wettability may also have a significant effect on the gas flow behavior in a slurry bubble column. Jamialahmadi and Muller-Steinhagen (1991) recorded that the addition of a small amount of non-wettable solids to an air-water system causes a considerable reduction in gas holdup. Lower gas holdup for hydrophobic particle systems was also observed by Van der Zon et al. (2002). The enhancement of bubble coalescence by hydrophobic particles is also known from antifoaming studies (Racz et al., 1996; Wang et al., 1999; Kluytmans et al., 2001) where hydrophobic particles tend to promote bubble coalescence by enhancing film rupture when two bubbles approach. In contrast, wettable particles tend to repel the gas interface, acting as a buffer between two adjacent gas bubbles and result in a decrease in bubble coalescence (Kluytmans et al., 2001). Chen and Fan (1989) also showed that non-wettable particles suppress bubble breakup. Both the promotion of bubble coalescence and the suppression of bubble breakup will considerably reduce gas holdup in systems with hydrophobic solids.

The degree of affinity the fiber has to water also has an impact on the fiber-fiber adhesive force. Chaouche and Koch (2001) showed adhesive force played an important role in the strength of fiber flocs, where a large force made the flocs easy to form and difficult to breakup. They also showed that the adhesive force of Nylon fiber in a glycerin/water mixture was ~20 times higher than in silicone oil and attributed this to the hydrophobicity of Nylon fiber. It can be postulated that the adhesive force among Nylon fibers is greater than Rayon

fiber because Nylon fiber has a lower affinity to water. This is supported by the fact that attempts to uniformly disperse small mass fractions of 12 mm long Nylon fiber in water were unsuccessful; after the suspension was agitated for a period of time through bubble-induced mixing, fiber bundles were formed. In contrast, 12 mm long Rayon fiber disperses easily in water (Su and Heindel, 2003). Larger adhesive forces among Nylon fibers also require a larger buoyant force to break through the fiber flocs, resulting in larger bubbles and a decrease in gas holdup.

The difference in gas holdup between Nylon and Rayon fiber suspensions may also be attributed to other fiber properties such as fiber flexibility that leads to different effective suspension viscosities, resulting in different gas flow behavior. Nylon fiber is less flexible than Rayon fiber (Bennington et al., 1995) and this tends to lower the Nylon suspension viscosity, leading to a higher gas holdup when compared to Rayon suspensions, which conflicts with the experimental results. This suggests that the effect of other factors, like Nylon fiber hydrophobicity, overshadow the effect of fiber flexibility.

4.3.3 Time-Dependent Gas Holdup in Nylon Fiber Suspensions

One important observation of the gas holdup behavior in Nylon fiber suspensions is that gas holdup varies with length of time the fiber is in the suspension. For example, four replicate experiments were completed with Nylon fiber L = 3 mm and C = 0.25% over a period of 84 hours after the fiber was added to the bubble column. Figure 4.15 clearly shows that the gas holdup varies with time and tends to increase with long-term system exposure. The first data set was taken 12 hours (t = 12 hours) after which the fiber was added to the bubble column. Large bubbles are observed even at very low superficial gas velocities ($U_g <$

0.9 cm/s), and the gas flow regime is pure heterogeneous. The gas holdup obtained at t = 36 and 60 hours is higher than that of t = 12 hours, but the bubbles have no visual difference than those of t = 12 hours. Heterogeneous flow is still observed over the entire range of superficial gas velocities. Also, no foam is observed for t = 12, 36, and 60 hours.

After t = 84 hours, the gas holdup increases and the bubbles are visually smaller than those of t < 84 hours with no large bubbles at low superficial gas velocities ($U_g \leq 2$ cm/s). Foam, which is not observed when t < 84 hours, appears at the top of fiber suspension surface. From Figure 4.15, a change in gas holdup trend is exhibited at t = 84 hours; this deviation is characteristic of three separate gas flow regimes (homogeneous, transitional, and heterogeneous flow).

The gas flow characteristics of Nylon fiber suspensions are not only affected by the experimental time in the bubble column, but also affected by the time the fiber is soaked in tap water prior to experiment initiation. Figure 4.16 shows the difference in gas flow behavior between 2 mm Nylon fiber soaked for five days and two weeks. The gas holdup behavior of 2 mm fiber soaked for five days has the same magnitude as that of 3 and 6 mm Nylon fiber at the same mass fraction of C = 0.05% (soaked for 3-5 days). However, the gas holdup of fiber soaked for two weeks is much higher, and a maximum gas holdup is exhibited. Although some fiber flocculation is observed at low superficial gas velocities in the fiber soaked for 2 weeks, a significant amount of fiber is uniformly dispersed in the bubble column, not adhering to other fiber or bubbles; this is not observed in the fiber that was soaked for 3-5 days.

To confirm the time-varying characteristic of Nylon material, the gas holdup in a Nylon powder system was also investigated. The gas holdup data in a C = 0.05% Nylon particle system, with a particle size range between 105 and 180 microns was repeated five times within t = 108 hours after which the powder was added to the bubble column. The gas holdup variation is also observed in the Nylon powder suspension, as shown in Figure 4.17. The gas holdup behavior is the same as that of Nylon fiber; that is, gas holdup increases with time. The increase in gas holdup with time is more apparent at intermediate superficial gas velocities, when the gas flow is in the transitional flow regime.

It is hypothesized that some Nylon fiber suspension properties change with time when exposed to an air-water hydrodynamic field, and these changes affect the gas flow hydrodynamics by promoting bubble breakup and/or hindering bubble coalescence. This influences the bubble size distribution, resulting in an increase in gas holdup in the Nylon suspension. To test this hypothesis, surface tension, electrical conductivity, total dissolved solids, and pH of the filtrate from the Nylon fiber and powder suspension were measured before and after each data set. No significant change in these properties was recorded.

Several possible additional mechanisms may cause changes in the Nylon fiber suspension properties during long-term water exposure that are not recorded when measuring surface tension, electrical conductivity, total dissolved solids, and pH; these include (i) Nylon fiber surface additive influence, (ii) fiber degradation, (iii) reduced fiber hydrophobicity, and (iv) deformation of the Nylon fiber shape. The time-varying gas holdup caused by the Nylon system changes may be attributed to one or more of these mechanisms.

4.3.3.1 Mechanism 1: The effect of Nylon fiber surface additives

During the manufacture of Nylon fiber, many additives may be used to satisfy industrial process requirements. For example, a spin finish will be applied to yarn to control static electricity, and as an aid for further processing. These spin finishes are usually composed of a proprietary mix of a lubricant, an emulsifier, an antistatic agent, and other components (Slade and Hild, 1992). Although the fibers were well washed in water before the experiment, perhaps it was not sufficient to remove all the materials. Some of the remaining additives may dissolve in water during the experiment and change the water properties, further affecting the bubble behavior in the fiber suspension. For example, foam was observed only after several hours of bubble column operating and the foam appearance could be the result Nylon fiber additives leaching into the water. Also, the fiber surface property and suspension filtrate chemistry may change with time due to the additives dissolving in the water, resulting in the change in inter-fiber forces and thus variation in apparent viscosity of fiber suspension. This may be the main source of the variation in gas flow hydrodynamics in Nylon fiber suspensions.

4.3.3.2 Mechanism 2: Nylon fiber degradation

Nylon is a polymer, and polymers encounter various kinds of degradation throughout their life, starting from the reactor where the polymer is synthesized, the extruder where it is processed, during service life, and after its failure when it is discharged into the environment (Thanki, 1999). The degradation involves several chemical and physical processes accompanied by small structural changes. In the current experiment, the Nylon fiber length is short and has a relatively large surface area to volume ratio, and undergoes long-term

exposure to water and air in a complex hydrodynamic field. In this environment, several types of degradation are possible: (i) hydrolytic degradation, (ii) oxidative degradation, and (iii) mechanical degradation.

Many polymers, mainly those synthesized by the polycondensation method (like Nylon), undergo hydrolysis that leads to degradation of the polymeric material by scission of the polymer backbone (Mathisen et al., 1991). Thanki (1999) claims that Nylon fiber is prone to hydrolytic degradation in moist environments. In the current study, hydrolytic degradation would be enhanced due to the Nylon long-term exposure to water. Fragments of a suitable size, broken from the main Nylon chain become water-soluble (Mikolajewski et al., 1964), which could change the properties of the suspension filtrate.

All polymers are subject to degradation by oxygen, and the stability of Nylon decreases in the presence of air (Kohan, 1995). Mikolajewski et al. (1964) observed faster oxidation occurred when Nylon fiber was wet. In the current study, Nylon is exposed to water, and air is continuously bubbled through the suspension. Oxidative degradation may be enhanced because the rate of oxygen diffusion into Nylon fiber would increase in the bubble-induced turbulent flow field.

Mechanical energy, applied in shear, can be converted to main chain bond energy resulting in polymer bond scission. Hunston and Zakin (1980) and Nagashiro and Tsunoda (1977) suggest that hydrodynamic fields can cause the decomposition of polymer macromolecules. Muller and Davidson (1994) bubbled hydrogen peroxide through aqueous solutions of carboxymethy cellulose (CMC), and suggested that CMC chains were mechanically broken due to shear forces caused by bubble-induced mixing. In the current

study, the Nylon is a solid of individual fibers and it may not experience significant mechanical degradation; however, under long-term exposure to water and bubble-induced mixing forces, mechanical degradation may contribute to the observed time-varying results.

The degradation of the Nylon fiber suspension may have an effect on gas flow hydrodynamics and the apparent viscosity of the fiber suspension. There is limited information on the effect of degradation on Nylon fiber properties. However, Lavrenko et al. (1994) studied the stability of poly (napthoyleneimidobenzimidazole) (PNIB) fiber under atmospheric conditions and showed that the material experienced slow hydrolytic degradation of the macromolecules, leading to a drop in intrinsic viscosity and changes in mechanical properties such as tensile strength and elastic modulus. They also showed that the decrease in molecular weight is significantly accelerated for PNIB in the powered state. It is postulated that Nylon fiber would experience similar changes as PNIB. The gas flow behaviors observed in Nylon fiber suspensions, such as increasing gas holdup with time, and a more apparent gas holdup change with time in a Nylon powder suspension, indirectly confirm this postulation. The time-varying gas holdup may be partly attributed to the change in fiber elastic modulus resulting from degradation; this may change the Nylon fiber deformation under the turbulence experienced in a bubble column, which could affect the fiber-fiber interaction and thus the apparent fiber suspension viscosity.

To test the possibility of mechanisms 1 and 2, approximately C = 1% fiber suspension was formed in a 4000 ml beaker, and surface tension, electrical conductivity (EC), total dissolved solids (TDS), and pH of the filtrate were measured at t = 6 and 300 hours after which the fiber suspension was formed (Table 4.1). Surface tension and pH decreased and

EC and TDS increased with soaking time, which may indirectly indicate that some fiber additives leach into the water and, perhaps, the fiber has experienced some degree of degradation. The reason why no change in these properties was recorded by the bubble column filtrate sample is that the changes are relatively small, they may be damped by the large water volume and low fiber concentration, and the equipment used is not sensitive enough to record small changes.

Table 4.1: Selected property variations of Nylon fiber soaked in water.

Soaking Time (hours)	Surface tension (mN/m)	EC (ms/cm)	TDS (ppm)	pH (-)
6	57	0.49	330	8.7
300	46	0.57	380	7.1

4.3.3.3 Mechanism 3: Reduced hydrophobicity of Nylon fiber

The loss of hydrophobicity of Nylon in a wet condition has been observed by Tokoro and Hackam (1995). Hydrophobicity loss of other polymers such as Polyethylene in a wet condition has also been studied by Khan and Hackam (1997). The enhanced dispersion of fiber in water with longer soaking time implies a reduced degree of hydrophobicity. The Nylon fiber surface becomes more hydrophilic during long-term water exposure due to fiber surface additives leaching into the water, leading to an increase in gas holdup. Although the surface tension of the suspension filtrate (i.e. gas-liquid interface surface tension) has no apparent change, the surface tension of the gas-solid and solid-liquid interface will change when Nylon fibers become more hydrophilic. This has a significant effect on bubble hydrodynamics, hindering bubble coalescence. The loss of hydrophobicity also reduces the

adhesive forces between fibers, which make Nylon fiber flocs easier to disrupt which was observed in our experiments after prolonged water exposure.

4.3.3.4 Mechanism 4: Nylon fiber shape deformation

Fiber deformation has a significant effect on fiber suspension viscosity (Joung et al., 2002). Blakeney (1966) found that a suspension of slightly curved fibers could increase the apparent suspension viscosity by 10-15% above that of a relative straight fiber suspension. Joung et al. (2002) provide numerical results that show fiber curvatures of between 5-10 degree have the greatest effect on suspension viscosity, and viscosity decreases when fiber curvatures are beyond this range. From the results of Joung et al. (2002), the time variation of gas holdup in Nylon fiber suspensions is influenced by the change in Nylon fiber deformation during an experiment, leading to a change in suspension viscosity. According to Lavrenko et al. (1994), fiber degradation affects fiber properties like elastic modulus, which, in turn, affects fiber deformation. Nylon fiber deformation would continue to change during exposure in a hydrodynamic field, leading to an increase in gas holdup with time.

4.3.4 Effect of Nylon Fiber Mass Fraction on Gas Holdup – Revisited

Figure 4.12 was obtained from data taken on the same day fiber was added to the bubble column. However, the effect of fiber mass fraction on gas holdup also depends on the length of the time the fiber is in the column. Figure 4.18 shows that the gas holdup at a Nylon fiber mass fraction of C = 0.4% and taken at t = 48 hours is higher than that of C = 0.25% taken at t = 12 hours. This conflicts with the trend that increasing mass fraction decreases gas holdup, as shown in Figure 4.12, as well as the results in Rayon fiber suspensions (section 4.1 and

4.2). The gas holdup time dependence makes it extremely difficult to study the effect of Nylon fiber mass fraction on gas holdup because the results depend on when the data are collected.

Selected experiments were completed in Rayon fiber suspensions to determine if gas holdup in these suspensions also varies with time. Excellent reproducible results of gas holdup in Rayon fiber suspensions with L = 3 mm is shown in Figure 4.19. There is no change in gas holdup during 84 hours after which Rayon fiber was added to the bubble column, which implies that Rayon fiber degradation is very slow, if at all, and has no effect on gas holdup. Thus, the gas holdup results in Rayon fiber suspensions are reliable, and Rayon fiber is a good material to investigate gas holdup behavior in synthetic fiber suspensions. In contrast, Nylon fiber is not appropriate for the study of fiber effects on gas holdup.

4.4 Gas Holdup in Short Rayon Fiber Suspensions (L = 0.38 and 1 mm)

In previous studies, fibers with a large aspect ratio ($74 \leq r \leq 580$) were employed which showed that, as expected, fiber mass fraction has a significant effect on gas holdup and flow regime transition. This is because fiber-fiber interaction (flocculation) occurs even at low fiber mass fractions in long fiber suspensions and fiber addition significantly modifies the suspension rheology from that of water. Short fibers reduce the flocculation tendency, and thus, more closely approximates a particulate system. This section investigates the effect of fiber mass fraction with L = 0.38 and 1 mm long Rayon fiber.

Figure 4.20 depicts the gas holdup variation with fiber mass fraction with A = 0.57%. The results are significantly different from those obtained from high aspect ratio fiber suspensions (L = 3, 6, and 12 mm). Similar results are obtained with aeration plates of A = 0.99% and 2.14%. Fiber mass fraction does have an effect on gas holdup which decreases with increasing fiber mass fraction. However, the effect is not as significant as those found when the fiber aspect ratio is large. As shown in Figure 4.20, only large fiber mass fractions lead to a significant gas holdup reduction. It can be seen that the presence of L = 0.38 mm Rayon fiber has little effect on gas holdup even at C = 0.6% (see, for comparison, Figure 4.1 for long Rayon fiber results). The flow pattern is also insensitive to fiber addition; homogeneous, transitional, and heterogeneous flow regimes exist even at fiber mass fractions as high as C = 3.0% for L = 0.38 mm. This indicates that fiber mass fraction has less effect on gas holdup and flow regime transitions for fiber suspensions with small fiber aspect ratios than large aspect ratios.

It is known that fiber addition leads to a decrease in gas holdup mainly due to the increased suspension viscosity. From the results in Figure 4.20, it is apparent that the effective viscosity may be influenced by fiber aspect ratio, in addition to fiber mass fraction, and small aspect ratio fibers can have a significant effect on the rheology of the fiber suspension. Fiber flexibility also influences the suspension viscosity and, according to Joung et al. (2001), the viscosity would increase by 7-10% when simulating flexible fibers compared to straight rigid fibers. Forgas and Mason (1959) contend that fiber flexibility is related to fiber aspect ratio (see Eq. (2.11)). They state that fiber flexibility cannot be neglected for large aspect ratio fibers and it has a significant impact on the rheology of the

fiber suspension. However, the flexibility is less important when the fiber aspect ratio is small.

Fiber aspect ratio also influences the fiber orientation distribution, which affects the suspension viscosity; a large fiber orientation distribution enhances apparent viscosity. Sundararajakumar and Koch (1997) showed that when $N_f L^2 d << 1$, the fiber orientation is controlled by hydrodynamic interaction, and Chaouche and Koch (2001) stated that in the "hydrodynamic regime", fiber addition has only a small contribution to the shear viscosity because the fiber is primarily aligned along the flow direction. When $N_f L^2 d = O(1)$, where N_f is the number of fibers per volume, mechanical contacts dominate, which cause the fiber to flip more frequently, resulting in the fiber orientation distribution to deviate from the flow direction (Sundararajakumar and Koch, 1997). As $N_f L^2 d$ is proportional to CL/d, where L/d is the fiber aspect ratio, the fiber mass fraction at which mechanical contacts dominate and influence the fiber suspension viscosity is larger when the fiber is L = 0.38 mm Rayon fiber than long fiber (i.e., L = 3, 6, and 12 mm).

Another factor contributing to gas holdup and flow pattern insensitivity to fiber addition is that foam is observed on the surface of the 0.38 mm long Rayon fiber slurries, and the amount of foam increases with increasing fiber addition. Foam generation is attributed to the fact that additives on the fiber surface may leach into the water and reduce the surface tension. Although the fiber was soaked in a bucket for two days and washed with tap water before it was added to bubble column, it was difficult to wash effectively because the fibers are so short and are easily lost during the washing procedure. It is hypothesized that the washing procedure was compromised to minimize the fiber loss. Thus, the slight change of

gas holdup with fiber mass fraction is partly attributed to the fact that the decrease in gas holdup caused by fiber addition is compensated by the increase in gas holdup due to foam formation.

Rayon fiber with L = 1 mm, whose length is between L = 0.38 and 3 mm, is used to try to check the transition length at which gas holdup behavior deviates from particulate systems. It is found from Figure 4.21 that gas holdup reduces with fiber mass fraction is more evident than L = 0.38 mm, and the effect of fiber mass fraction is more pronounced in the transitional flow regime. However, the flow pattern is similar to that L = 0.38 mm; it is weakly dependent on fiber addition, and pure heterogeneous flow regime is not observed over the range of fiber mass fractions ($C \leq 1.8$). Note that for L = 3 and 6 mm, the critical fiber mass fractions at which the flow changes from homogeneous to pure heterogeneous flow regime are around 0.6%. Figure 4.21 shows that L = 1 mm fiber behavior is between the L = 0.38 mm and L = 3 mm, and a critical fiber length where the fiber aspect ratio differentiates between fiber and particulate systems is between r = 48.5 (L = 1 mm) and r = 145 (L = 3 mm).

4.5 Effect of Bubble Column Diameter

In this section, three bubble column diameters (D = 10.2, 15.2, and 32.1 cm) are employed to study the scale-up effect on gas holdup in an air-water system and cellulose fiber (hardwood, softwood, and BCTMP) suspensions. For all three bubble columns, similar perforated plate gas distributors are using where the nominal open area ratio is 0.5%. The exact open area ratios are A = 0.62% (D = 10.2 cm), A = 0.57% (D = 15.2 cm), and A =

0.49% (D = 32.1 cm). The aeration plate hole diameter in all cases is d_o = 1 mm. Some of the data used in this section were taken by other researchers in our laboratory, but the combined analysis is part of this thesis.

4.5.1 Air-Water

Figure 4.22 shows the scale-up effect on gas holdup in an air-water system. For all three column diameters (D = 10.2, 15.2, and 32.1 cm), homogeneous, transitional, and heterogeneous flows and a local maximum gas holdup are observed over the range of superficial gas velocities, although the maximum is not prevalent for D = 10.2 cm. When the superficial gas velocity is low, which corresponds to the homogeneous flow regime, gas holdup is independent of column diameter. When the superficial gas velocity is increased and the flow is in the transitional regime, gas holdup is enhanced by decreasing column diameter. When gas holdup is further increased and the flow becomes heterogeneous, the difference in gas holdup between D = 15.2 and 32.1 cm is negligible, both of which are lower than that of D = 10.2 cm. This phenomenon is consistent with that of Zahradnik et al. (1997) who observed that bubble column diameter had no effect on gas holdup in the homogeneous and heterogeneous flow regime when D > 15 cm, but it influenced gas holdup in the transitional flow regime.

Bubble column size has two effects on bubble column hydrodynamics. One is that the liquid circulation velocity is affected by column diameter, and it increases with increasing column diameter (Zehner, 1989). Liquid circulation accelerates the bubble rise velocity. Krishna et al. (2001) numerically proved that the bubble swarm velocity is scale dependent and increases with increasing bubble column diameter. This reduces the bubble residence

time and thus, gas holdup. Another influence is the column diameter wall effects. Krishna et al. (1999b) pointed out that wall effects play an important role with respect to bubble rise velocity and hinder bubble rise when d_b/D (ratio of bubble diameter to column diameter) > 0.125. Thus, smaller bubbles and/or larger column diameters produce smaller wall effects.

At low superficial gas velocity, where liquid circulation in the column is not important and the flow is homogeneous, gas holdup is independent of bubble column diameter (see Figure 4.22) because the small bubble sizes typical of this regime are not influenced by the column wall. In the transitional and heterogeneous flow regimes, where bubble coalescence is significant leading to large bubble diameters, wall effects become important for the small column diameter; these effects hinder bubble rise and increase gas holdup. Additionally, significant liquid circulation appears for all column diameters in transitional and heterogeneous flow, and liquid circulation drives bubbles to rise faster in larger diameter columns (Krishna et al., 2001). Thus, gas holdup in the D = 10.2 cm column is higher than that of D = 15.2 and 32.1 cm for the transitional and heterogeneous flow. When $D \geq 15$ cm, gas holdup is affected by column diameter only in the transitional flow regime, resulting in a higher gas holdup when D = 15.2 cm compared to D = 32.1 cm. This is attributed to a lower liquid circulation velocity in the D = 15.2 cm column than the D = 32.1 cm column, leading to a longer bubble residence time and thus a higher gas holdup. Also, very large bubbles in the D = 15.2 cm column may be influenced by wall effects, which further increases gas holdup. In heterogeneous flow, the effect of column diameter disappears for D = 15.2 and 32.1 cm. This could be attributed to the fact that the turbulent intensity of large diameter column may be stronger due to a higher liquid circulation velocity. This increases the

possibility of bubble breakup in the large diameter column, which dominates in heterogeneous flow (Prince and Blanch, 1990). The decrease in gas holdup due to a higher bubble rise velocity by increased liquid circulation is compensated by the increase in gas holdup due to bubble breakup.

4.5.2 Fiber Suspensions

Figure 4.23 shows gas holdup in BCTMP suspensions as a function of superficial gas velocity for various fiber mass fractions and three bubble column diameters. Similar gas holdup trends are found in all three bubble columns. When the fiber mass fraction is low, there is a local maximum gas holdup and three flow regimes (homogeneous, transitional, and heterogeneous) are observed, which is similar to that of air-water system. When the fiber mass fraction is beyond a critical value, pure heterogeneous flow is observed. This critical value is independent of column diameter and $C_{critical} \approx 0.4\%$ for all three bubble columns. These phenomena are also observed in softwood and hardwood fiber suspensions, the only difference is that $C_{critical}$ is lower for softwood. Table 4.2 shows the critical fiber mass fraction for BCTMP, softwood and hardwood fiber suspensions in all three bubble columns. It indicates that the flow pattern is not affected by column diameter. The similar flow patterns for both the air-water system and the three cellulose fiber suspensions, in all three bubble columns, implies that for a given fiber type and fiber mass fraction, the flow pattern is determined primarily by the gas distributor. Since all three bubble columns used perforated plate gas distributors with a nominal open area ratio of ~ 0.5%, and all holes are the same diameter (d_o = 1 mm), similar flow patterns result.

Table 4.2: The critical fiber mass fraction beyond which the pure heterogeneous flow regime appears for different bubble column diameters.

	Column diameter, D (cm)		
	10.2	15.2	32.1
BCTMP	0.4%	0.4%	0.4%
Softwood	0.25%	0.25%	0.25%
Hardwood	0.4%	0.4%	0.4%

Figure 4.23 also shows that at high fiber mass fractions ($C \geq 1.0\%$), the effect of fiber addition disappears for D = 10.2 and 15.2 cm, however, gas holdup continues to decrease with increasing fiber mass fraction for D = 32.1 cm. This different phenomenon for the largest column diameter may be attributed to a different slurry dispersion coefficient for the D = 32.1 cm bubble column. In gas-liquid-fiber semi-batch bubble columns, fibers disperse with liquid carried up by the bubble wake. At high fiber mass fractions, some fiber settling occurs, which may lead to channeling, this is observed for all three bubble columns at the high fiber mass fractions. In section 4.1, it was explained that gas channeling in the lower column region resulted in a negligible decrease in gas holdup when additional fiber is added to the column because the fiber dispersion is not uniform. Krishna (2000) argued that the slurry dispersion coefficient is proportional to the liquid circulation velocity and bubble column diameter. At the fiber mass fraction where channeling is observed, more fibers disperse in the larger diameter bubble column leading to a more uniform fiber dispersion. However, when C is further increased to 1.8% in the D = 32.1 cm column, gas holdup does not change from C = 1.4%, which is similar to that observed when D = 10.2 and 15.2 cm (see Figure 4.24). It is noted that at the high fiber mass fractions, it is possible that the decrease in gas holdup due to bubble coalescence is compensated by the increase in gas holdup due to

the hindrance effect the fibers have on the bubble rise velocity, trapping small bubbles, which increase bubble residence time and gas holdup.

Figure 4.24 shows the gas holdup variation with BCTMP fiber mass fraction for different column diameters. At U_g = 5 cm/s, gas holdup is not influenced by fiber addition when the fiber mass fraction is very low for all three bubble columns. As seen from Figure 4.24, this fiber mass fraction is a function of bubble column diameter and is 0.4%, 0.1%, and 0.1% for D = 10.2, 15.2, and 32.1 cm, respectively. The negligible influence of the fiber addition on gas holdup at low fiber mass fractions is attributed to the fact that when the fiber mass fraction is low, the flow is homogeneous at U_g = 5 cm/s. In the homogeneous flow, there is negligible bubble coalescence and it is assumed that bubble size is only weakly dependent on fiber addition at low fiber mass fractions. Thus, at low superficial gas velocities (i.e., U_g = 5 cm/s), gas holdup does not change with fiber mass fraction. When the fiber mass fraction is further increased, the flow deviates from the homogeneous regime at U_g = 5 cm/s and gas holdup decreases with increasing fiber mass fraction. The gas holdup decreases with the same trend with increasing fiber mass fraction for all three bubble columns when C ≥ 0.6%; this fiber mass fraction results in heterogeneous flow, indicating that for heterogeneous flow and low superficial gas velocities, the fiber addition affects gas holdup in a similar manner for all bubble column diameters of this study.

At U_g = 10 cm/s, gas holdup decreases with a steeper slope with increasing fiber mass fraction for D = 10.2 and 15.2 cm than for D = 32.1 cm when C < 0.6%. Note that when C < 0.6% and U_g = 10 cm/s, the flow is in the transitional regime with a maximum gas holdup for D = 10.2 and 15.2 cm but is heterogeneous flow for D = 32.1 cm (see Figure 4.23). Figure

4.24b indicates that gas holdup is more sensitive to fiber addition in the transitional flow regime. The possible reason for this trend is that bubble coalescence dominates in the transitional flow regime and fiber addition enhances bubble coalescence. Also, the slope of the D = 15.2 cm data is steeper than that of D = 10.2 cm, this may be attributed to the fact that for D = 10.2 cm, the decrease in gas holdup due to fiber addition enhancing bubble coalescence is partly offset by an increase in gas holdup due to wall effects. However, for D = 15.2 cm, the liquid circulation velocity is more important to the gas holdup behavior than wall effects, and this tends to decrease gas holdup. This unfavorable effect on gas holdup is enhanced by fiber addition.

When $0.6\% \leq C \leq 1\%$, the slopes in Figure 4.24b are the same for all three bubble columns. In this range of fiber mass fraction, the flow is heterogeneous for all bubble columns at $U_g = 10$ cm/s. There are three competing effects determining gas holdup: (i) wall effects that lead to an increase in gas holdup which is more pronounced in the small diameter bubble column; (ii) liquid circulation that accelerates bubble rise velocity, and thus reduces gas holdup, which is enhanced by the larger bubble diameter column; and (iii) liquid circulation that increases the turbulent intensity, which encourages bubble breakup (Prince and Blanch, 1990), and it is more significant in the larger diameter column. The similar slope in this region of Figure 4.24b indicates that the net balance of these three effects is independent of column diameter.

When $C > 1\%$ and $U_g = 10$ cm/s, gas holdup in the D = 10.2 and 15.2 cm columns is independent of fiber mass fraction; the results for D = 32.1 cm column are influenced by fiber mass fraction until C = 1.4%. The reason has been discussed previously.

At U_g = 15 cm in Figure 4.24c, where the flow is heterogeneous for all three bubble columns, the slopes are the same until C > 1.0%, which further proves that the effects of fiber addition are not a function of bubble column diameter in the heterogeneous flow regime. Note that gas holdup levels off when C > 1.0% for D = 10.2 and 15.2 cm, but this does not occur until C > 1.4% for D = 32.1 cm for all three superficial gas velocities.

The gas holdup variation with superficial gas velocity for different fiber mass fractions and fiber types (softwood, hardwood, and BCTMP) in all three bubble columns is shown in Figure 4.25. It is seen that the effect of bubble column diameter on gas holdup is similar for all three fiber suspensions except hardwood suspension with C = 0.25%.

When fiber mass fraction is low (C = 0.25%) where homogeneous, transitional, and heterogeneous flow regimes occur, the gas holdup behavior for all three fiber suspensions is similar to that of the air-water system. Gas holdup is independent of bubble column diameter in the homogeneous flow for all three column diameters and in the heterogeneous flow regime when D ≥ 15 cm, but affected by column diameter in the transitional flow regime. In the transitional flow regime, gas holdup generally increases with decreasing column diameter. The possible reasons for these results are similar to those discussed with the air-water system. Note that for the transitional flow regime in the hardwood fiber suspension, the gas holdup of D = 10.2 cm column is lower than that of D = 15.2 cm and 32.1 cm columns (see Figure 4.25c(i)) and the reason for this is currently unknown.

When C = 0.8%, the flow is pure heterogeneous for all three bubble columns and the effect of column diameter disappears when D ≥ 15 cm. This phenomenon was also observed

by other researchers (Yoshida and Akita, 1965; Shah et al., 1982; Wilkinson, 1991; Deckwer, 1992; Zahradnik et al., 1997; Krishna et al., 2001). However, when C is further increased to C = 1.4%, the effect of column diameter is evident even when D > 15 cm. It is obvious that gas holdup in the D = 10.2 cm bubble column is higher than that of D = 15.2 and 32.1 cm because wall effects are more significant (Krishna et al., 1999b), and there is lower liquid circulation velocity for a smaller diameter column (Zehner, 1989), both of which result in a lower bubble rise velocity and a higher gas holdup.

The possible explanations to no difference in gas holdup between D = 15.2 and 32.1 cm at C = 0.8% are: although bubble size increases with increasing fiber mass fraction because of bubble coalescence (Heindel and Garner, 1999), wall effects are not significant for both D = 15.2 and 32.1 cm due to the small ratio of d_b/D (Krishna et al., 1999b). Liquid circulation plays a more important role than wall effects for this condition. Liquid circulation velocity is higher in the D = 32.1 cm bubble column compared to the D = 15.2 cm column (Zehner, 1989). On one hand, the enhanced liquid circulation velocity accelerates the bubble rise velocity, which decreases gas holdup; on the other hand, increasing liquid circulation velocity enhances bubble breakup due to increased turbulence intensity, which increases gas holdup. The competition of these two effects leads the gas holdup in the D = 32.1 cm bubble column to be similar to that of the D = 15.2 cm column.

At C = 1.4%, bubble size is further increased (the suspension is more viscous) so that wall effects become important to bubble behavior, and wall effects for D = 15.2 cm are stronger than that of D = 32.1. Additionally, the liquid circulation velocity is higher for D = 32.1 cm and increases the bubble rise velocity, however, it does not provide enough turbulent

intensity to break up bubbles due to a high effective viscosity. Therefore, the gas holdup is lower in the larger bubble diameter when the fiber mass fraction is high.

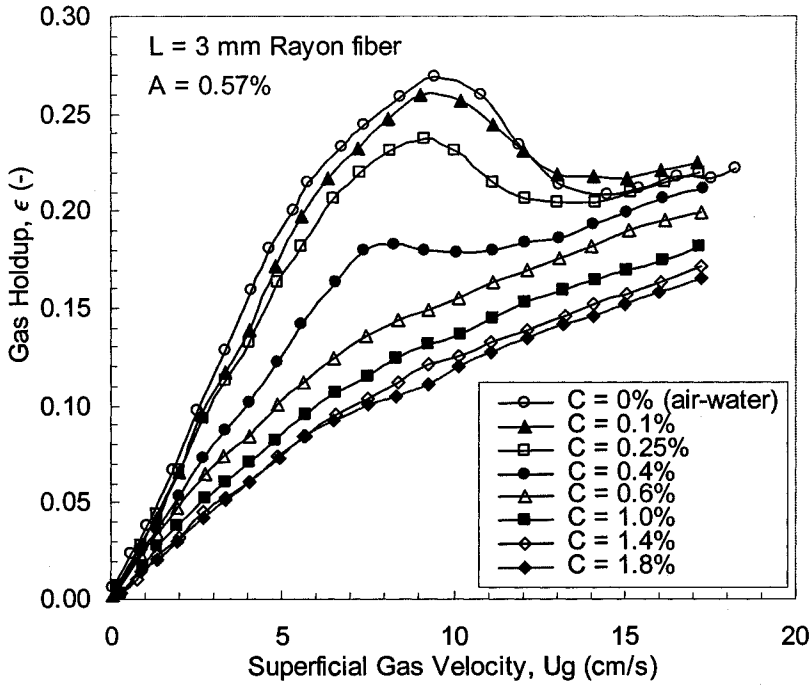

Figure 4.1: Gas holdup as a function of superficial gas velocity for various Rayon fiber mass fractions with L = 3 mm and A = 0.57%.

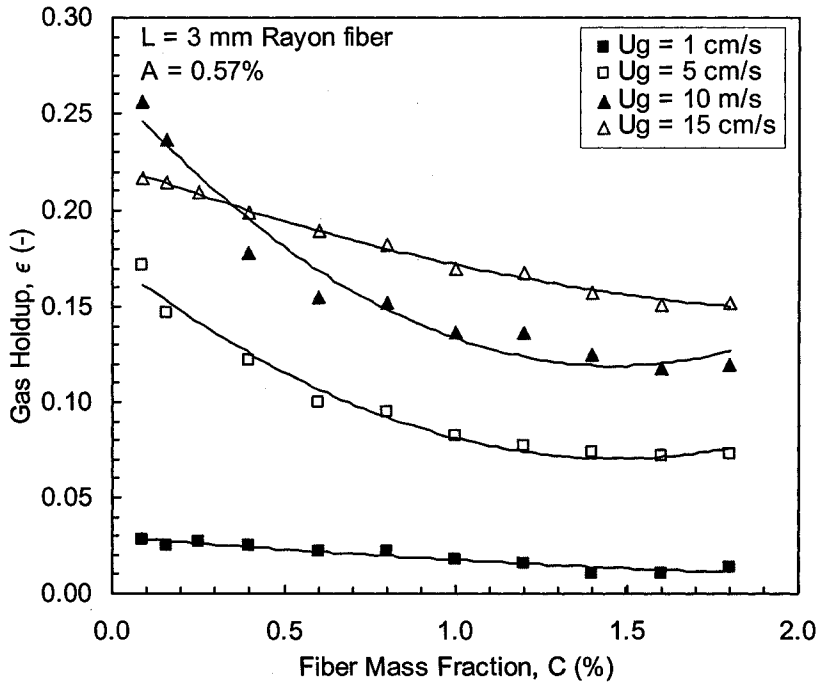

Figure 4.2: Gas holdup as a function of Rayon fiber mass fraction for L = 3 mm and A = 0.57%.

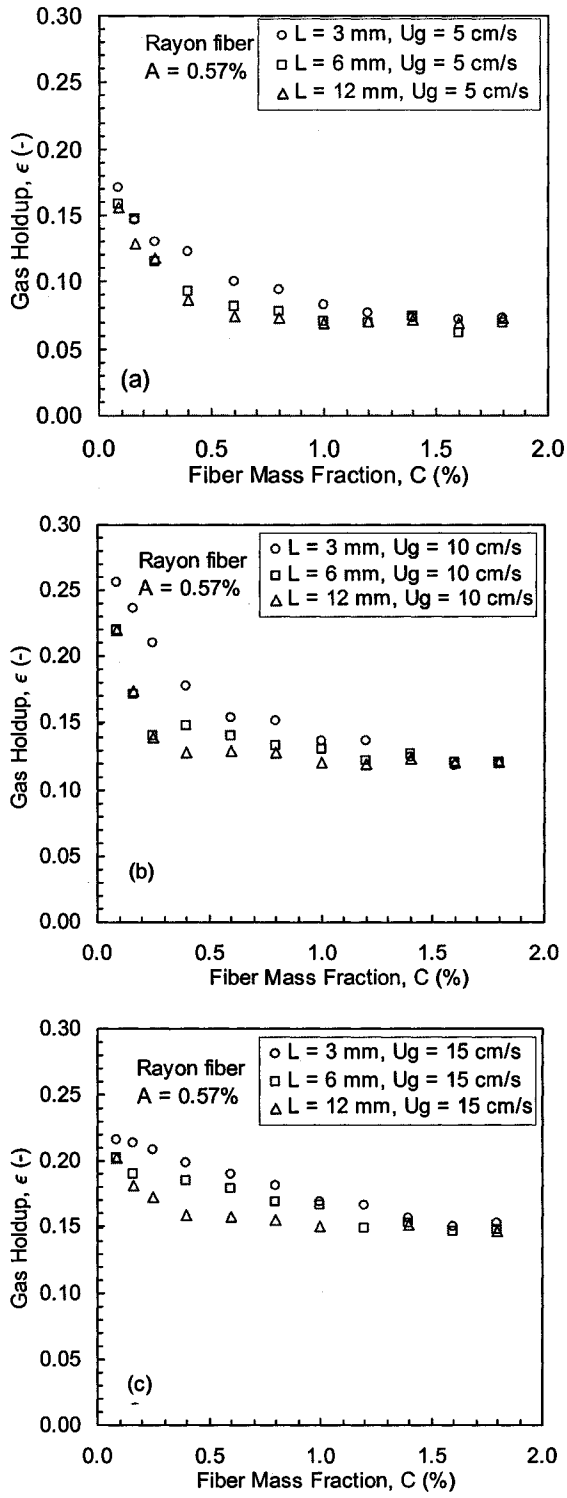

Figure 4.3: The effect of fiber mass fraction on gas holdup for different Rayon fiber lengths and superficial gas velocities with A = 0.57%; (a) U_g = 5 cm/s, (b) U_g = 10 cm/s, and (c) U_g = 15 cm/s.

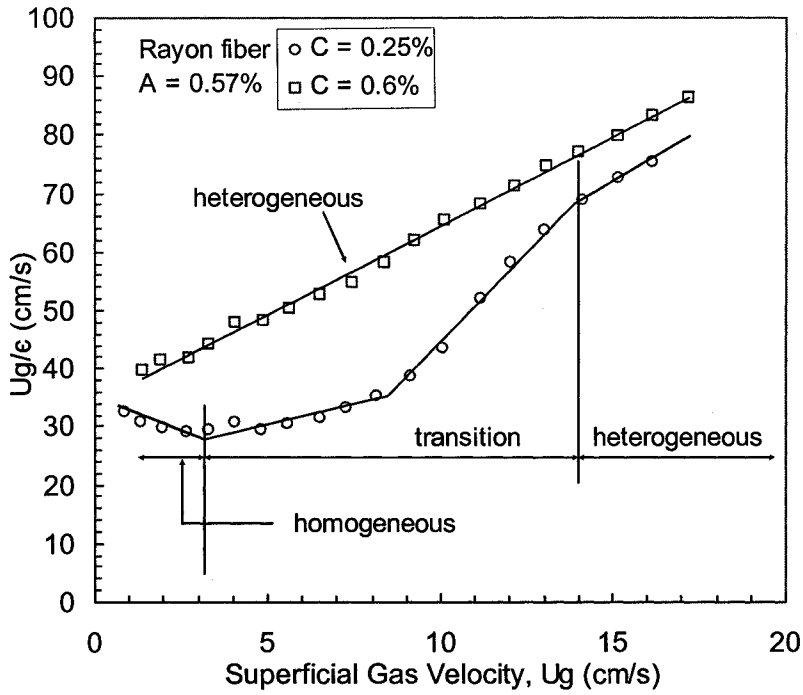

Figure 4.4: Drift flux model to identify the regime transition: L = 3 mm and A = 0.57%.

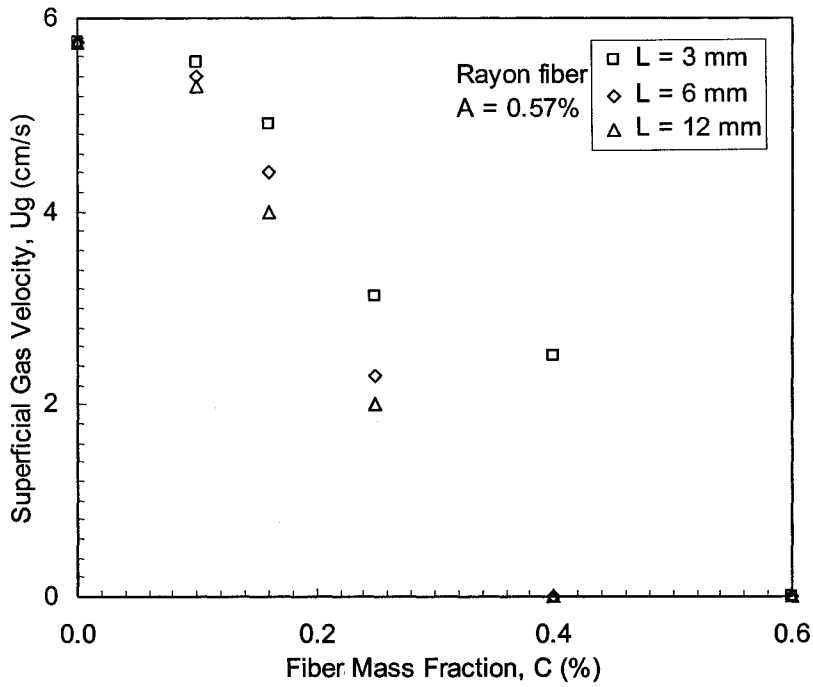

Figure 4.5: Superficial gas velocity at which transition flow is observed in Rayon fiber suspensions for A = 0.57%.

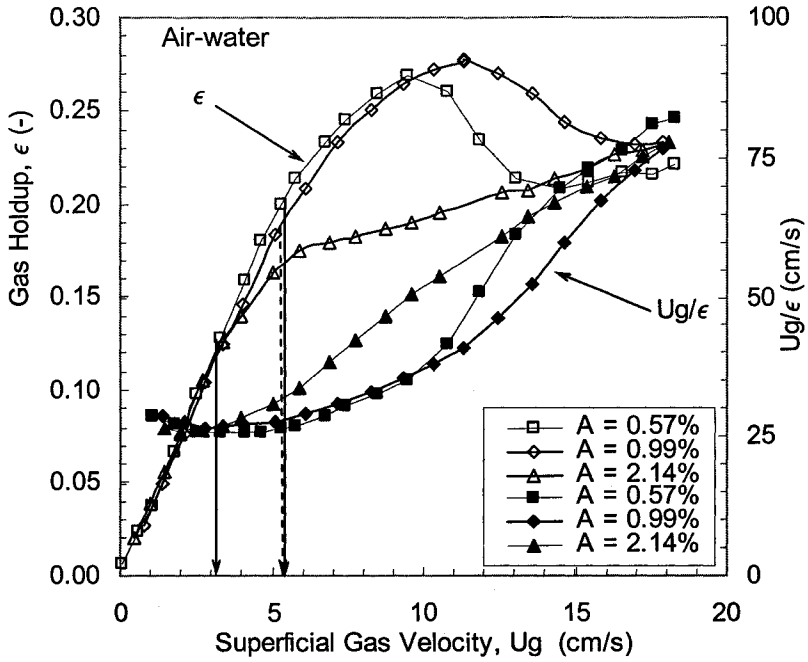

Figure 4.6: Gas holdup and flow regime transitions for various aeration plates in an air-water system.

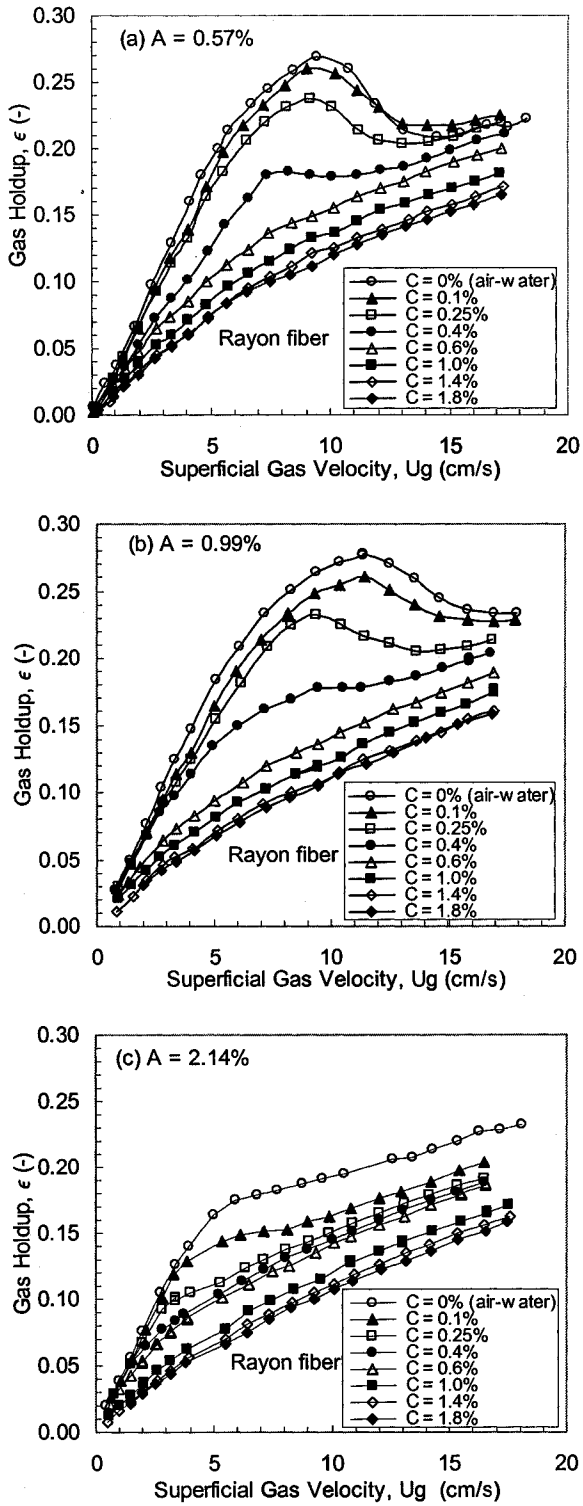

Figure 4.7: The effect of fiber mass fraction on gas holdup with different aeration plates for L = 3 mm Rayon fiber suspensions; (a) A = 0.57%, (b) A = 0.99%, and (c) A = 2.14%.

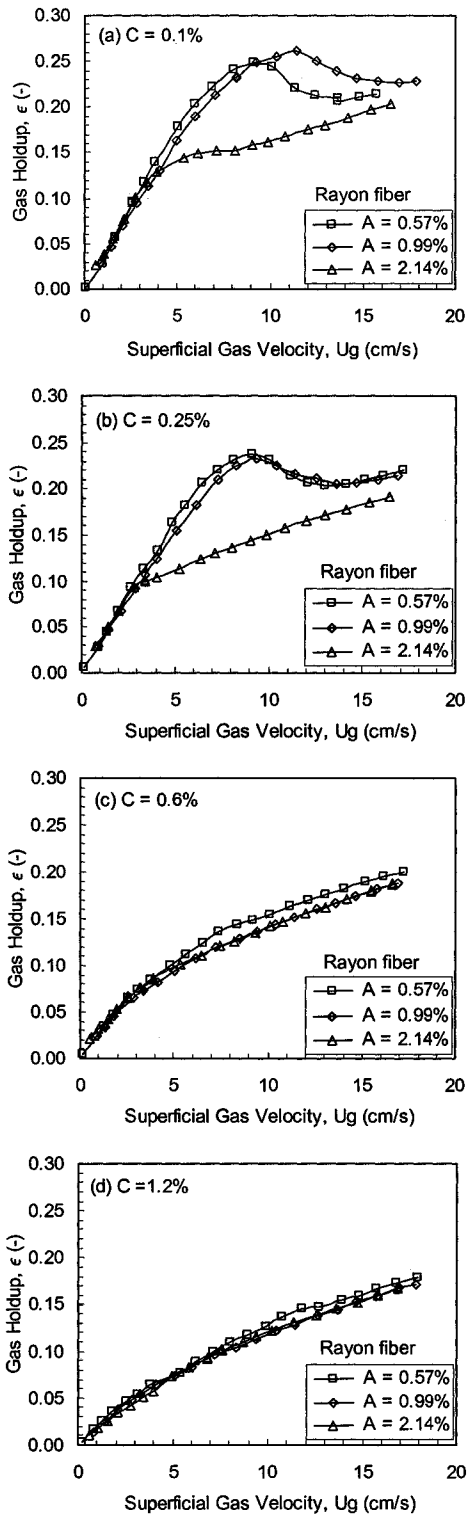

Figure 4.8: Effect of aeration plate open area on gas holdup at various fiber mass fractions (Rayon fiber L = 3 mm); (a) C = 0.1%, (b) C = 0.25%, (c) C = 0.6%, and (d) C = 1.2%.

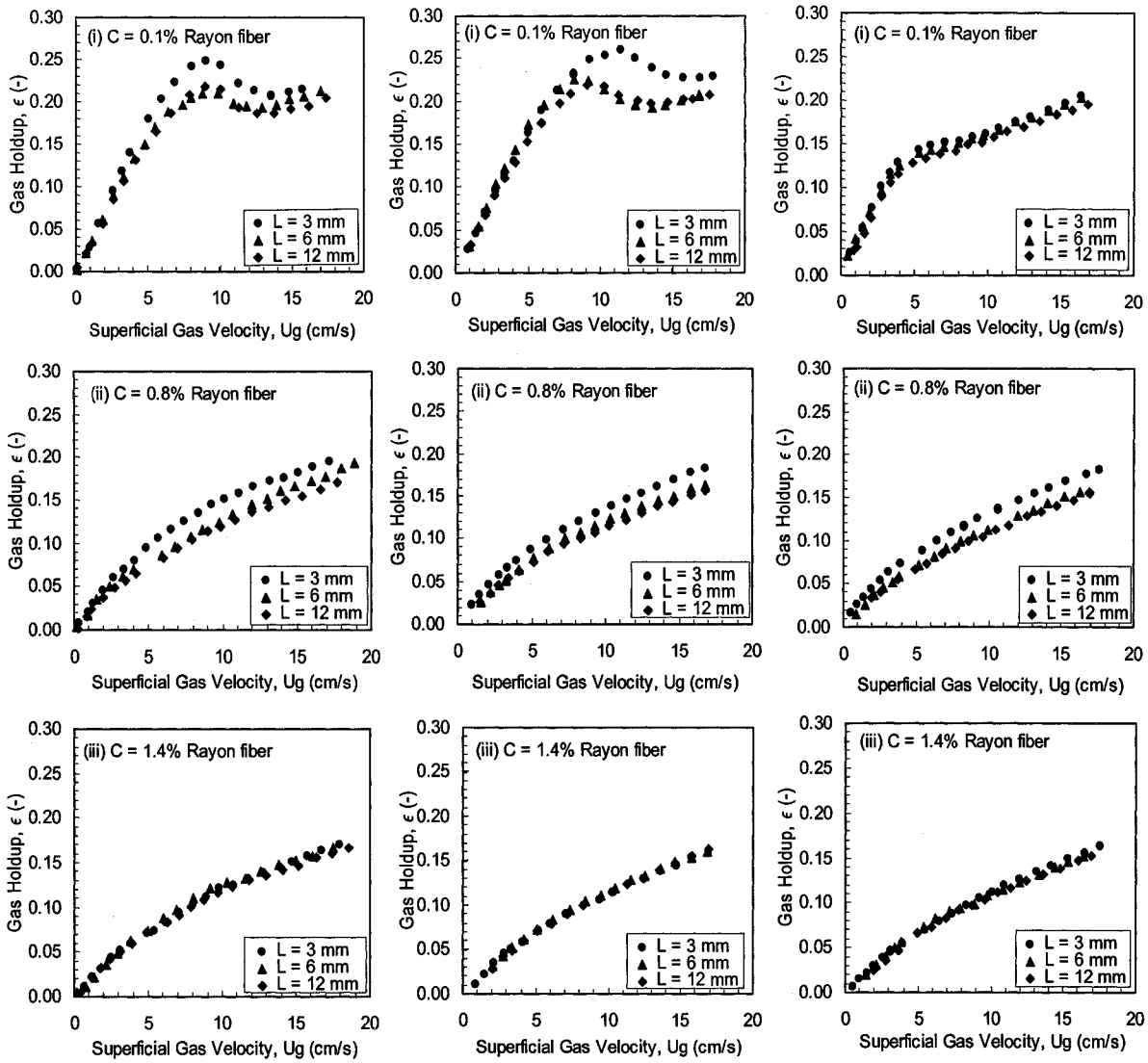

(a) A = 0.57% (b) A = 0.99% (c) A = 2.14%

Figure 4.9: The effect of Rayon fiber length on gas holdup; (a) A = 0.57%, (b) A = 0.99%, and (c) A = 2.14%.

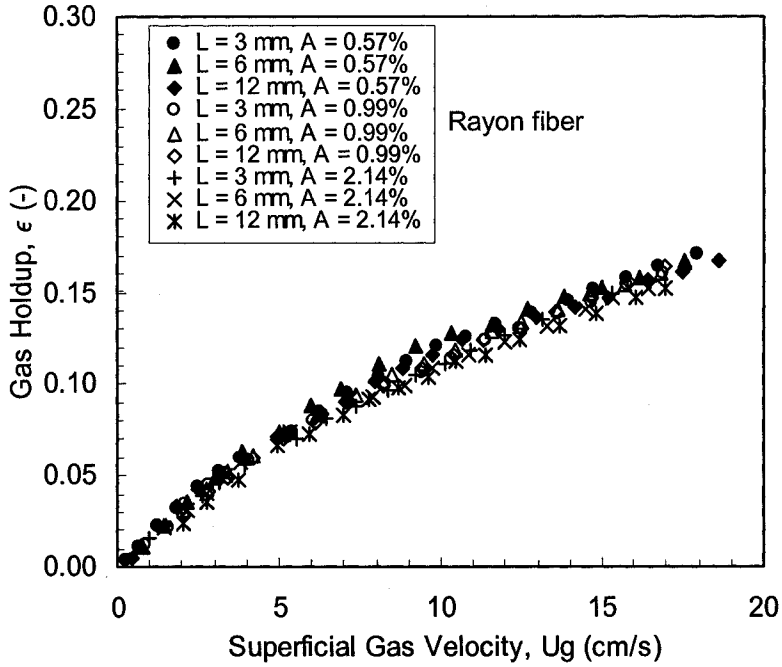

Figure 4.10: Effect of Rayon fiber length and aeration plate open area on gas holdup at C = 1.4%.

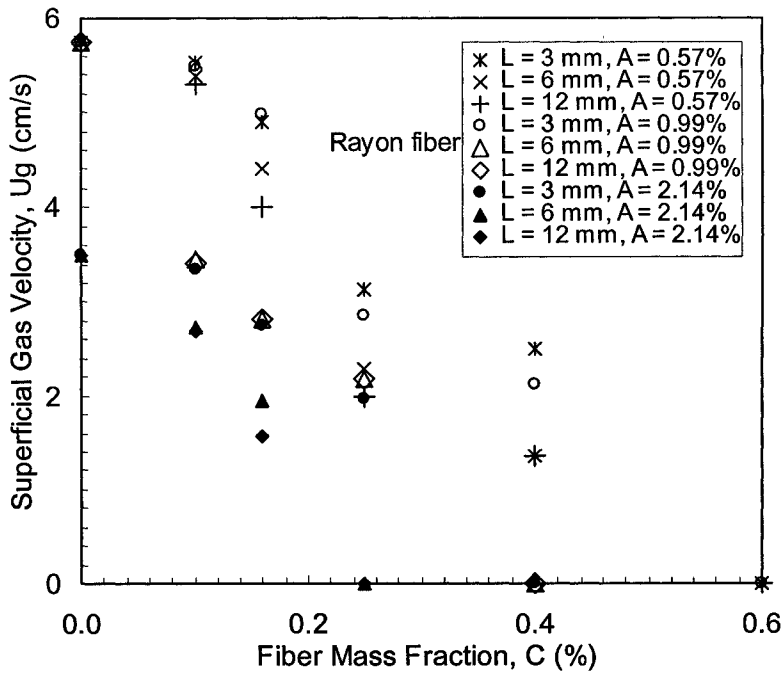

Figure 4.11: The effect of aeration plate open area, fiber mass fraction, and fiber length on the superficial gas velocity at which flow regime transition is initiated.

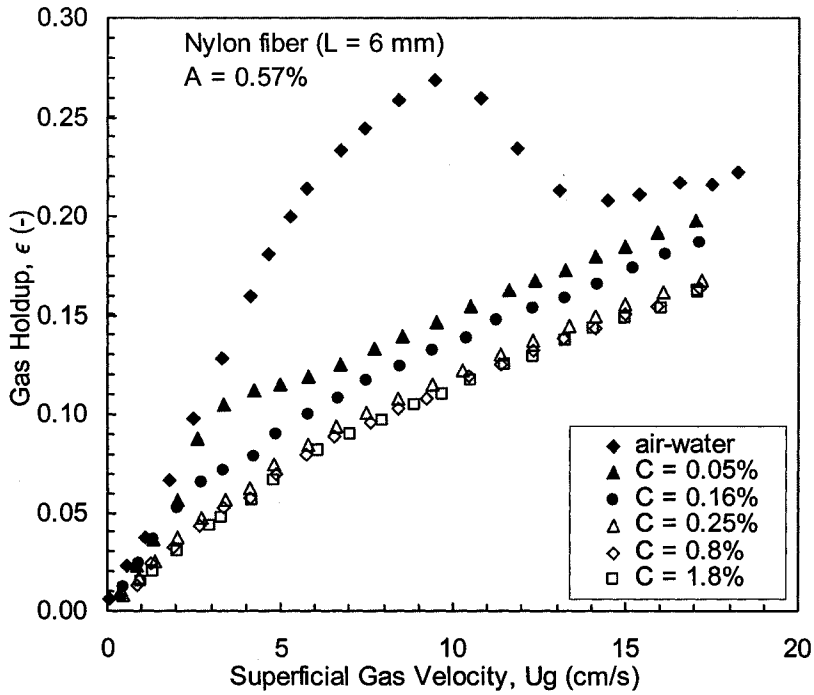

Figure 4.12: Gas holdup as a function of superficial gas velocity for various Nylon fiber mass fractions and L = 6 mm.

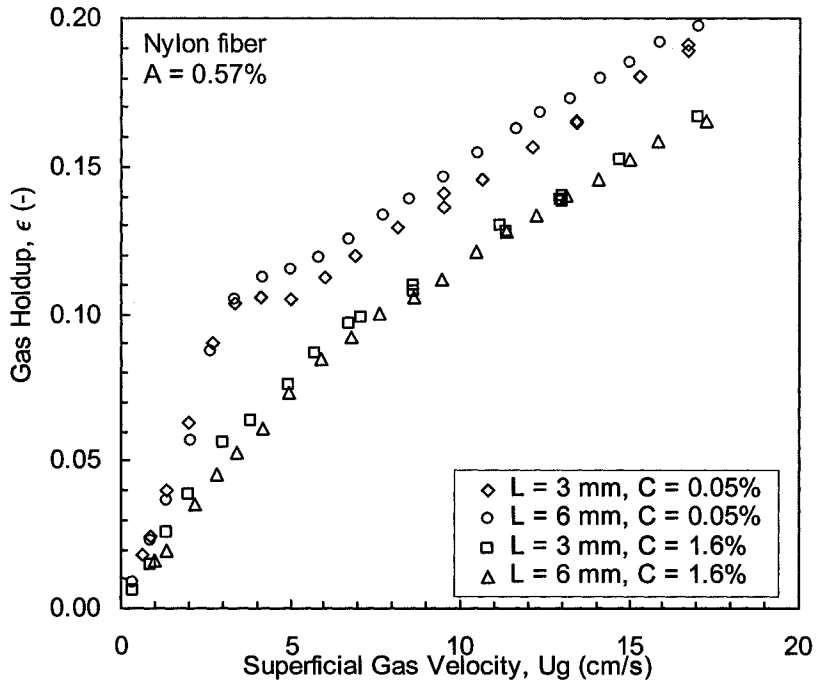

Figure 4.13: Effect of Nylon fiber length on gas holdup at various fiber mass fractions.

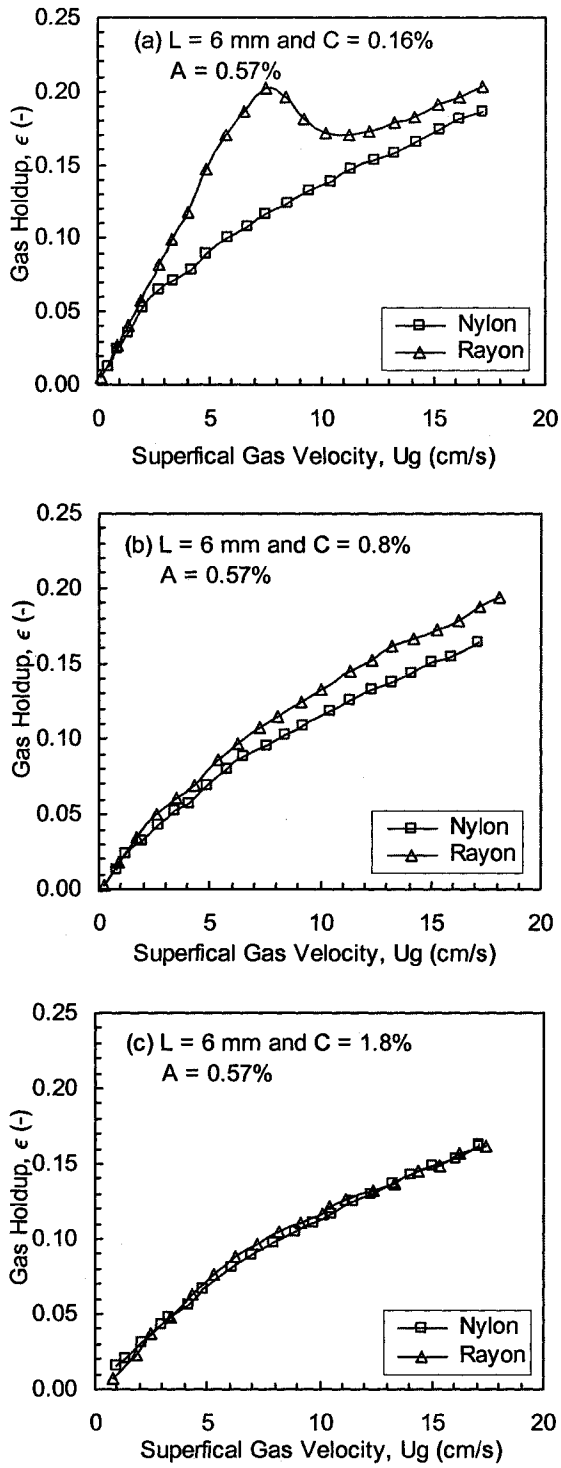

Figure 4.14: Gas holdup comparison of Nylon and Rayon fiber suspensions (L = 6 mm) at various fiber mass fractions; (a) C = 0.16%, (b) C = 0.8%, and (c) C = 1.8%.

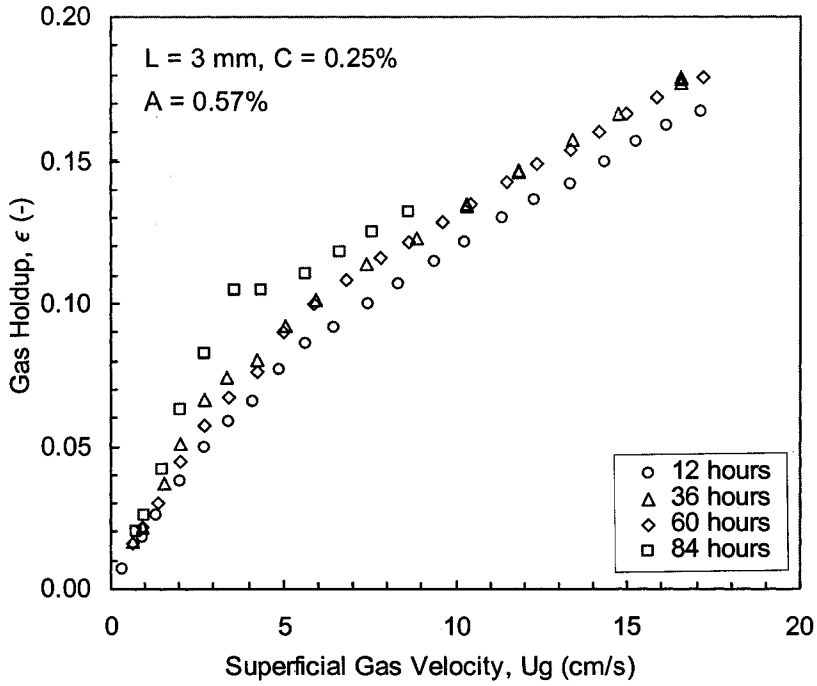

Figure 4.15: Gas holdup dependence on time for a Nylon fiber suspension.

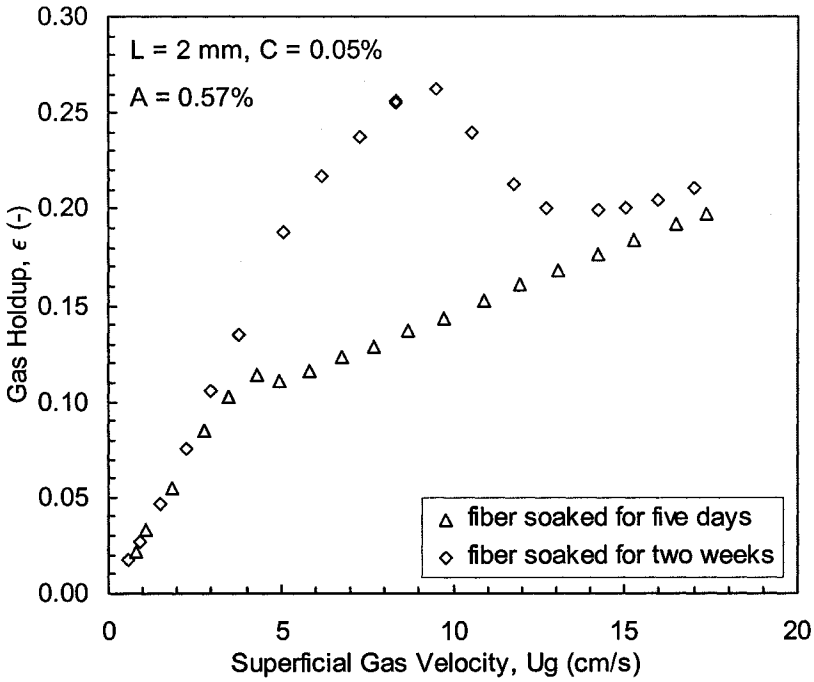

Figure 4.16: The effect of Nylon fiber soaking time on gas holdup.

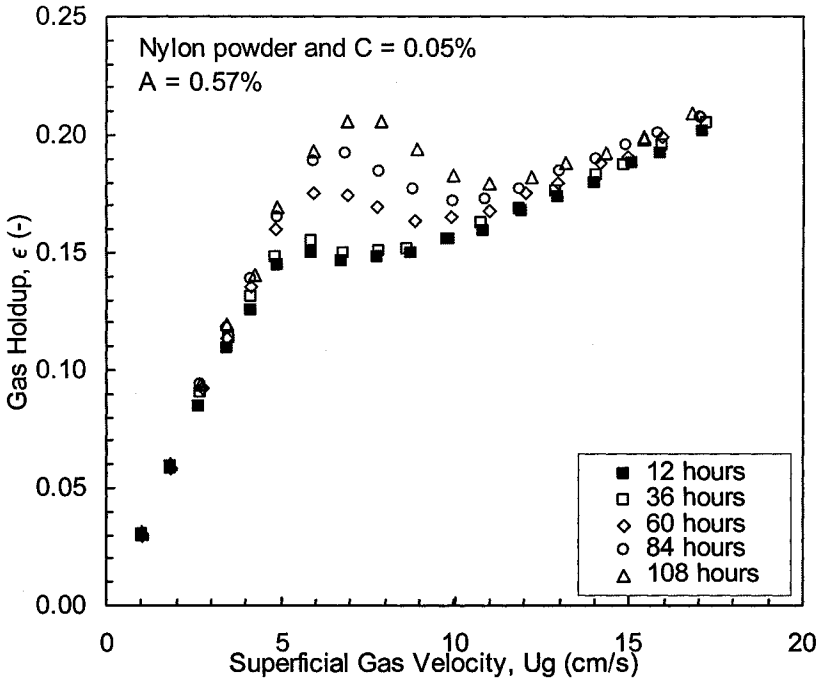

Figure 4.17: Gas holdup dependence on time for a Nylon powder suspension.

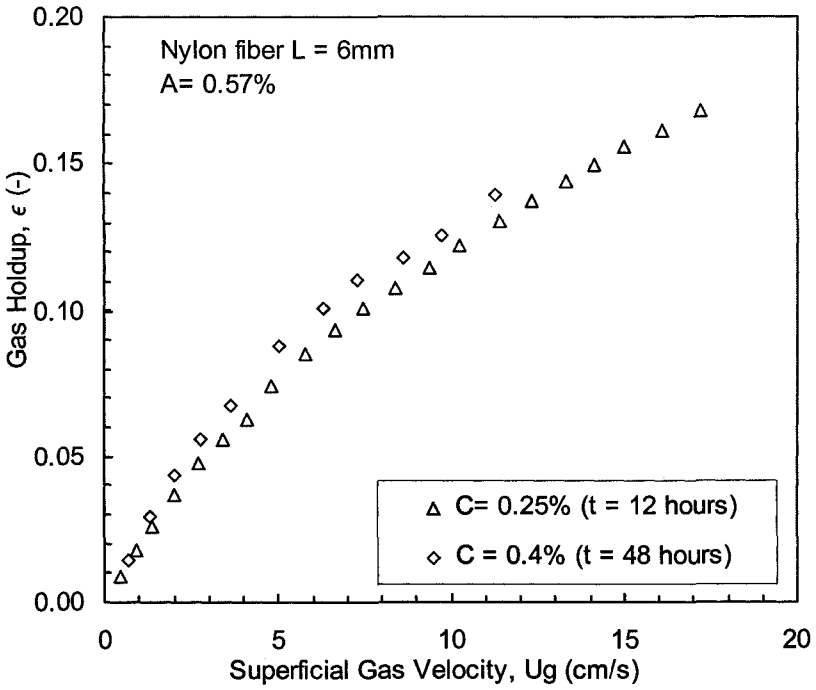

Figure 4.18: Time dependence of Nylon fiber mass fraction effect on gas holdup.

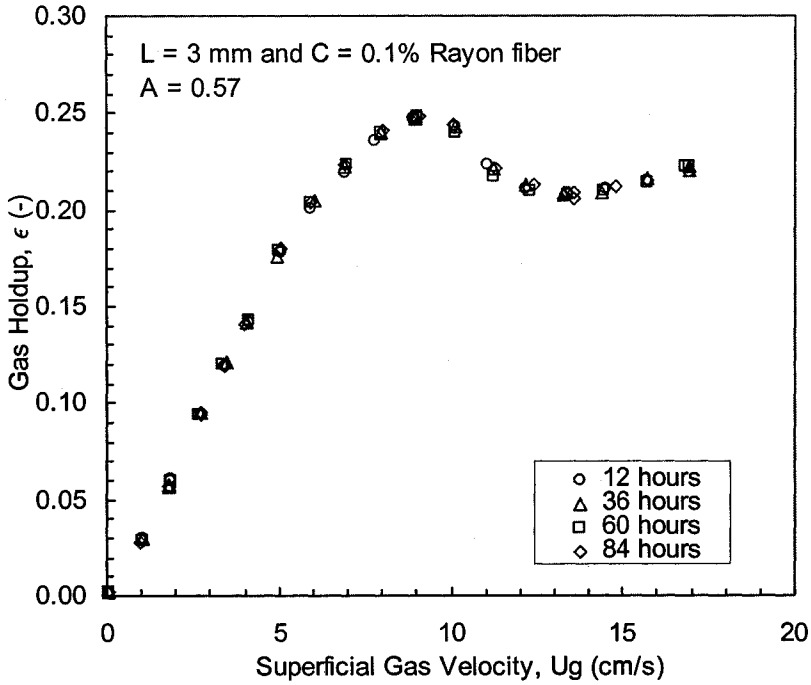

Figure 4.19: Gas holdup repeatability in a Rayon fiber suspension with A = 0.57%.

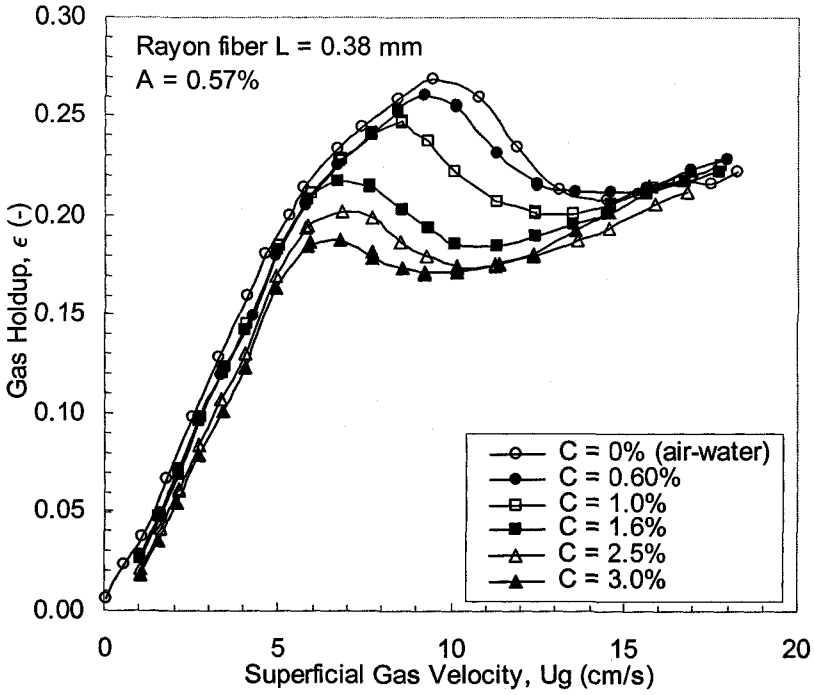

Figure 4.20: Gas holdup variations with fiber mass fraction in 0.38 mm long Rayon fiber suspensions with A = 0.57%.

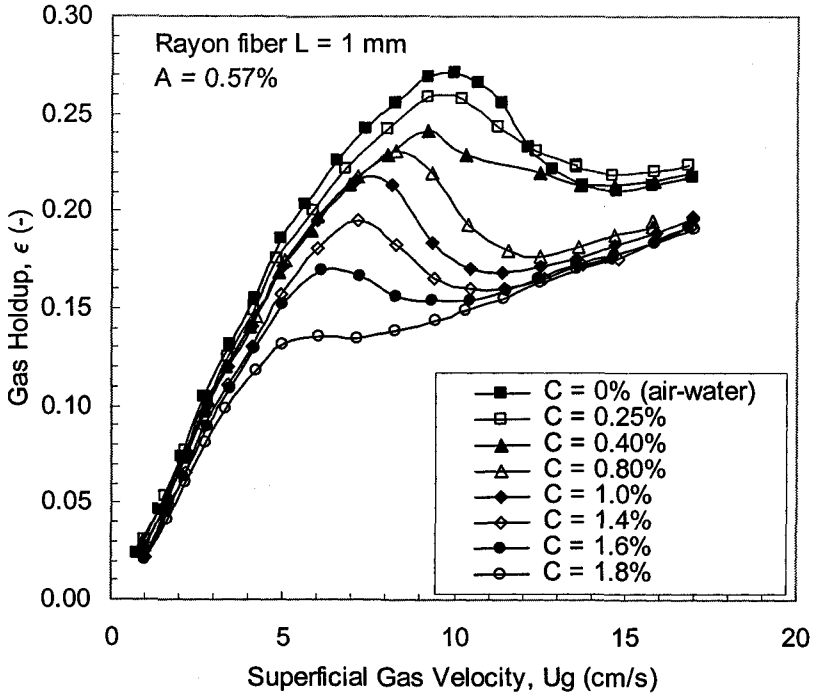

Figure 4.21: Gas holdup variations with fiber mass fraction in 1 mm long Rayon fiber suspensions with A = 0.57%.

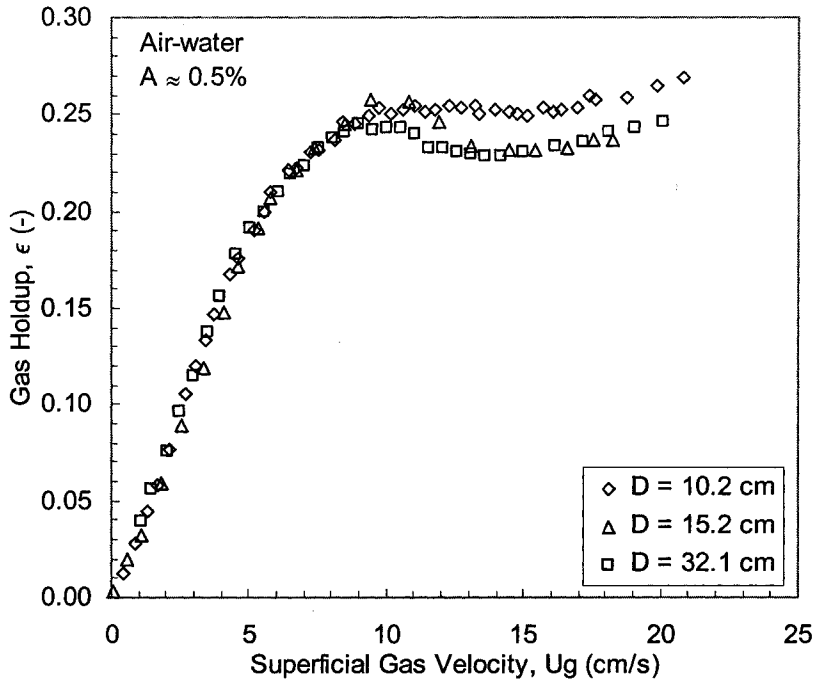

Figure 4.22: The effect of column diameter on gas holdup for an air-water system and a nominal open area ratio of A ≈ 0.5%.

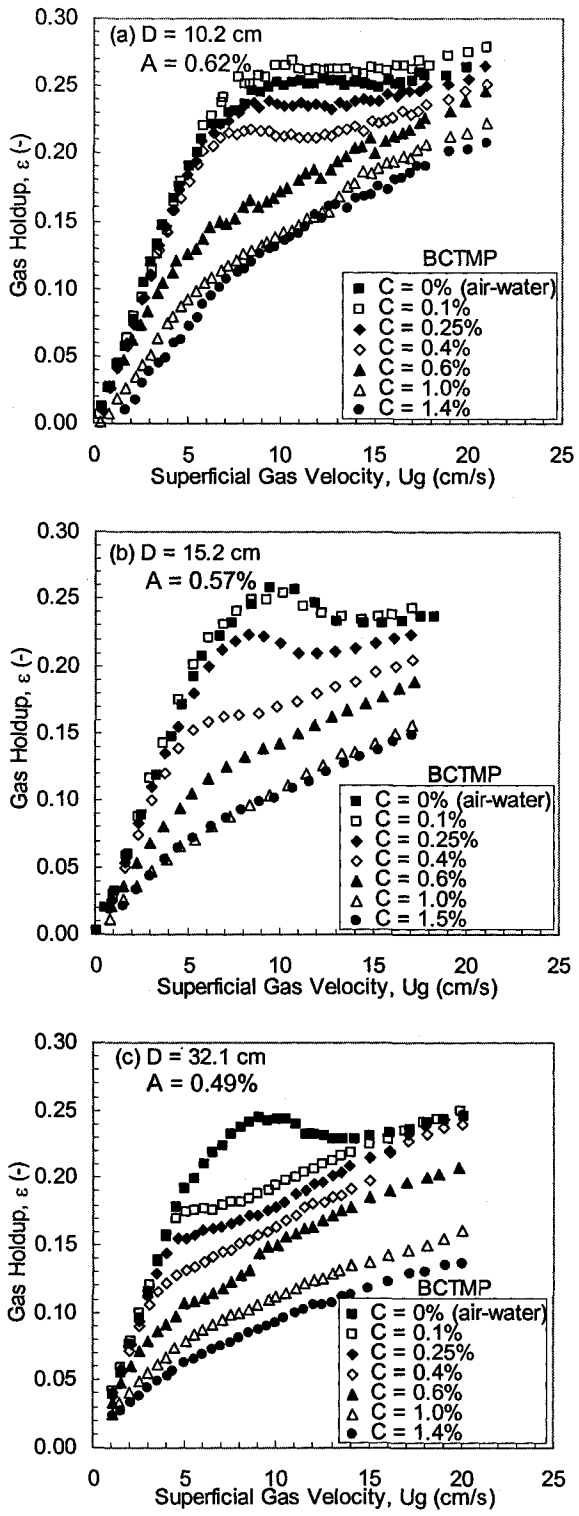

Figure 4.23: Gas holdup in BCTMP suspensions for different column diameters with A ≈ 0.5%; (a) D = 10.2 cm, (b) D = 15.2 cm, and (c) D = 32.1 cm.

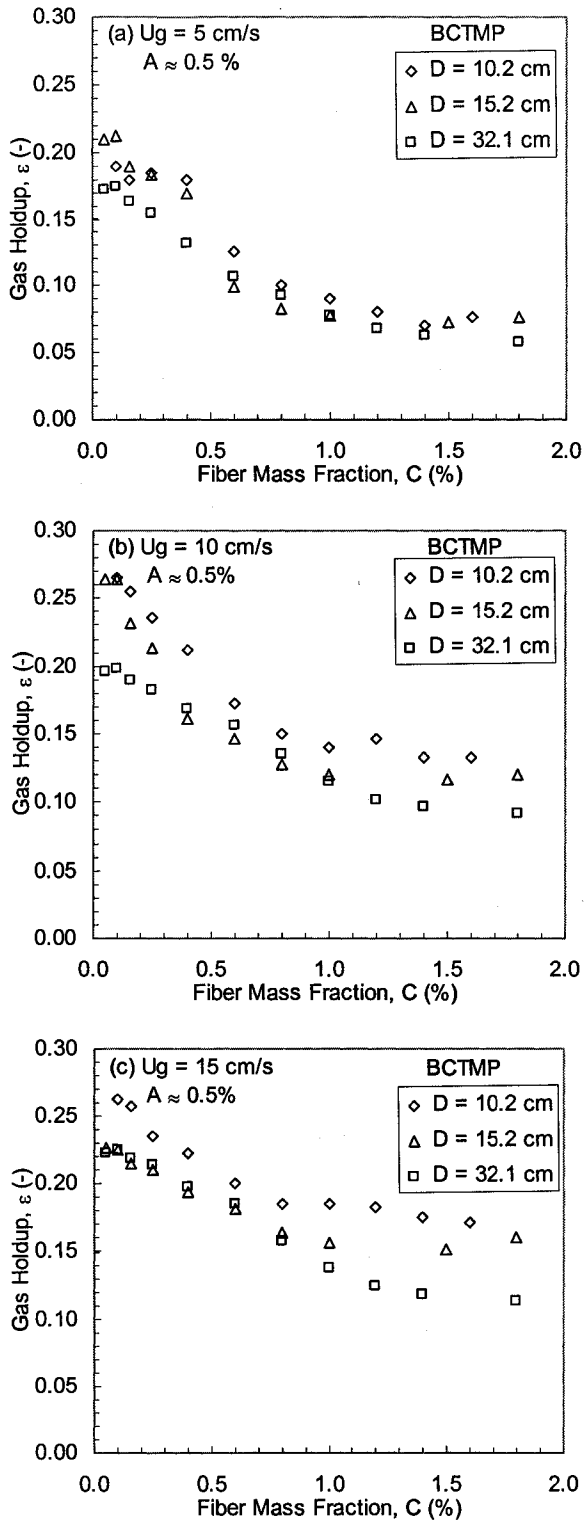

Figure 4.24: Gas holdup as a function of BCTMP fiber mass fraction for different column diameters at (a) Ug = 5 cm/s, (b) Ug = 10 cm/s, and (c) Ug = 15 cm/s.

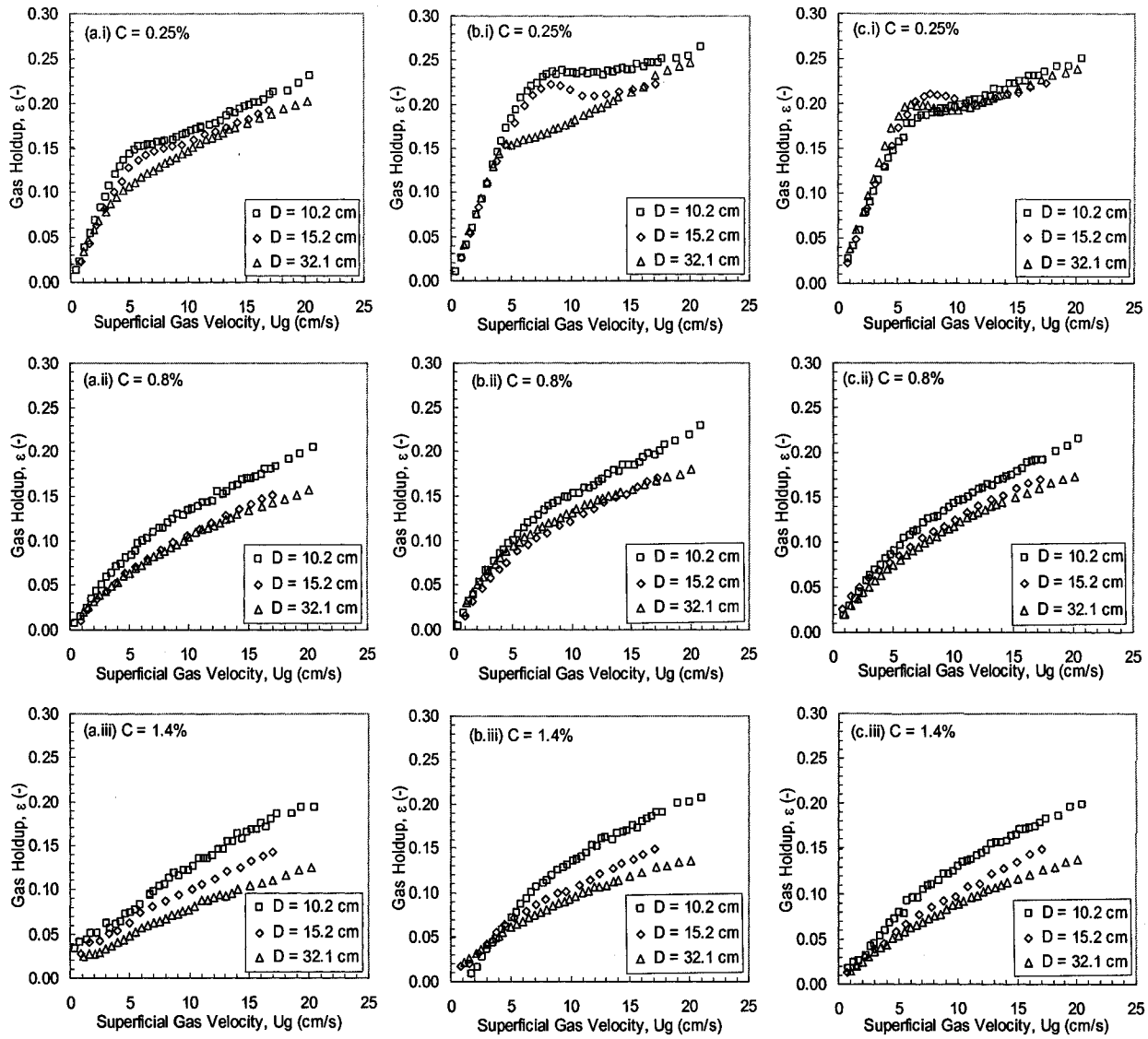

Figure 4.25: The comparison of gas holdup in three bubble columns at different fiber mass fraction; (a) softwood, (b) BCTMP, and (c) hardwood.

CHAPTER 5: GAS HOLDUP MODEL DEVELOPMENT

In this section, gas holdup models for A = 0.57%, 0.99%, and 2.14% are developed and compared with experimental data. The effects of superficial gas velocity (U_g), fiber type, fiber length (L), and fiber mass fraction (C) are included in the models. Note that in the models, superficial gas velocity, fiber length, and fiber mass fraction are in units of m/s, m, and percent, respectively. As suggested by the data in Chapter 4, gas holdup patterns as a function of superficial gas velocity follows general flow regime trends, depending on fiber mass fraction and aeration plate open area (Figure 5.1). Two flow patterns result as the fiber mass fraction increases: three-regime flow and pure heterogeneous flow. Thus, these two flow patterns will be studied separately.

For the three-regime flow, it has been shown in Chapter 4 that for A = 0.57% and 0.99%, there is a local maximum gas holdup with increasing superficial gas velocity, and this local maximum divides the transitional flow regime into two parts: the first part characterized by increasing gas holdup with increasing superficial gas velocity and the second part characterized by decreasing gas holdup with increasing superficial gas velocity; for A = 2.14%, no local maximum gas holdup appears. Therefore, for A = 0.57% and 0.99%, two different methods are used to deal with these two gas holdup behaviors (as shown in Figure 5.1): Model I for the homogeneous and the first part of the transitional flow regime and Model II for the second part of the transitional flow and heterogeneous flow regime. Model I is also used for the entire three-regime flow for A = 2.14% (i.e., it is applicable when homogeneous flow is initially observed at low gas flow rates and applied as long as gas

holdup increases with increasing superficial gas velocity). Model III is developed for pure heterogeneous flow for all three open area ratios. The models do not account for the effect of open area ratio. From Chapter 4, it is known that gas holdup is not a monotonic function of open area ratio and there is a critical open area ratio which generates a maximum gas holdup. However, there are only three open area ratios in the current study which do not provide enough information to determine an exact mathematic description of the open area ratio effect. Hence, Models I, II, and III have different coefficients and exponents for different open area ratios.

The models are developed using Rayon fiber suspensions with L = 3, 6, and 12 mm and C up to 1.8% in a D = 15.24 cm semi-batch bubble column for three open area ratios. In addition, data for A = 0.57% also includes softwood, hardwood, and BCTMP with C up to 1.8%. Note that data when $U_g < 1$ cm/s is not included in the models because when the gas flow rate is low, the gas holdup is also low and experimental error maybe significant ($> \pm$ 20%).

5.1 Influential Factors on Gas Holdup in Fiber Suspensions

This section identifies the factors that influence gas holdup in fiber suspensions that are considered in the gas holdup models. For completeness, a nondimensional analysis is summarized in Appendix A.

Fibers are flexible and of large aspect ratio, thus, fibers tend to flocculate and form network structures. This leads to a complex suspension rheology which has a significant effect on bubble behavior in fiber suspensions. Hence, factors that affect fiber flocculation

and the resulting suspension characteristics (i.e., yield stress, suspension viscosity, etc.) will influence gas holdup.

According to the literature review in Chapter 2, fiber flocculation is affected by fiber mass fraction, fiber aspect ratio, and fiber type, and the combination of these factors can be represented by the crowding number (N) (Kerekes and Schell, 1992). In addition, fiber stiffness (EI), friction coefficient, and fiber shape have a significant contribution to fiber flocculation (Schmid et al., 2000).

It has been shown that stiffness, fiber mass fraction, and fiber aspect ratio play important roles in yield stress (Bennington et al., 1990). Additionally, Wikstrom et al. (1998) found that the fiber length distribution has an important effect on network strength. Andersson et al. (1999) included fiber number density in the yield stress correlation.

Fiber concentration ($N_f L^3$) (Sundararajakumar and Koch, 1997), fiber stiffness (especially for large aspect ratio fibers) (Schmid et al., 2000), fiber shape (Joung et al., 2002), and fiber orientation (Petrich et al., 2000) also affect fiber suspension viscosity.

Fiber stiffness, friction coefficient, and shape are difficult to measure and control and depend, to some extent, on fiber origin (e.g., type) and processing conditions (Smook, 1992), hence, only fiber type, fiber mass fraction, and aspect ratio are considered in this gas holdup model development. Since the crowding factor (N) accounts for the effect of fiber mass fraction and aspect ratio on fiber flocculation, it will be used to replace fiber mass fraction and fiber aspect ratio in the models. The crowding factor also includes the effect of fiber coarseness. From the Eq. (2.7), fiber length has a more significant effect on flocculation than

fiber mass fraction. However, this relative importance between fiber mass fraction and fiber length does not apply to the effect on gas holdup. As shown in section 4.1.3, the same crowding number does not produce the same gas holdup and this phenomenon is attributed to the fact that the crowding number exaggerates the effect of fiber length on gas holdup, especially when fiber is long.

Fiber length has a significant effect on yield stress and suspension viscosity. Yield stress and suspension viscosity have two opposite effects on gas holdup: on one hand, they hinder bubble rise and thus increase bubble residence time, which tends to increase gas holdup; on the other hand, they enhance bubble coalescence and suppress bubble break up, which leads to a decrease in gas holdup. Gas holdup behavior is the combination of these two effects. Thus, fiber length does not affect gas holdup as much as it affects yield stress and effective viscosity. Therefore, the crowding factor may combine with another (other) quantity (quantities) to describe the fiber effect on gas holdup.

Fiber number density (N_f), with units of number of fibers per unit volume, was used by some researchers to account for the effect of fiber concentration on yield stress (Andersson et al., 1999) and suspension viscosity (Sundararajakumar and Koch, 1997). N_f is expressed as

$$N_f = \frac{\rho_w \frac{C}{100}}{\pi \frac{d^2}{4} L \rho_f} \tag{5.1a}$$

for Rayon fiber, and

$$N_f = n_f \frac{C}{100} \rho_{eff} \tag{5.1b}$$

for cellulose fiber, with n_f the number of fibers per gram of oven dry material, C the fiber mass fraction in percent, and ρ_{eff} effective fiber suspension density. For this study, cellulose fiber analysis was completed by Kimberly-Clark Corp. and provided $n_f = 21.4 \times 10^6$, 6.37×10^6, and 4.25×10^6 per gram for hardwood, softwood, and BCTMP fiber, respectively.

For fiber with a uniform diameter like Rayon, N_f is proportional to C/L in Eq. (5.1a). Thus, the combination of N_f with N adjusts the effect of fiber length.

5.2 Gas Holdup Model Development

5.2.1 Three-Regime Flow

This flow pattern exists when the fiber mass fraction is low. The critical fiber mass fraction at which the flow pattern changes from three-regime flow to pure heterogeneous flow differs for different open area ratios and fiber lengths. The fiber mass fraction range within which three-regime flow is observed is summarized in Table 5.1; this range becomes narrower with increasing fiber length and weakly depends on open area ratio.

Table 5.1: Fiber mass fraction (%) ranges within which three-regime flow occurs.

Open area ratio (A)	Rayon fiber L (mm)			Hardwood	Softwood	BCTMP
	3	6	12			
0.57%	C < 0.6	C < 0.4	C < 0.4	C < 0.6	C < 0.4	C < 0.6
0.99%	C < 0.6	C < 0.4	C < 0.4	-	-	-
2.14%	C < 0.6	C < 0.4	C < 0.25	-	-	-

5.2.1.1 Correlations for Superficial Gas Velocity at Which Local Maximum Gas Holdup is Reached (U_{gmax})

The superficial gas velocity at which the local maximum gas holdup is reached (U_{gmax}) is the demarcation of the conditions that apply to Model I and II; hence, it is necessary to determine a correlation of U_{gmax} for A = 0.57% and 0.99%. Kuncova and Zahradnik (1995) and Zahradnik et al. (1997) have showed that flow regime transition is affected by viscosity, and increasing viscosity enhances the flow regime transition. Thus, it can be predicted that U_{gmax} is influenced by fiber mass fraction and fiber length because they affect the fiber suspension effective viscosity. It is reasonable to assume that U_{gmax} is a function of N and N_f because they take into account the effect of fiber mass fraction and fiber length.

Figure 5.2 shows U_{gmax} as a function of NN_f for A = 0.57% and 0.99%, respectively. It is seen that U_{gmax} decreases with increasing NN_f (i.e., with increasing fiber mass fraction and fiber length). This is consistent with the observations of Kuncova and Zahradnik (1995) and Zahradnik et al. (1997) that flow regime transition is enhanced by increasing the suspension viscosity (by increasing the fiber mass fraction and fiber length). It also shows that U_{gmax} can be assumed to be a log function of NN_f. Since the data are still scattered for both A's, it is suggested to change NN_f to $N^aN_f^b$. Thus, a correlation for U_{gmax} may take on the form

$$U_{gmax} = a_1 + \ln(N^{a_2} N_f^{a_3}) \tag{5.2}$$

The coefficient a_1 and exponents a_2 and a_3 are determined by nonlinear curve fitting using MATLAB. The U_{gmax} correlations are:

$$U_{gmax} = 0.21 + \ln(N^{-0.0053} N_f^{-0.005}) \qquad (A= 0.57\%) \tag{5.3}$$

$$U_{gmax} = 0.27 + \ln(N^{-0.011} N_f^{-0.007}) \qquad (A = 0.99\%) \qquad (5.4)$$

The comparisons of predicted and experimental U_{gmax} are shown in Figure 5.3 for A = 0.57% and 0.99%. The models reproduce most U_{gmax} data within ± 10%. It is noted that the experimental U_{gmax} is not a clearly defined value but may occur over a certain range. Also, U_{gmax} is sensitive to the liquid properties (Maruyama et al., 1981) which may change if any fiber additives leach into the suspension water, and the coalescing behavior of the liquid which can change by the presence of trace impurities (Krishna et al., 1999a). This partly contributes to the data scatter in Figure 5.3.

5.2.1.2 Model I

5.2.1.2.1 Homogeneous and the first part of the transitional flow regime (A = 0.57% and 0.99%)

Based on a force balance on bubbles bubbling through a bubble column, Mersmann (1978) derived a gas holdup correlation in a dilute bubble swarm. It was assumed that bubble motion was in a quasi-steady state, hence, the velocity of the bubble in a swarm was determined by the balance of the buoyant and drag forces.

$$C_d \frac{\pi d_b^{\,2}}{4} \frac{\rho_c v_r^2}{2} = \frac{\pi d_b^{\,3}}{6} \Delta\rho_d g \qquad (5.5)$$

where C_d is the bubble drag coefficient in a swarm, d_b is the bubble diameter, v_r is the relative bubble velocity, ρ_c is the density of the continuous phase, and $\Delta\rho_d$ is the density difference between the mixture (gas and liquid) and gas.

In the present study, ρ_c is the effective fiber–water slurry density (ρ_{eff}), and $\Delta\rho_d$ is the density difference between gas-liquid-fiber mixture and bubbles. Additionally, v_r and $\Delta\rho_d$ are, respectively:

$$v_r = \frac{U_g}{\varepsilon} \tag{5.6}$$

for a semi-batch bubble column and

$$\Delta\rho_d = \rho_m - \rho_g = (1-\varepsilon)(\rho_{eff} - \rho_g) = (1-\varepsilon)\Delta\rho \tag{5.7}$$

where ρ_m is the density of the gas-liquid-fiber system and can be calculated from

$$\rho_m = \varepsilon\rho_g + (1-\varepsilon)\rho_{eff} \tag{5.8}$$

Substituting Eq. (5.6) and Eq. (5.7) into Eq. (5.5) and rearranging yields

$$\varepsilon(1-\varepsilon)^{1/2} = c\left(\frac{C_d}{d_b}\right)^{1/2} U_g \tag{5.9}$$

where $c = \left(0.75\frac{\rho_{eff}}{\Delta\rho g}\right)^{1/2}$. In the present study, fiber addition has a negligible effect on the overall slurry density, so c is assumed to be constant.

Based on other researchers' experimental data, Mersmann (1978) suggested a more exact expression obtained by a modification of Eq. (5.9) as follows:

$$\varepsilon(1-\varepsilon)^{n} = c\left(\frac{C_d}{d_b}\right)^{1/2} U_g \tag{5.10}$$

The exponent n depends on the density ratio of the continuous phase to the disperse phase. When the ratio is greater than 200, n = -4. This agrees with the result of Akita and Yoshida (1973). For the present study, the continuous phase can be assumed to be a homogeneous

water-fiber slurry and the dispersed phase is air. For these conditions, the density ratio is greater than 200, thus, n = -4 for this model.

Mersmann (1978) also discussed in detail that both C_d and d_b are functions of fluid properties, such as surface tension, viscosity, and density difference between the two phases. For the experimental conditions in the present study, it is assumed that in these three quantities, only the effective viscosity varies with fiber addition. The effective viscosity depends on fiber type, fiber mass fraction, fiber length, and shear rate (Joung et al., 2001). Switzer and Klingenberg (2003) argued that the effective viscosity is a function of N_fL^3 and increases with increasing N_fL^3. As $N_f \propto C/(d^2L)$, $N_fL^3 \propto CL^2/d^2$. It is known that the crowding number $N \propto CL^2/d^2$; thus, the effective viscosity is a function of the crowding number N. Shamlou et al. (1998) and Al-Masry (1999) showed that shear rate is a function of superficial gas velocity in non-Newtonian liquids, which indicates that the effective viscosity in a fiber suspension is also a function of superficial gas velocity.

In addition, yield stress has an important effect on bubble diameter. The bubble diameter is required to be large enough to produce enough buoyant force to break through the fiber network (Pelton and Piette, 1992; Walmsley, 1992; Su and Heindel, 2003). Andersson et al. (1999) reported that the number of fiber-fiber contacts has an important contribution to yield stress, which is proportional to fiber number density N_f.

Therefore, it is reasonable to introduce two quantities, the crowding number (N) and the fiber number density (N_f), to account for the fiber effect on effective slurry viscosity and yield stress, which have a significant effect on the drag coefficient and bubble diameter. The

influence on the bubble diameter is visually apparent; increasing the fiber mass fraction (i.e. N and N_f) increases the bubble diameter (Heindel, 1999; Heindel and Garner, 1999). Additionally, Hebrard et al. (1996) observed that bubble diameter depends on superficial gas velocity and is related to gas distributor type. They determined that for a perforated plate gas distributor (which is the case in the present study), bubble diameter decreases with increasing U_g.

Based on the above analysis, the quantity C_d/d_b should be a function of U_g, N_f, and N. Hence, Eq. (5.10) can be rewritten as

$$\frac{\varepsilon}{(1-\varepsilon)^4} = f(U_g, N_f, N)U_g \tag{5.11}$$

Figures 5.4 and 5.5 plot $\varepsilon/(1-\varepsilon)^4$ as functions of U_g and NN_f, respectively, for A = 0.99%. The log-log scale in these figures reveals a straight line dependence, indicating that $\varepsilon/(1-\varepsilon)^4$ can be expressed as a power function of U_g and NN_f. The product NN_f is proportional to C^2L, which implies that the effect of fiber mass fraction (to the power 2) is more important than fiber length (to the power 1). This is consistent with the observations in Chapter 4 that when the fiber is long, the fiber length effect is less significant than fiber mass fraction. Although $\varepsilon/(1-\varepsilon)^4$ correlates well with NN_f in Figure 5.5 for A = 0.99%, the data are scattered for A = 0.57% when $\varepsilon/(1-\varepsilon)^4$ is plotted as a function of NN_f (Figure 5.6). Hence, a N and N_f variation in the form $N^aN_f^b$, as opposed to $(NN_f)^\alpha$, may be more appropriate to may be more appropriate to generalize it to more conditions (i.e., other open area ratios or other bubble column diameters). Therefore, a gas holdup model is proposed in the following form

$$\frac{\varepsilon}{(1-\varepsilon)^4} = a_1 U_g^{a_2} N^{a_3} N_f^{a_4} \tag{5.12}$$

The coefficient a_1 and exponents a_2, a_3, and a_4 in Eq. (5.12) are determined by nonlinear curve fitting tools in MATLAB. Thus, the resulting gas holdup correlations are:

$$\frac{\varepsilon}{(1-\varepsilon)^4} = 40.5 U_g^{1.4} N^{-0.146} N_f^{-0.006} \qquad (A = 0.57\%) \tag{5.13}$$

and

$$\frac{\varepsilon}{(1-\varepsilon)^4} = 183.7 U_g^{1.289} N^{-0.128} N_f^{-0.106} \qquad (A = 0.99\%) \tag{5.14}$$

Table 5.2 summarizes the various model parameters and provides a 95% confidence interval for the coefficients and exponents.

Table 5.2: Coefficient and exponents in Model I Eq. (5.12) and their 95% confidence interval for A = 0.57% and 0.99%.

	A = 0.57%			A = 0.99%		
	a_i	95% confidence interval		a_i	95% confidence interval	
a_1	40.5	30.9	52.9	183.7	126.280	267.227
a_2	1.4	1.372	1.428	1.289	1.265	1.313
a_3	-0.146	-0.164	-0.128	-0.128	-0.144	-0.112
a_4	-0.006	-0.017	0.005	-0.106	-0.123	-0.088

Figuers 5.7 and 5.8 compare the predicted results with the experimental data. It can be seen from the graph that 94% (214 out of 225) and 98.4% (125 out of 127) of the data can be predicted within ±15%, and the average absolute deviations are 3.7% and 4.5% for A = 0.57% and 0.99%, respectively.

Equations (5.13) and (5.14) show that the exponents of N and N_f are negative, indicating that gas holdup decreases with increasing N and N_f. This is consistent with the physical mechanism: the larger N and N_f, the larger viscosity and yield stress, which leads to the larger bubble diameter and faster bubble rise velocity, resulting in smaller gas holdup.

5.2.1.2.2 Homogenous, transitional, and heterogeneous flows (A = 2.14%)

For this open area ratio, there is no maximum gas holdup over the range of superficial gas velocity. It is convenient that all three flow regimes are considered in one model. Although Model I is based on the assumption of a quasi-steady state, Mersmann (1978) argued that the resulting expression for gas holdup is applicable to heterogeneous flow. Akita and Yoshida (1973) applied the similar correlation as Mersmann (1978) to a wide range of superficial gas velocity encompassing both homogeneous and heterogeneous flow. Also, good agreement of the predictions with experimental data shown in Figure 5.9 proves that this model is also applicable to heterogeneous flow.

Through a nonlinear curve fitting package in MATLAB, the gas holdup correlation for three-flow-regime with A = 2.14% is

$$\frac{\varepsilon}{(1-\varepsilon)^4} = 26.52 U_g^{0.781} N^{-0.11} N_f^{-0.11} \tag{5.15}$$

The 95% confidence intervals for the coefficient and exponents are listed in Table 5.3.

Figure 5.9 shows the comparison between predicted gas holdup and experimental data. It is shown that Eq (5.15) can produce 96% (155 out of 162) of the data within ±15%. The average absolute deviation is 6.9%.

Table 5.3: Coefficient and exponents in Model I Eq. (5.12) and their 95% confidence interval for A = 2.14%.

	A = 2.14%		
	a_i	95% confidence interval	
a_1	26.52	15.30	45.96
a_2	0.781	0.754	0.809
a_3	-0.112	-0.135	-0.090
a_4	-0.110	-0.135	-0.084

Equation (5.15) shows that at a given superficial gas velocity, gas holdup decreases with increasing N and N_f for the range of superficial gas velocity. It is noted that when A = 2.14%, gas holdup depends on U_g to the power less than 1 instead of greater than 1 (as for A = 0.57% and 0.99%), which indicates that when A = 2.14%, gas holdup increases with increasing superficial gas velocity less than when A = 0.57% or 0.99%. This can be attributed to the fact that for A = 2.14%, bubbles tend to coalesce near the distribution plate with increasing U_g because of the small hole spacing, resulting in an increased probability of bubble interactions with bubbles from adjacent holes.

5.2.1.3 Model II

5.2.1.3.1 Heterogeneous and the second part of the transitional flow regime (A = 0.57% and 0.99%)

After a maximum gas holdup is reached when A = 0.57% and 0.99%, a local minimum gas holdup is observed before heterogeneous flow is reached (see Figure 5.1). However, when $U_g/(1-\varepsilon)$ is plotted as a function of U_g for various fiber mass fraction, a straight line results (Figure 5.10).

Figure 5.10 also shows that for each open area ratio, the difference among slopes is negligible, but the intercepts change with different fiber lengths and mass fractions. Therefore, the correlation for this regime is assumed to follow:

$$\frac{U_g}{1-\varepsilon} = a_1 U_g + f(C,L) \tag{5.16}$$

As with Model I, N and N_f are used to account for the effect of C and L. The effects of N and N_f on the intercept f(C, L) are shown in Figure 5.11 and Figure 5.12, respectively, for A = 0.57% and 0.99%. These figures reveal the data are widely scattered. However, when data are plotted as a function of the parameter $N^a N_f^b$, where a and b are different for different open area ratios and determined through trial and error (as shown in Figure 5.13), the trend becomes clear: f(L, C) decreases with increasing $N^a N_f^b$ and follows a logarithmic function well. Additionally, to generalize $U_g/(1-\varepsilon)$, U_g is assumed to vary as a power function. Hence, the correlation for the second part of the transitional and the heterogeneous flow regime for A = 0.57% and 0.99% is proposed to be

$$\frac{U_g}{1-\varepsilon} = a_1 U_g^{a_2} + \ln\left(N^{a_3} N_f^{a_4}\right) + a_5 \tag{5.17}$$

The coefficients a_1 and a_5 and exponents a_2, a_3, and a_4 for A = 0.57% and 0.99% and their 95% confidence interval are listed in Table 5.4. Note that from Table 5.4, the exponents a_3 and a_4, respectively, of N_f and N in the proposed model (Eq. (5.17)) are different from those shown on the x-axis in Figure 5.13, but the corresponding ratios of the two exponents are similar.

Table 5.4: Coefficients and exponents in Model II Eq. (5.17) for A = 0.57% and 0.99%.

	A = 0.57%			A = 0.99%		
	a_i	95% confidence interval		a_i	95% confidence interval	
a_1	1.617	1.4670	1.7663	1.469	1.258	1.68
a_2	1.209	1.1352	1.2826	1.1267	1.0	1.25
a_3	-0.0039	-0.0043	-0.0036	-0.0039	-0.0044	-0.0035
a_4	-0.0013	-0.0015	-0.0011	-0.0026	-0.0031	-0.0021
a_5	0.0648	0.0548	0.0747	0.0817	0.0605	0.1029

Figure 5.14 shows that the model can produce 97% (207 out of 214) of the data within ±15% for A = 0.57%, and Figure 5.15 shows that the model can produce 99% (93 out of 94) data within ±15%. Average absolute deviations are 4.4% and 4.7%, for A = 0.57% and 0.99%, respectively.

5.2.2 Pure Heterogeneous Flow Regime (A = 0.57%, 0.99%, and 2.14%)

5.2.2.1 Model III

Model III is used to describe the flow when pure heterogeneous flow is observed at all superficial gas velocities (see Figure 5.1), and it is based on the Zuber and Findlay drift flux model (Zuber and Findlay, 1965). The drift flux model considers the mixture as a whole and reduces the difficulties associated with interface interactions. For a semi-batch bubble column, the drift velocity is expressed by

$$V_{oj} = v_g - U_g \tag{5.18}$$

thus,

$$v_g = \frac{U_g}{\varepsilon} = V_{oj} + U_g \tag{5.19}$$

The average gas velocity (averaged over the cross-sectional area of the bubble column) is obtained by

$$\langle v_g \rangle = \left\langle \frac{U_g}{\varepsilon} \right\rangle = \langle U_g \rangle + \langle V_{oj} \rangle \tag{5.20}$$

where, for example, the average value of quantity F is defined by

$$\langle F \rangle = \frac{1}{A} \int_A F dA \tag{5.21}$$

Hence, the weighted mean gas velocity $\bar{v}_g$ is given by

$$\bar{v}_g = \frac{\langle v_g \varepsilon \rangle}{\langle \varepsilon \rangle} = \frac{\langle U_g \rangle}{\langle \varepsilon \rangle} = C_o \langle U_g \rangle + \frac{\langle \varepsilon V_{oj} \rangle}{\langle \varepsilon \rangle} \tag{5.22}$$

where the distribution parameter $C_o = \dfrac{\langle \varepsilon U_g \rangle}{\langle \varepsilon \rangle \langle U_g \rangle}$ is constant for a specified flow pattern and reflects the effect of the nonuniform flow and gas holdup profiles. For uniform flow $C_o = 1$. However, in general, C_o depends on flow regime, pressure, channel geometry, and flow rates (Wallis, 1969). The nomenclature <> is typically omitted from the drift flux model for convenience.

Zuber and Finlay (1965) argued that the weighted mean drift velocity $\dfrac{\langle \varepsilon V_{oj} \rangle}{\langle \varepsilon \rangle} \approx V_{oj}$ represents the terminal bubble rise velocity for heterogeneous flow, and the value is independent of bubble size. In this model V_{oj} is called the terminal bubble rise velocity. For heterogeneous flow, the plot of the weighted mean gas velocity ($\bar{v}_g$) against U_g is a straight line whose slope represents C_o and intercept is the terminal bubble rise velocity.

Plots of U_g/ε against U_g for different fiber mass fractions and fiber lengths are shown in Figure 5.16. The slopes are weakly dependent on fiber length and mass fraction for A = 0.57%, however, the intercepts, representing terminal bubble rise velocities, are influenced by fiber mass fraction and length. Similar behavior is observed for A = 0.99% and 2.14%. By using Eq. (5.22), the drift flux parameter C_o and terminal bubble rise velocity are determined for different fiber mass fractions and fiber lengths with A = 0.57%, 0.99% and 2.14% and shown in Figures 5.17 and 5.18, respectively.

Figure 5.17 shows that C_o can be approximated by a constant for different fiber lengths and fiber mass fractions for all A = 0.57%, 0.99%, and 2.14%.

Figure 5.18 shows that the terminal bubble rise velocity is a function of fiber mass fraction and length and increases with increasing fiber mass fraction for all three fiber lengths. When the fiber mass fraction is high, terminal bubble rise velocity varies only slightly with fiber mass fraction.

Based on the above analysis, the gas holdup model for this flow regime can be assumed to be

$$\frac{U_g}{\varepsilon} = C_o U_g + g(C,L) \tag{5.23}$$

where g(C, L) represents the terminal bubble rise velocity V_{oj}. Assume g(C, L) can be described by a functional relationship involving N and N_f,

$$V_{oj} = g'(N, N_f) \tag{5.24}$$

Terminal bubble rise velocities for different fiber mass fractions and lengths are plotted as a function of the parameter $N^aN_f^b$ (a = b for all three open area ratios by trail and error) in Figure 5.19. The figure shows that the terminal bubble rise velocities for each open area ratio gather into one single line and follow a logarithmic function of $N^aN_f^b$. Therefore, the gas holdup model for pure heterogeneous flow is proposed to be of the form

$$\frac{U_g}{\varepsilon} = C_o U_g + \ln\left(N^{C_1} N_f^{C_2}\right) + C_3 \tag{5.25}$$

Table 5.5 lists the coefficients and exponents of Eq. (5.25) and their 95% confidence intervals.

Table 5.5: Coefficients and exponents of Eq. (5.25) for A = 0.57%, 0.99%, and 2.14%.

	A = 0.57%			A = 0.99%			A = 2.14%		
	C_i	95% confidence interval		C_i	95% confidence interval		C_i	95% confidence interval	
C_o	3.0	2.917	3.077	3.11	3.03	3.18	3.13	3.04	3.21
C_1	0.078	0.073	0.083	0.069	0.065	0.073	0.057	0.053	0.061
C_2	0.044	0.041	0.047	0.074	0.068	0.080	0.053	0.048	0.059
C_3	-0.917	-1.01	-0.823	-1.50	-1.644	-1.346	-0.958	-1.097	-0.818

From Table 5.5, the distribution parameter C_o for all three open area ratios is very close, which indicates that when the fiber mass fraction is high, the influence of open area ratio on gas holdup distribution is negligible. This implies that for high fiber mass fraction suspensions, bubble behavior is weakly dependent on gas distribution plate and mainly depends on slurry mixing.

Figures 5.20 – 5.22 show the comparison of predicted gas holdup to experimental data for A = 0.57%, 0.99%, and 2.14%, respectively. It is shown that the model produces 99% (581 out of 587) of the data for A = 0.57%, 100% (305 out of 305) of the data for A = 0.99%, and

99% (397 out of 401) of the data for A = 2.14% within ±15%. The average absolute deviations are 5.0%, 3.3%, and 3.8%, for A = 0.57%, 0.99%, and 2.14%, respectively.

5.3 Model Evaluation

The models that were developed for a 15.2 cm semi-batch bubble column were applied to data obtained in a 32.1 cm ID semi-batch bubble column with a perforated plate gas distributor with A = 0.49% (Hol, 2005). The gas holdup behavior in the large bubble column is similar to that of D = 15.2 cm with A = 0.57%. Based on these data, model coefficients and exponents are determined to be

$$\frac{\varepsilon}{(1-\varepsilon)^4} = 30.8 U_g^{1.326} N^{-0.115} N_f^{-0.0113} \qquad \text{(Model I)} \qquad (5.26)$$

$$\frac{U_g}{1-\varepsilon} = 1.57 U_g^{1.15} + \ln(N^{-0.0022} N_f^{-0.0012}) + 0.044 \qquad \text{(Model II)} \qquad (5.27)$$

and

$$\frac{U_g}{\varepsilon} = 4.1 U_g + \ln(N^{0.119} N_f^{0.0756}) - 1.8411 \qquad \text{(Model III)} \qquad (5.28)$$

Figures 5.23 – 5.25 compare the predicted and experimental data. It shows that the predictions agree well with experimental data: Eqs. (5.26) - (5.28) can reproduce, respectively, 99.3% (285 out of 287) of the data for Model I, 99.7% (369 out of 370) of the data for Model II, and 98% (1147 out 1167) of the data for Model III within ±15%. The good agreement between the predictions and experimental data proves that Model I, II, and III can be successfully used to reproduce gas holdup for gas-liquid-fiber semi-batch bubble columns with perforated gas distributors.

Figure 5.26 compares the experimental data and their predictions at selected fiber mass fractions for L = 3 mm Rayon fiber with A = 0.99%.

5.4 Summary

Three basic gas holdup models are developed to predict gas holdup for (i) the homogeneous and the first part of the transitional flow regime (A = 0.57% and 0.99%) and the entire three-regime flow (A = 2.14%), (ii) the second part of the transitional and the heterogeneous flow regime (A = 0.57% and 0.99%), and (iii) pure heterogeneous flow regime (A = 0.57%, 0.99%, and 2.14%). The models can reproduce most of the data within ±15% for the bubble column used in this study (D = 15.2 cm), as well as a similar bubble column (D = 32.1 cm) used in a companion study. A significant limitation of the models, due to limited experimental data, is that the model coefficients and exponents vary with different bubble column diameters and open area ratios; thus, they currently can not be used for scale-up.

A reliable parameter was show to be $N^aN_f^b$ in both U_{gmax} and the gas holdup modes to take into account the complex effect of fiber type, fiber mass fraction, and fiber length. The exponents a and b are functions of bubble column flow regime, open area ratio, and column diameter, but independent of fiber type and length.

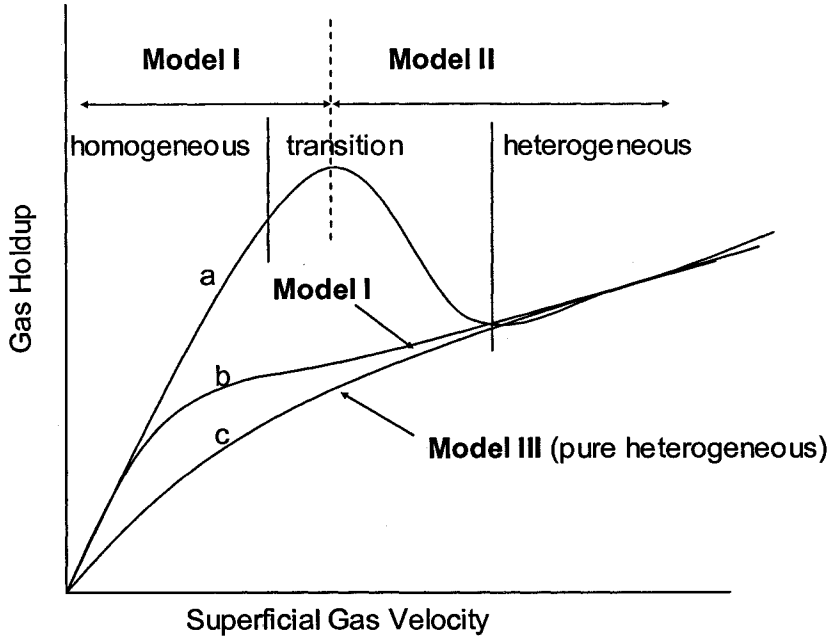

Figure 5.1: Gas holdup models for different flow regimes.

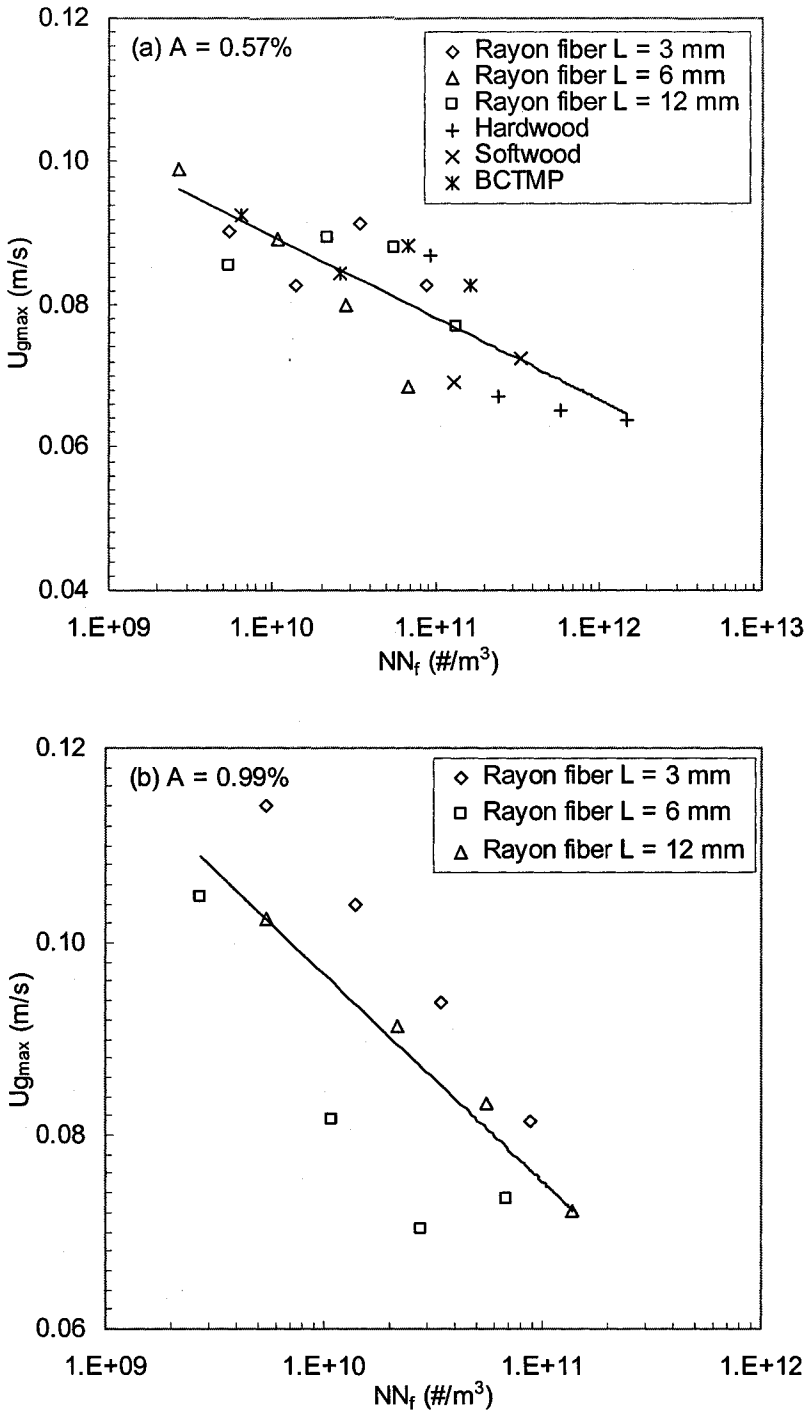

Figure 5.2: U_{gmax} as a function of NN_f for (a) A = 0.57% and (b) A = 0.99%.

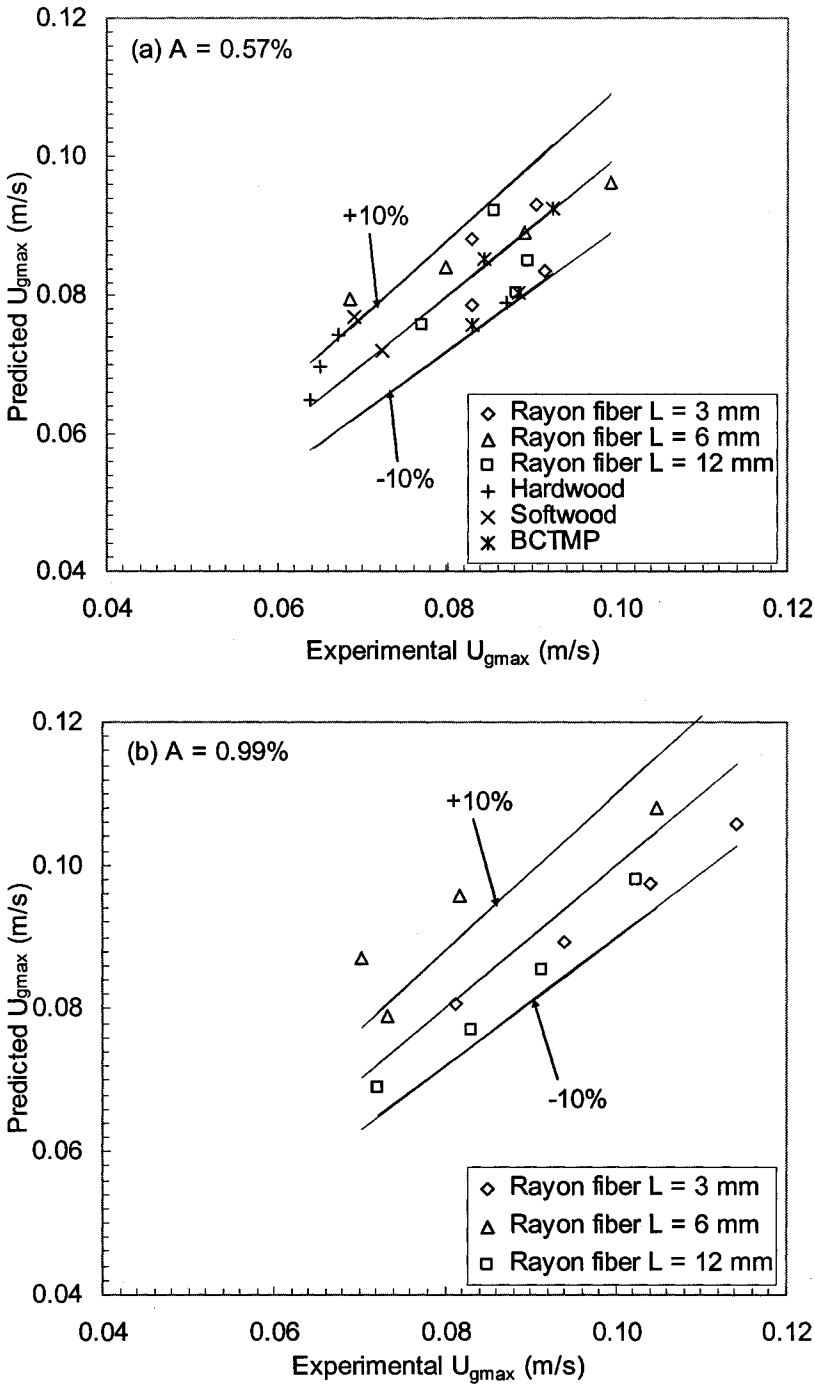

Figure 5.3: The comparison of predicted and experimental U_{gmax} for (a) A = 0.57% and (b) A = 0.99%

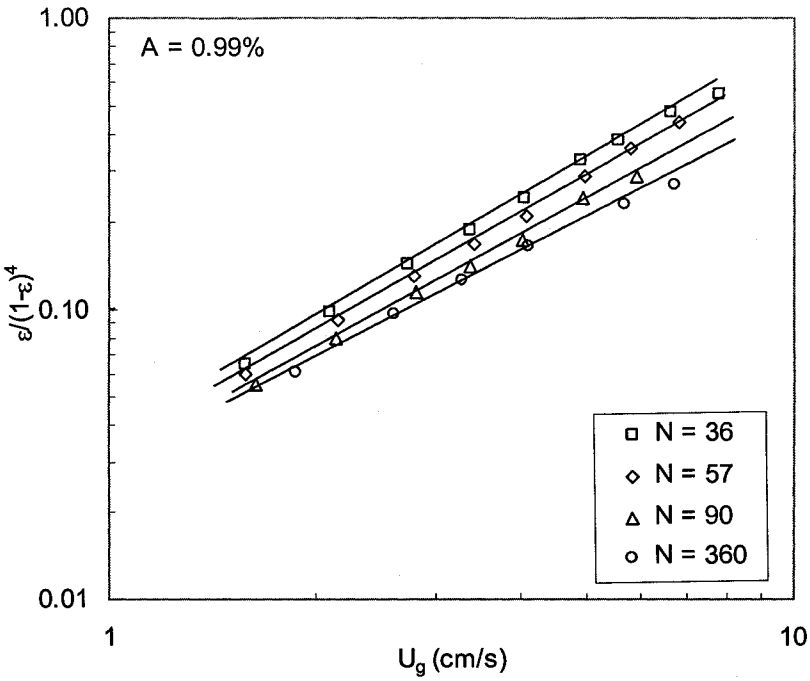

Figure 5.4: The effect of superficial gas velocity on $\varepsilon/(1-\varepsilon)^4$ for A = 0.99%.

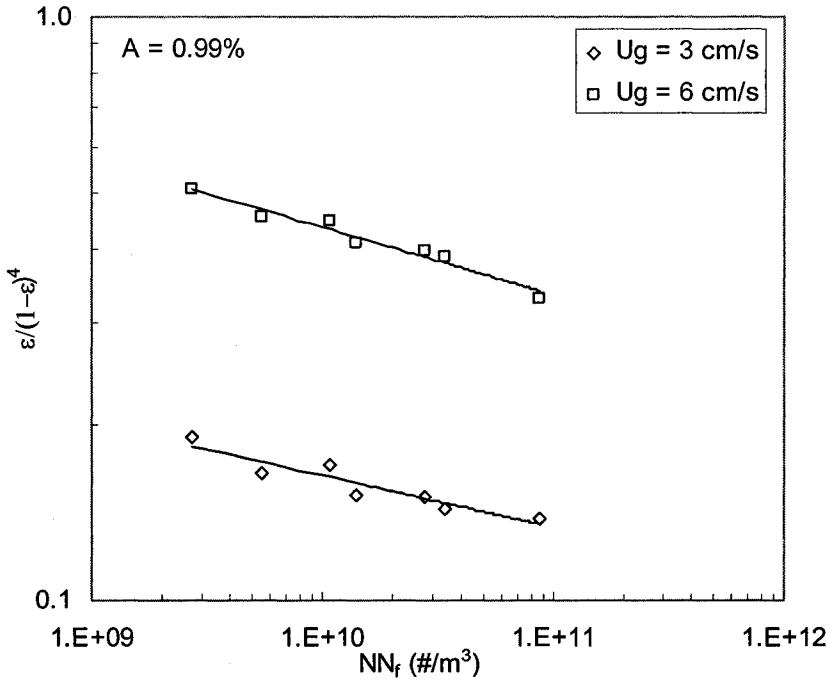

Figure 5.5: The effect of the product of crowding factor and fiber number density on $\varepsilon/(1-\varepsilon)^4$ for A = 0.99%.

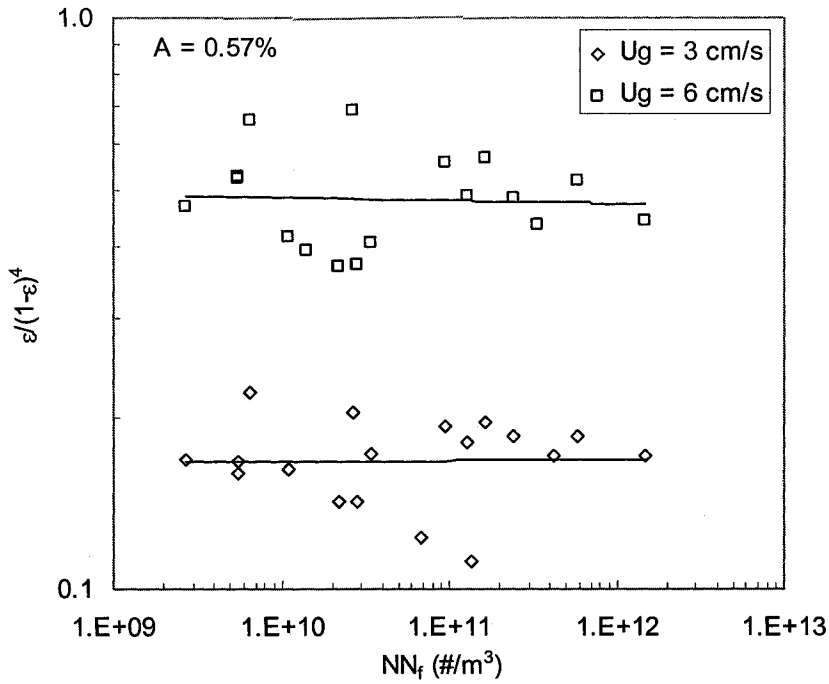

Figure 5.6: The effect of the product of crowding factor and fiber number density on $\varepsilon/(1-\varepsilon)^4$ for A = 0.57%.

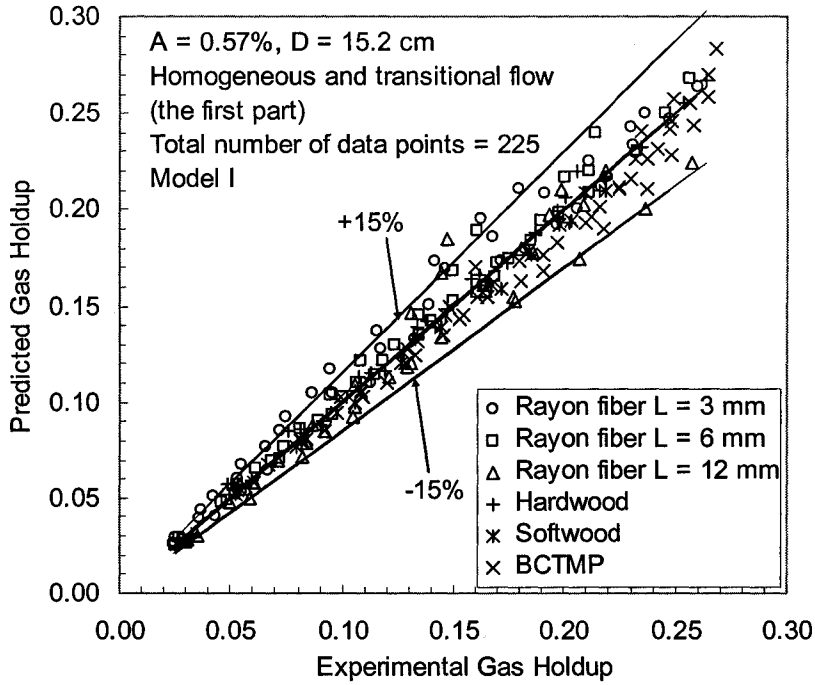

Figure 5.7: Comparison of the experimental values of gas holdup with those predicted from Eq. (5.13) for A = 0.57%.

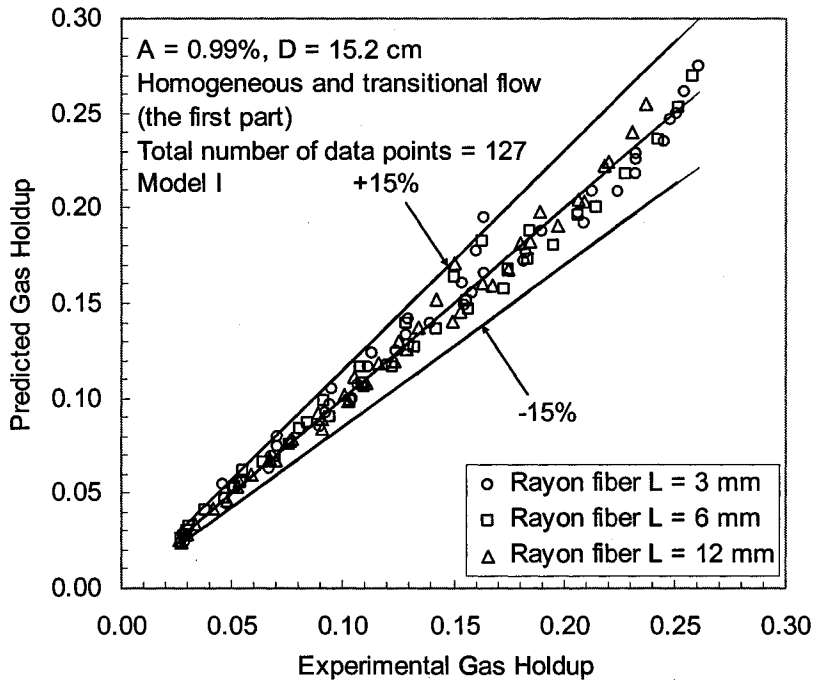

Figure 5.8: Comparison of the experimental values of gas holdup with those predicted from Eq. (5.14) for A = 0.99%.

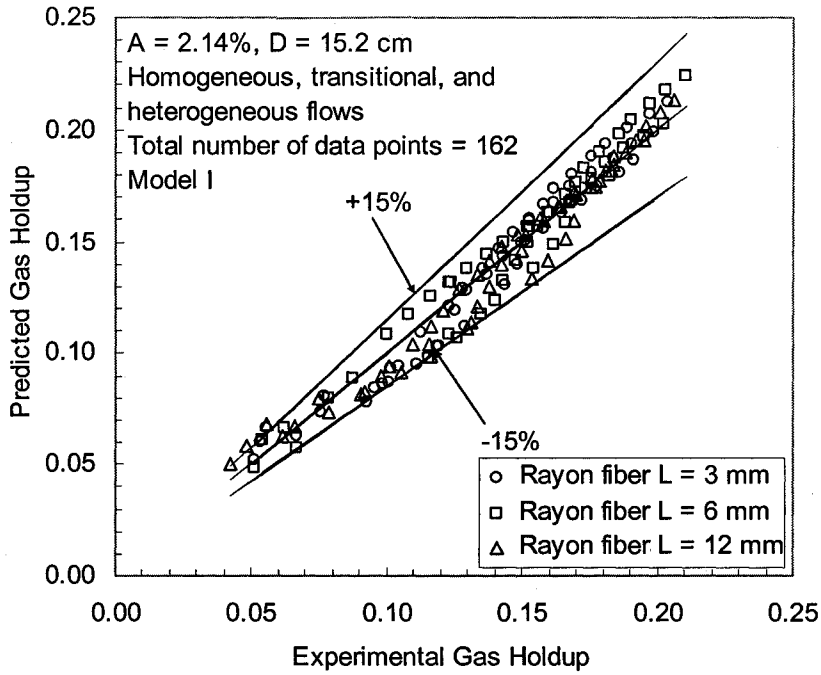

Figure 5.9: Comparison of the experimental values of gas holdup with those predicted from Eq. (5.15) for A = 2.14%.

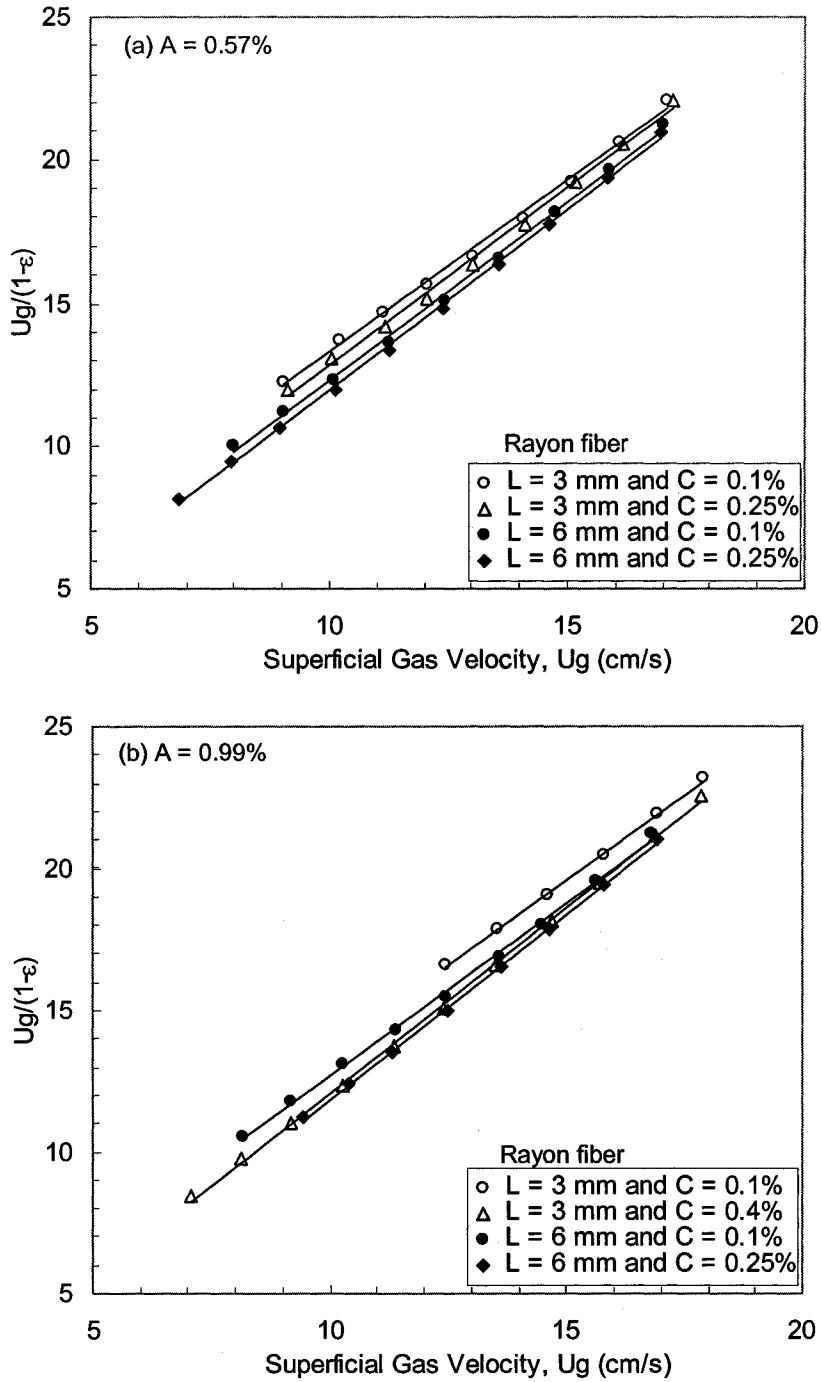

Figure 5.10: $U_g/(1-\varepsilon)$ as a function of superficial gas velocity for different fiber lengths and mass fractions with (a) A = 0.57% and (b) A = 0.99%.

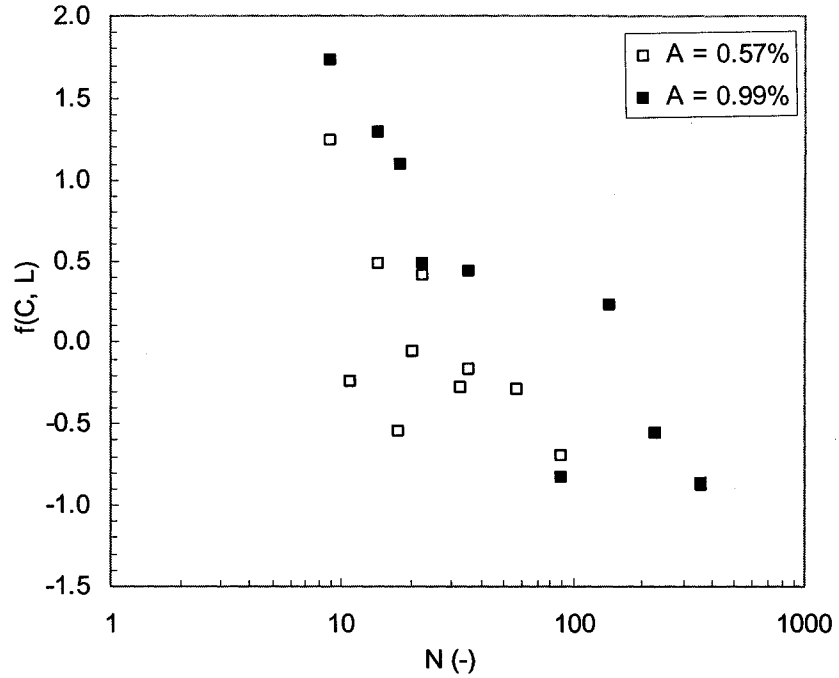

Figure 5.11: Effect of N on the intercept f(C, L) in Eq. (5.16).

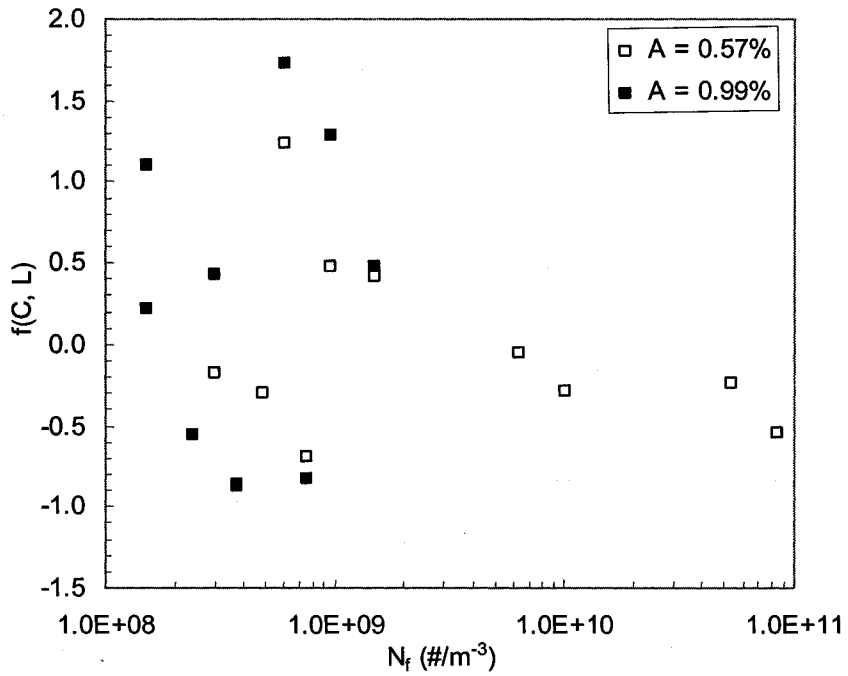

Figure 5.12: Effect of N_f on the intercept f(C, L) in Eq. (5.16).

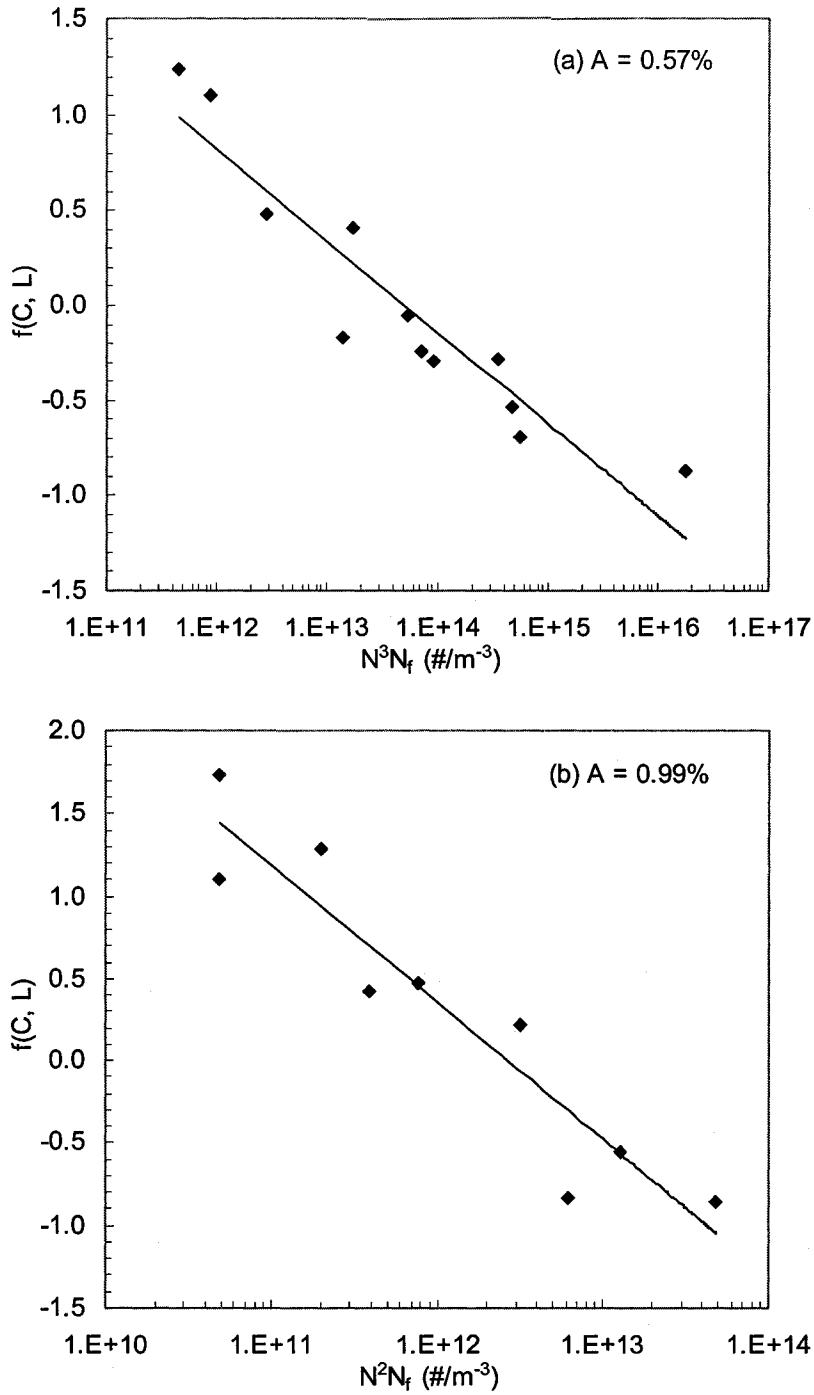

Figure 5.13: Effect of the parameter $N^aN_f^b$ on the intercept f(C, L) in Eq. (5.16) for (a) A = 0.57% and (b) A = 0.99%

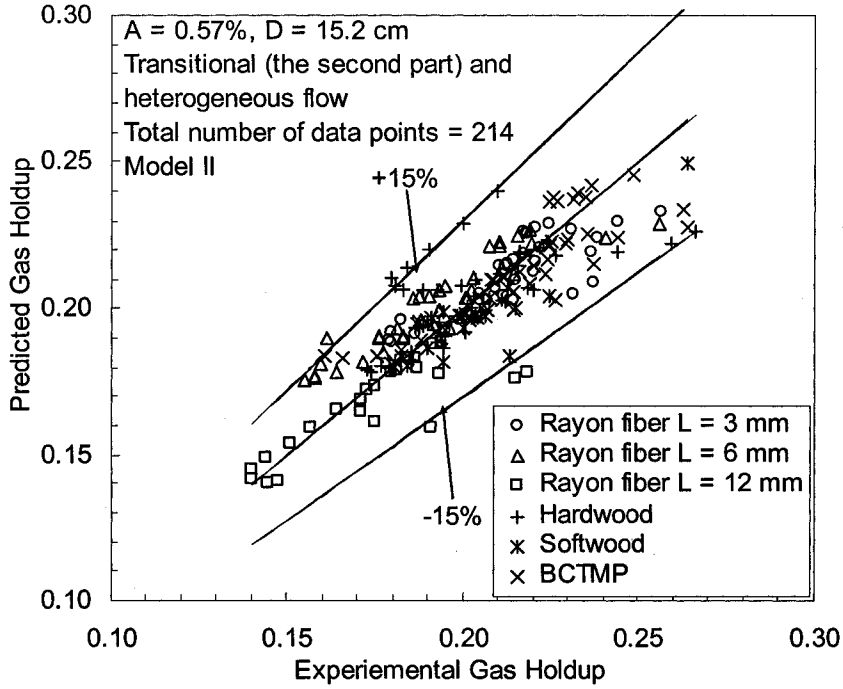

Figure 5.14: Comparison of predicted and experimental data of the second part of transitional and heterogeneous flows for A = 0.57%.

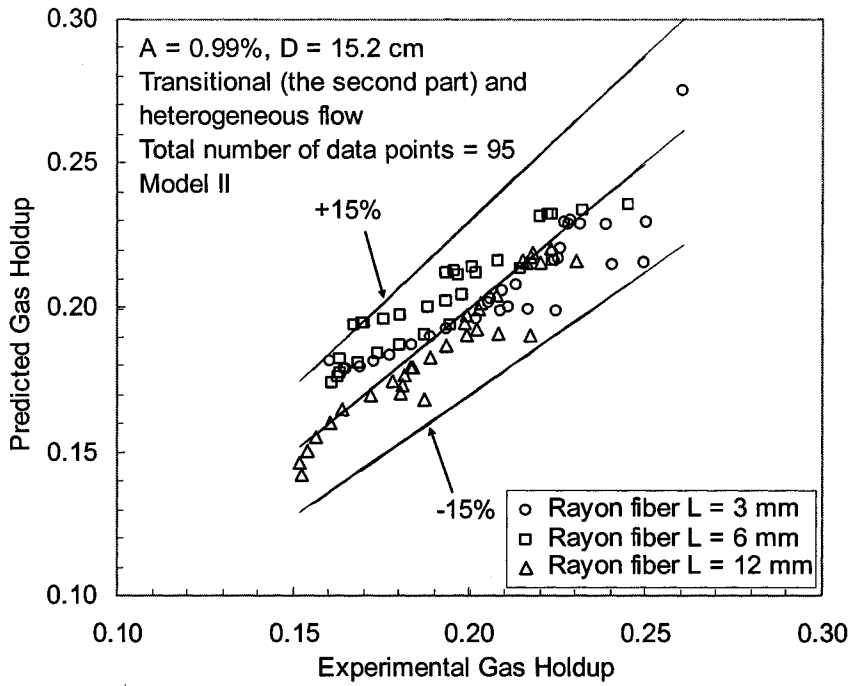

Figure 5.15: Comparison of predicted and experimental data of the second part of transitional and heterogeneous flows for A = 0.99%.

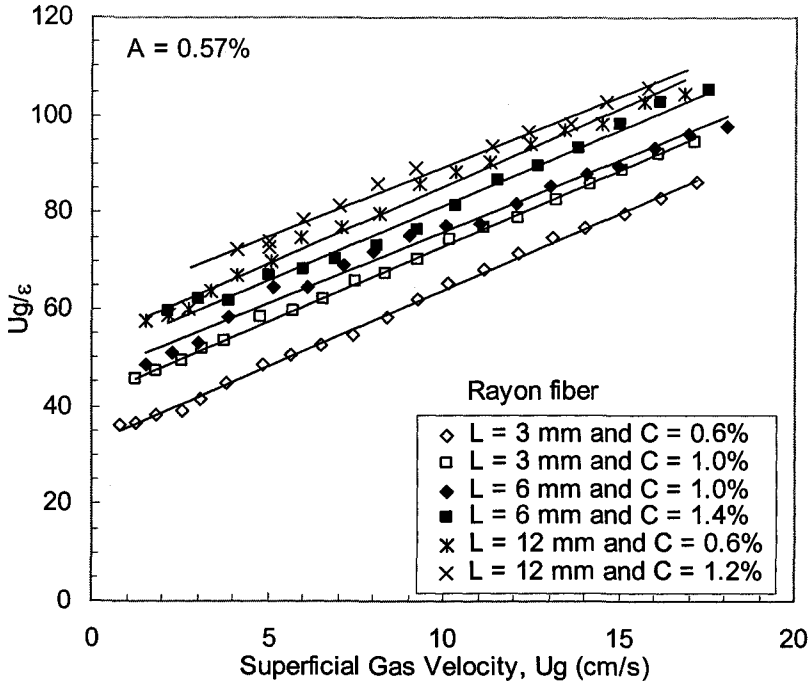

Figure 5.16: Drift flux model for different fiber lengths and mass fractions for A = 0.57%.

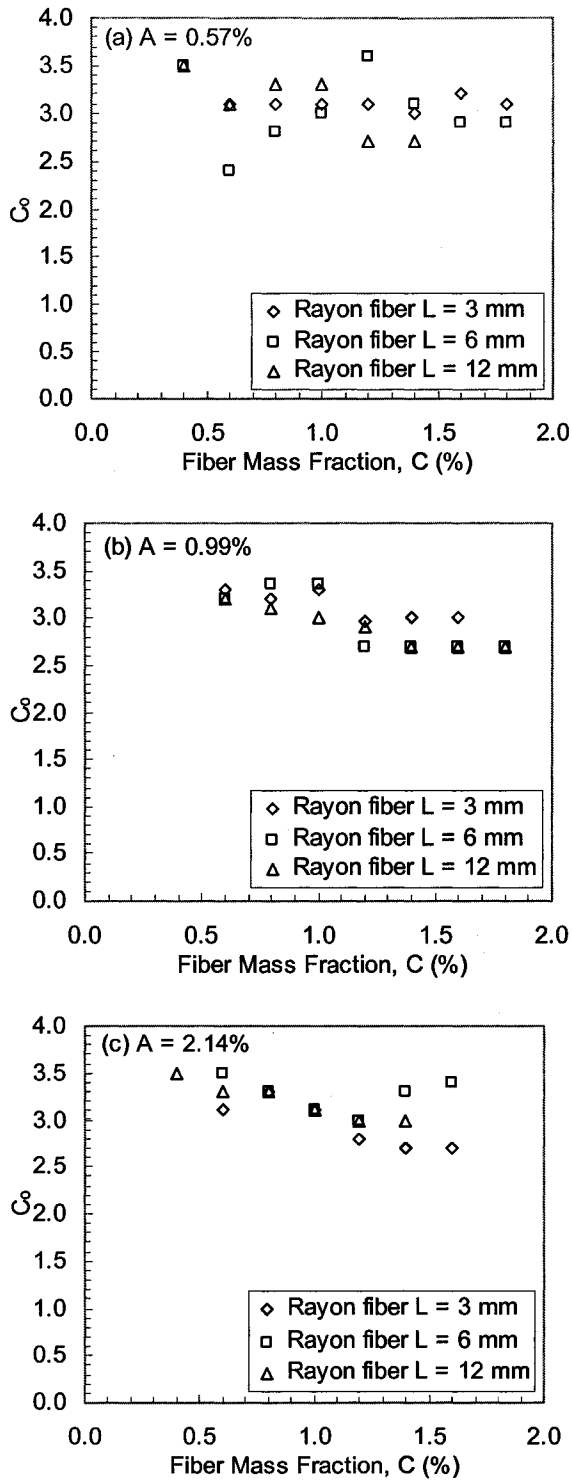

Figure 5.17: The drift flux parameter C_o with respect to different fiber mass fractions for (a) A = 0.57%, (b) A = 0.99%, and (c) A = 2.14%.

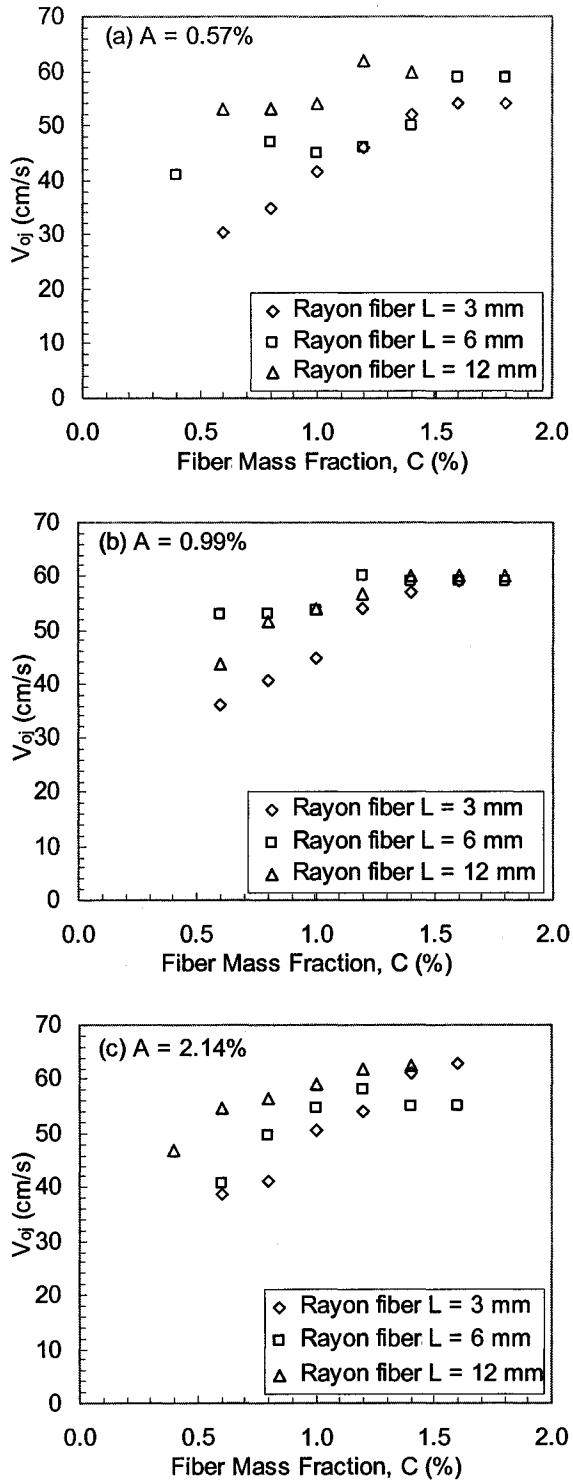

Figure 5.18: Terminal bubble rise velocity with respect to fiber mass fraction for (a) A = 0.57%, (b) A = 0.99%, and (c) A = 2.14%.

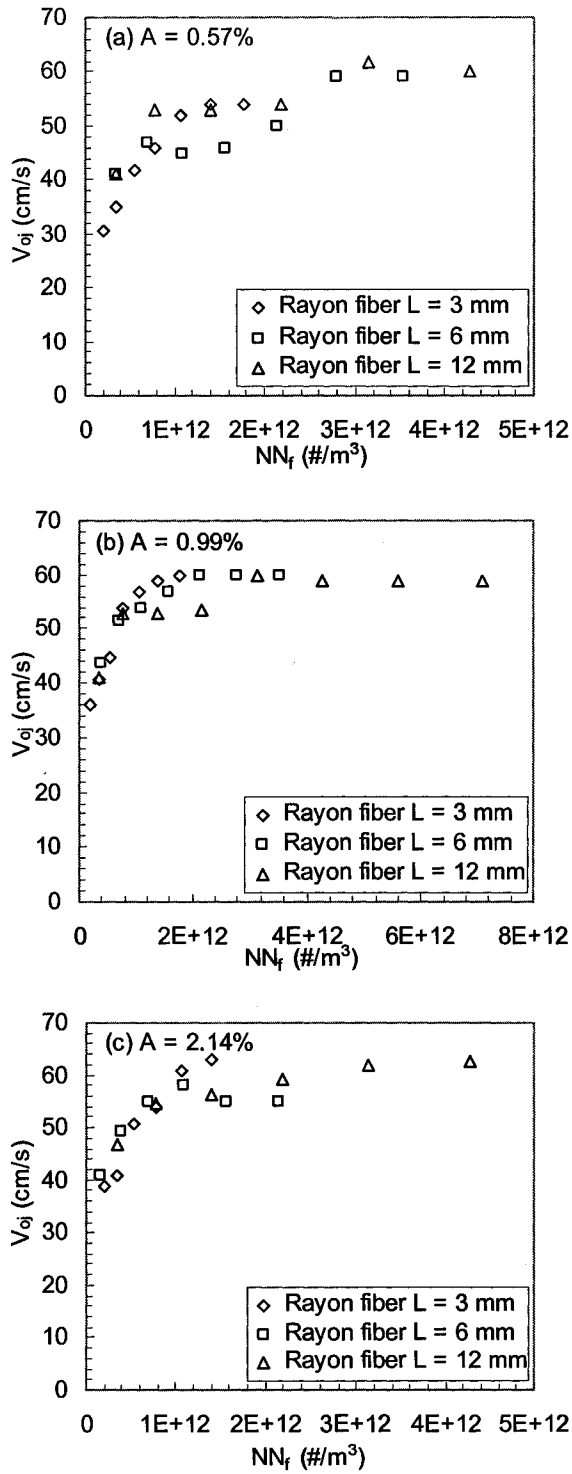

Figure 5.19: Terminal bubble rise velocity as a function of the product of N and N_f for (a= 0.57%, (b) A = 0.99%, and (c) A = 2.14%.

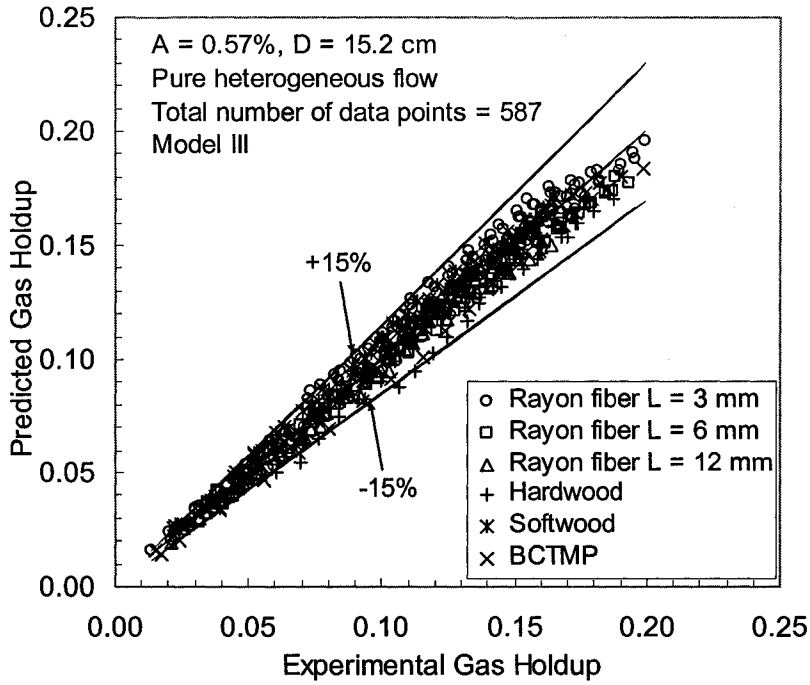

Figure 5.20: Comparison of predicted gas holdup to experimental data in pure heterogeneous flow regime for A = 0.57%.

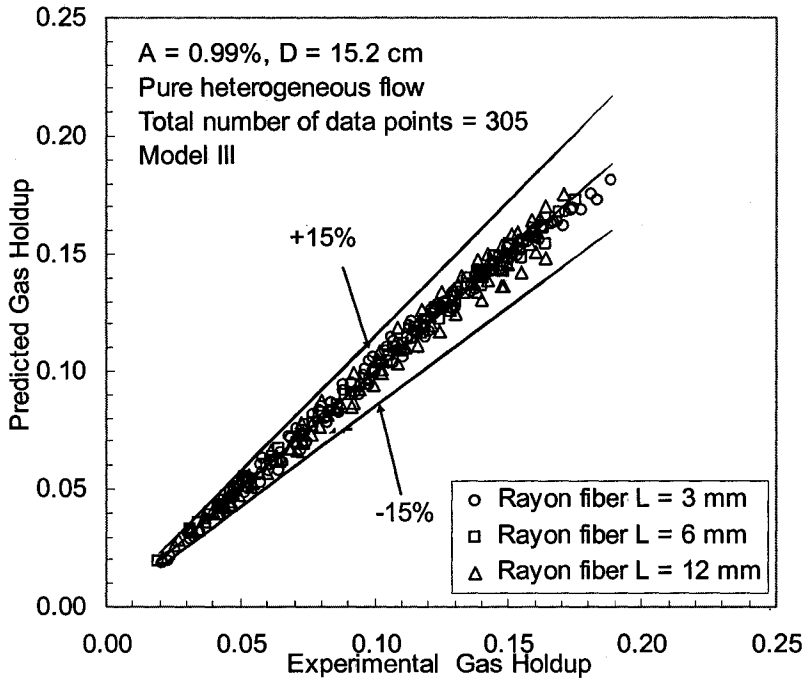

Figure 5.21: Comparison of predicted gas holdup to experimental data in pure heterogeneous flow regime for A = 0.99%.

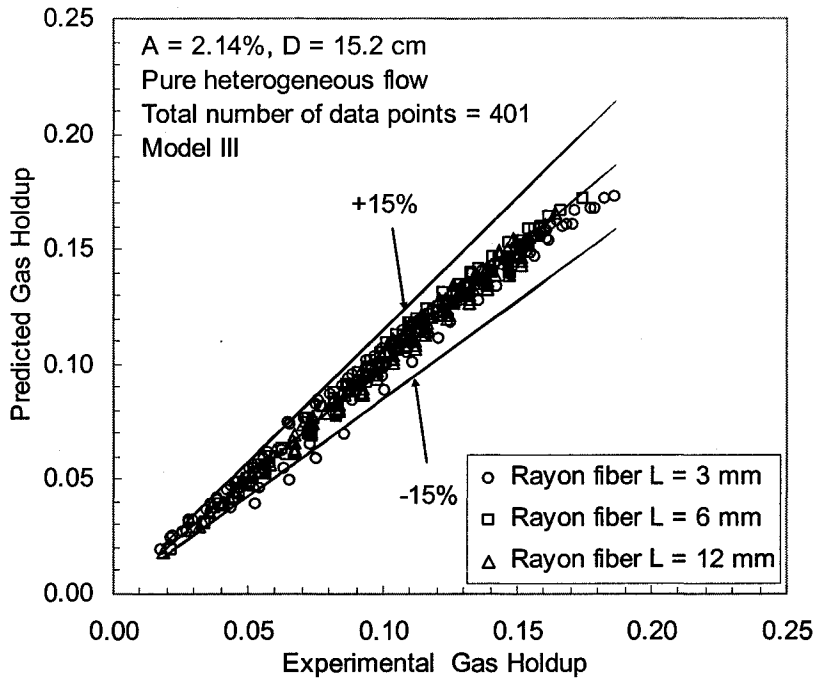

Figure 5.22: Comparison of predicted gas holdup to experimental data in pure heterogeneous flow regime for A = 2.14%.

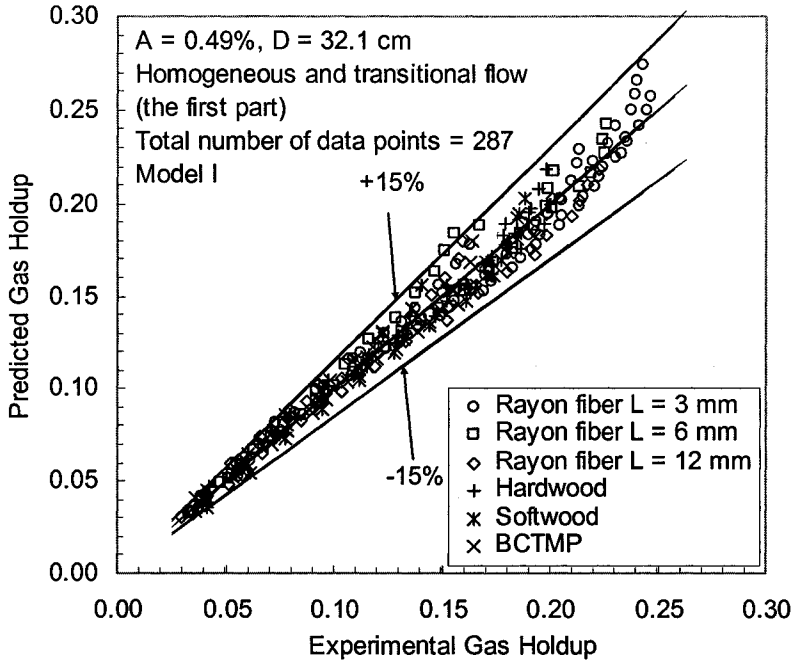

Figure 5.23: Comparison of prediction to experimental data in homogeneous and the first part of transitional flow regimes for D = 32.1cm and A = 0.49%.

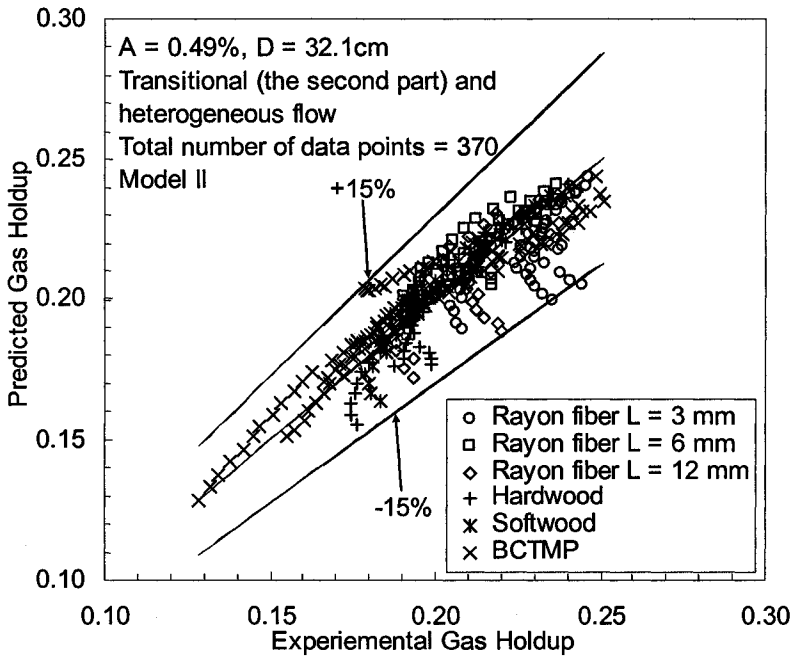

Figure 5.24: Comparison of prediction to experimental data in the second part of transitional and heterogeneous flow regimes for D = 32.1cm and A = 0.49%.

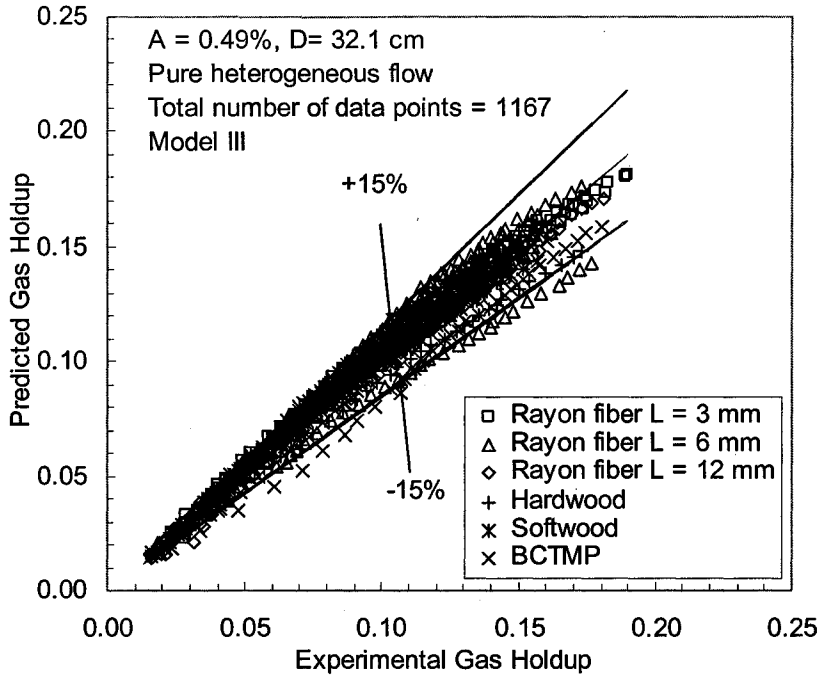

Figure 5.25: Comparison of prediction to experimental data in pure heterogeneous flow regime for D = 32.1cm and A = 0.49%.

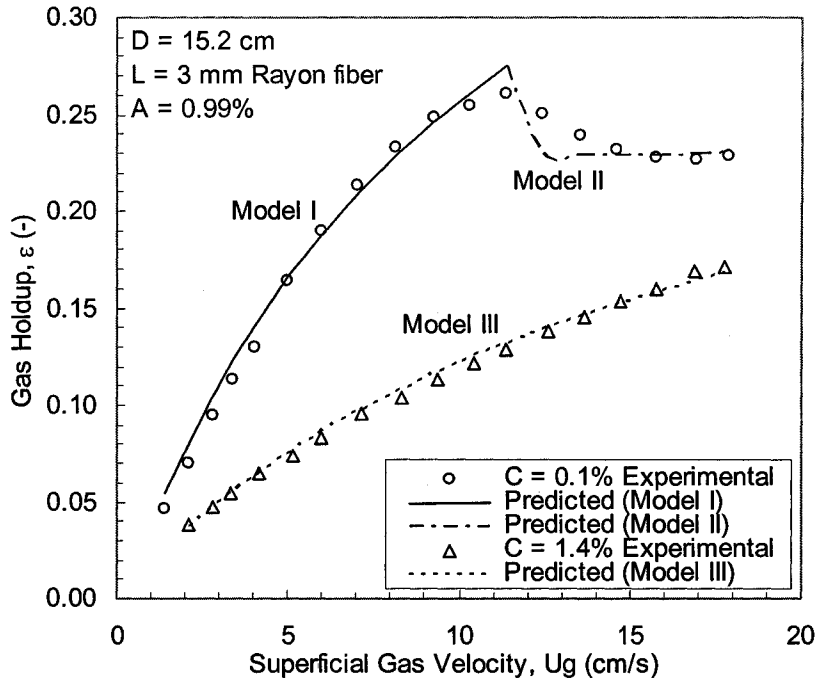

Figure 5.26: Comparison between predictions and experimental data at specified fiber mass fractions for Rayon fiber (L = 3 mm).

CHAPTER 6: CONCLUSIONS AND RECOMMENDATIONS

Gas holdup in a gas-liquid-fiber semi-batch bubble column has been studied. The issues in this research included the effect of Rayon fiber mass fraction and length, the effect of Nylon fiber, the effect of gas distributor open area ratio, the effect of bubble column diameter in cellulose fiber suspensions, and gas holdup models in gas-liquid-fiber semi-batch bubble columns. The first part of this chapter gives conclusions of these issues and the second part provides the recommendations to further this study.

6.1 Conclusions

The main conclusions for this research are as follows:

1. Gas holdup in a semi-batch bubble column filled with a long fiber suspension decreased with increasing fiber mass fraction and fiber length, which was more pronounced when the fiber mass fraction was low. This was attributed to the fact that the effective fiber suspension viscosity increases with increasing fiber mass fraction. At high fiber mass fractions, the effects of fiber mass fraction and fiber length disappeared. Fiber mass fraction had more influence on gas holdup than fiber length. Gas flow patterns changed from the existence of homogeneous, transitional, and heterogeneous flow to pure heterogeneous flow as fiber mass fraction increased.

2. The wettability of the fiber surface had an effect on gas holdup and flow regime transition. Gas holdup of hydrophobic Nylon fiber suspensions was lower than that of hydrophilic Rayon fiber suspensions at the same fiber mass fraction and fiber length. Additionally, gas holdup in Nylon fiber suspensions varied with time, leading to

difficulties in interpreting the effect of fiber mass fraction. Hence, Nylon fiber is not recommended for further gas holdup studies. The mechanisms of the time-dependence of gas holdup include: (i) the effect of Nylon fiber surface additives; (ii) Nylon fiber degradation; (iii) reduced hydrophobicity of Nylon fiber; and (iv) Nylon fiber shape deformation.

3. The aeration plate open area ratio had an effect on gas holdup and flow regime transition. For an air-water system and fiber suspensions with low fiber mass fractions, gas holdup increased when A increased from 0.57% to 0.99%, but it dropped dramatically when A was further increased to 2.14%. Compared to that of A = 0.57%, the flow regime transition occurred at lower superficial gas velocities when A = 2.14%, but it did not change when A = 0.99%. In the midrange of fiber mass fractions addressed in this study, A = 0.99% generated the same gas holdup as that of A = 2.14%, both of which were lower than that of A = 0.57%. The effect of open area ratio diminished and all three aeration plates produced the same gas holdup results when $C \geq 1.2\%$. The reasons the lowest gas holdup was generated when A = 2.14% included: (i) reduced hole spacing enhances bubble coalescence; (ii) large A leads to bubble formation in the asynchronous regime; and (iii) A = 2.14% does not produce a stable plate operation.

4. The gas holdup behavior in short (small aspect ratio) Rayon fiber suspensions (L = 0.38 and 1 mm) was different from that of long (large aspect ratio) Rayon fibers (L = 3, 6, 12 mm). In L = 0.38 mm Rayon fiber suspensions, fiber addition did not reduce gas holdup significantly, and obvious gas holdup changes were observed only when the fiber mass fraction was $C \geq 0.6\%$. Also, fiber addition did not affect the various flow regimes, even

when the fiber mass fraction was as high as C = 3.0%. In L = 1 mm Rayon fiber suspensions, the effect of fiber addition on gas holdup is pronounced in the transitional flow regime, however, the flow pattern is insensitive to fiber addition and homogeneous flow regime was still observed at low superficial gas velocity when C is as high as 1.8%. These phenomena were attributed to the short fiber causing only small changes in the suspension rheology and possible foam formation due to incomplete fiber washing.

5. Three basic gas holdup models were developed to predict gas holdup for (i) the homogeneous and the first part of the transitional flow regime (A = 0.57% and 0.99%) and the entire three-regime flow (A = 2.14%), (ii) the second part of the transitional and the heterogeneous flow regime (A = 0.57% and 0.99%), and (iii) pure heterogeneous flow regime (A = 0.57%, 0.99%, and 2.14%). The models reproduce most of the experimental data within ±15% for the bubble column used in this study (D = 15.2 cm), as well as a similar bubble column (D = 32.1 cm) used in a companion study. A reliable parameter was shown to be $N^{a}N_{f}^{b}$ in both U_{gmax} and the gas holdup modes to take into account the complex effect of fiber type, fiber mass fraction, and fiber length. The exponents a and b are functions of bubble column flow regime, open area ratio, and column diameter and independent of fiber type and length.

6.2 Recommendations

1. More gas distributor open area ratios between A = 0.99% and 2.14% should be further studied to determine a critical open area ratio at which maximum gas holdup is reached. This work should also be done to other bubble column diameters to check the dependence

of gas distributor effects on bubble column diameter and fiber mass fraction. The information obtained may help to optimize equipment in the paper and pulp industry.

2. Gas distributor open area ratio and bubble column diameter should be added in gas holdup models in order that the gas holdup models can be used for scale-up. A significant limitation of the models in the current study, due to limited experimental data, is that the model coefficients and exponents vary with different bubble column diameters and open area ratios; thus, they currently can not be used for scale-up. The knowledge obtained in #1 can give the information for this intention.

3. Scale-up gas holdup model(s) should be developed to account for the effects of fiber type, fiber mass fraction, fiber length, bubble column diameter, and gas distributor open area ratio. To complete this intention, several other work needs to be done (refer to Appendix A).

4. Study the liquid (fiber slurry) height on gas holdup in fiber suspensions and determine the critical liquid (fiber slurry) aspect ratio (column height to diameter ratio) beyond which gas holdup is independent of liquid (fiber slurry) aspect ratio for the gas distribution plates with A = 0.57%, 0.99%, and 2.14%. Examine the relation of the critical value to fiber mass fraction for each plate and the interaction with open area ratios. The effect of aspect ratio in gas-liquid systems has been investigated (Wilkinson et al., 1992; Zahradnik et al., 1997; Veera and Joshi, 1999; Bando et al., 2003). Veera and Joshi (1999) showed that the effect of aspect ratio is dependent on aeration hole number, indicating that distributor open area ratio influences on the column aspect ratio effect. Bando et al. (2003) studied the aspect ratio effect on gas holdup in highly viscous liquid

and concluded that the critical aspect ratio is 8 and independent on liquid viscosity. No study to date has been done focusing on the column aspect ratio effect(s) in gas-liquid-fiber systems.

5. Study the effect of gas chamber volume on gas holdup in fiber suspensions. Determine the interaction of gas chamber volume and gas distributor with different open area ratios (A = 0.57%, 0.99%, and 2.14%). Hughes et al.(1955) pointed out that chamber volume has a strong effect on bubble formation size, and the smaller the gas chamber, the more stable is the bubble growth. Park et al. (1977) reported that when the gas chamber is small, bubbles grow slowly and smoothly. The bubble size is constant when the gas flow rate is below a certain value, otherwise it linearly increases with increasing gas flow rate. When the gas chamber is large enough, bubble size is independent of gas flow rate throughout the entire range of gas flow rates. Park et al. (1977) also pointed out that there are different trends of the change in bubble size with orifice diameter for different chamber volumes. Terasaka and Tsuge (2001) studied the bubble formation in viscous liquids having a yield stress and showed that at the bubble size increases with increasing chamber volume and shear stress. Ponter and Surati (1997) point out that the standardization of the equipment geometries, especially regarding volumes gas chambers and distribution plates, is very important to generate reproducible bubbles. Non-standard gas chambers and distribution plates can be used to explain why inconsistent and poorly reproducible data are obtained.

6. Study the effect of Rayon fiber length distribution on gas holdup to obtain information of the effect of fiber length distribution on gas holdup, and examine the dependence of this

effect on gas distributor open area ratio. Wikstrom et al. (1998) found that the fiber length distribution has a significant effect on yield stress. It is hypothesized that the fiber length distribution also has an effect on gas holdup.

7. Study gas holdup behavior and flow regime in 2 mm long Rayon fiber suspensions. From the current study, gas holdup and flow regime are different in long (L = 3, 6, and 12 mm) and short (L = 0.38 and 1 mm) Rayon fiber suspensions, where the flow regime in short Rayon fiber is insensitive to fiber addition. It is necessary to study 2 mm long Rayon fiber suspensions and try to identify one parameter to demark the long and short Rayon fiber results.

8. Use the current models to predict gas holdup in another hydrophilic fiber system and compare the predictions with the experimental data to determine the model predictive capabilities.

REFERENCES

Ajersch, M., and Pelton, R., "The Behavior of Air Bubbles in Aqueous Wood Pulp Suspensions," *Proceedings of the Research Forum on Recycling*, 97-112 (1999).

Akita, K., and Yoshida, F., "Gas Holdup and Volumetric Mass-Transfer Coefficient in Bubble Columns - Effects of Liquid Properties," *Industrial & Engineering Chemistry Process Design and Development*, 12 (1), 76-80 (1973).

Al-Masry, W., "Effect of Scale-up on Average Shear Rates for Aerated Non-Newtonian Liquids in External Loop Airlift Reactors," *Biotechnology and Bioengineering*, 62 (4), 494-498 (1999).

Andersson, S. R., Ringner, J., and Rasmuson, A., "The Network Strength of Non-Flocculated Fiber Suspensions," *Nordic Pulp & Paper Research Journal*, 14 (1), 61-70 (1999).

Bando, Y., Chaya, M., Hamano, S., Yasuda, K., Nakamura, M., Osada, K., and Matsui, M., "Effect of Liquid Height on Flow Characteristics in Bubble Column Using Highly Viscous Liquid," *Journal of Chemical Engineering of Japan*, 36 (5), 523-529 (2003).

Banisi, S., Finch, J. A., Laplante, A. R., and Weber, M. E., "Effect of Solid Particles on Gas Holdup in Flotation Columns. 1. Measurement," *Chemical Engineering Science*, 50 (14), 2329-2334 (1995a).

Banisi, S., Finch, J. A., Laplante, A. R., and Weber, M. E., "Effect of Solid Particles on Gas Holdup in Flotation Columns. 2. Investigation of Mechanisms of Gas Holdup Reduction in Presence of Solids," *Chemical Engineering Science*, 50 (14), 2335-2342 (1995b).

Beghello, L., and Eklund, D., "The Influence of the Chemical Environment on Fiber Flocculation," *Journal of Pulp and Paper Science*, 25 (7), 246-250 (1999).

Bennington, C. P. J., Kerekes, R. J., and Grace, J. R., "The Yield Stress of Fiber Suspensions," *The Canadian Journal of Chemical Engineering*, 68 (5), 748-757 (1990).

Bennington, C. P. J., Azevedo, G., John, D. A., Birt, S. M., and Wolgast, B. H., "The Yield Stress of Medium-Consistency and High-Consistency Mechanical Pulp Fiber Suspensions at High Gas Contents," *Journal of Pulp and Paper Science*, 21 (4), J111-J118 (1995).

Blakeney, W. R., "The Viscosity of Suspensions of Straight, Rigid Rods," *Journal of Colloid and Interface Science*, 22 324 (1966).

Camarasa, E., Vial, C., Poncin, S., Wild, G., Midoux, N., and Bouillard, J., "Influence of Coalescence Behaviour of the Liquid and of Gas Sparging on Hydrodynamics and Bubble Characteristics in a Bubble Column," *Chemical Engineering and Processing*, 38 (4-6), 329-344 (1999).

Chaouche, M., and Koch, D. L., "Rheology of Non-Brownian Rigid Fiber Suspensions with Adhesive Contacts," *Journal of Rheology*, 45 (2), 369-382 (2001).

Chen, R. C., Reese, J., and Fan, L. S., "Flow Structure in a 3-Dimensional Bubble-Column and 3-Phase Fluidized-Bed," *AIChE Journal*, 40 (7), 1093-1104 (1994).

Chen, Y. M., and Fan, L. S., "Bubble Breakage Due to Particle Collision in a Liquid-Medium -Particle Wettability Effects," *Chemical Engineering Science*, 44 (11), 2762-2767 (1989).

Clark, N. N., Vanegmond, J. W., and Nebiolo, E. P., "The Drift-Flux Model Applied to Bubble-Columns and Low Velocity Flows," *International Journal of Multiphase Flow*, 16 (2), 261-279 (1990).

Colella, D., Vinci, D., Bagatin, R., Masi, M., and Abu Bakr, E., "A Study on Coalescence and Breakage Mechanisms in Three Different Bubble Columns," *Chemical Engineering Science*, 54 (21), 4767-4777 (1999).

Crabtree, J. R., and Bridgwat, J., "Bubble Coalescence in Viscous Liquids," *Chemical Engineering Science*, 26 (6), 839-& (1971).

Cruz, M. M., "Rayons," *Synthetic Fibers in Papermaking*, Battista, O. A., Ed., Interscience Publishers, Princeton, New Jersey, 11-45 (1964)

De Swart, J. W. A., and Krishna, R., "Influence of Particles Concentration on the Hydrodynamics of Bubble-Column Slurry Reactors," *Chemical Engineering Research & Design*, 73 (A3), 308-313 (1995).

De Swart, J. W. A., van Vliet, R. E., and Krishna, R., "Size, Structure and Dynamics of "Large" Bubbles in a Two-Dimensional Slurry Bubble Column," *Chemical Engineering Science*, 51 (20), 4619-4629 (1996).

Deckwer, W. D., *Bubble Column Reactors*, John Wiley, New York (1992).

Douek, R. S., Hewitt, G. F., and Livingston, A. G., "Hydrodynamics of Vertical Co-Current Gas-Liquid-Solid Flows," *Chemical Engineering Science*, 52 (23), 4357-4371 (1997).

Eissa, S. H., and Schugerl, K., "Holdup and Backmixing Investigations in Cocurrent and Countercurrent Bubble Columns," *Chemical Engineering Science*, 30 (10), 1251-1256 (1975).

Figliola, R. S., and Beasley, D. E., *Theory and Design for Mechanical Measurement*, 3rd ed, John Wiley & Sons, Inc, New York (2000).

Forgas, O. L., and Mason, S. G., "Particle Motions in Sheared Suspension. 9. Spin and Deformation of Threadlike Particles," *Journal of Colloid Science*, 14 457-472 (1959).

Gandhi, B., Prakash, A., and Bergougnou, M. A., "Hydrodynamic Behavior of Slurry Bubble Column at High Solids Concentrations," *Powder Technology*, 103 (2), 80-94 (1999).

Gestrich, W., and Rahse, W., "Relative Gas Content of Bubble Layers," *Chemie Ingenieur Technik*, 47 (1), 8-13 (1975).

Haug, H. F., "Stability of Sieve Trays with High Overflow Weirs," *Chemical Engineering Science*, 31 (4), 295-307 (1976).

Hebrard, G., Bastoul, D., and Roustan, M., "Influence of the Gas Sparger on the Hydrodynamic Behaviour of Bubble Columns," *Chemical Engineering Research & Design*, 74 (A3), 406-414 (1996).

Heindel, T. J., "Bubble Size Measurements in a Quiescent Fiber Suspension," *Journal of Pulp and Paper Science*, 25 (3), 104-110 (1999).

Heindel, T. J., and Garner, A. E., "The Effect of Fiber Consistency on Bubble Size," *Nordic Pulp & Paper Research Journal*, 14 (2), 171-178 (1999).

Heindel, T. J., "Gas Flow Regime Changes in a Bubble Column Filled with a Fiber Suspension," *The Canadian Journal of Chemical Engineering*, 78 (5), 1017-1022 (2000).

Heindel, T. J., and Omberg, S. J., "Gas Bubble Size in a Synthetic Fiber Slurry." *Proceedings of the ICMF-2001(4th International Conference on Multiphase Flow),* May 27 to June 1, 2001, New Orleans, LA, (2001).

Heindel, T. J., "Bubble Size in a Cocurrent Fiber Slurry," *Industrial & Engineering Chemistry Research*, 41 (3), 632-641 (2002).

Hibiki, T., and Ishii, M., "One-Dimensional Drift-Flux Model for Two-Phase Flow in a Large Diameter Pipe," *International Journal of Heat and Mass Transfer*, 46 (10), 1773-1790 (2003).

Hikita, H., Asai, S., Tanigawa, K., Segawa, K., and Kitao, M., "Gas Hold-up in Bubble-Columns," *Chemical Engineering Journal and the Biochemical Engineering Journal*, 20 (1), 59-67 (1980).

Hol, P., "Gas Holdup in a 32 cm Bubble Column," MS Thesis, Iowa State University, 2005.

Hughes, R. R., Handlos, A. E., Evans, H. D., and Maycock, R. L., "The Formation of Bubbles at Simple Orifices," *Chemical Engineering Progress*, 51 (12), 557-563 (1955).

Hunston, D. L., and Zakin, J. L., "Flow-Assisted Degradation in Dilute Polystyrene Solutions," *Polymer Engineering and Science*, 20 (7), 517-523 (1980).

Inga, J. R., and Morsi, B. I., "Effect of Operating Variables on the Gas Holdup in a Large-Scale Slurry Bubble Column Reactor Operating with an Organic Liquid Mixture," *Industrial & Engineering Chemistry Research*, 38 (3), 928-937 (1999).

Jamialahmadi, M., and Muller-Steinhagen, H., "Effect of Solid Particles on Gas Hold-up in Bubble-Columns," *The Canadian Journal of Chemical Engineering*, 69 (1), 390-393 (1991).

Janse, P., Gomez, C. O., and Finch, J. A., "Effect of Pulp Fibers on Gas Holdup in a Flotation Column," *The Canadian Journal of Chemical Engineering*, 77 22-25 (1999).

Jordan, U., and Schumpe, A., "The Gas Density Effect on Mass Transfer in Bubble Columns with Organic Liquids," *Chemical Engineering Science*, 56 (21-22), 6267-6272 (2001).

Joung, C. G., Phan-Thien, N., and Fan, X. J., "Direct Simulation of Flexible Fibers," *Journal of Non-Newtonian Fluid Mechanics*, 99 (1), 1-36 (2001).

Joung, C. G., Phan-Thien, N., and Fan, X. J., "Viscosity of Curved Fibers in Suspension," *Journal of Non-Newtonian Fluid Mechanics*, 102 (1), 1-17 (2002).

Kara, S., Kelkar, B. G., Shah, Y. T., and Carr, N. L., "Hydrodynamics and Axial Mixing in a Three-Phase Bubble Column," *Industrial & Engineering Chemistry Process Design and Development*, 21 (4), 584-594 (1982).

Kataoka, Y., Suzuki, H., and Murase, M., "Drift-Flux Parameters for Upward Gas-Flow in Stagnant Liquid," *Journal of Nuclear Science and Technology*, 24 (7), 580-586 (1987).

Kelkar, B. G., Shah, Y. T., and Carr, N. L., "Hydrodynamics and Axial Mixing in a Three-Phase Bubble Column - Effects of Slurry Properties," *Industrial & Engineering Chemistry Process Design and Development*, 23 (2), 308-313 (1984).

Kerekes, R. J., Soszynski, R. M., and Tam Doo, P. A., "The Flocculation of Pulp Fibers." *Transactions of 8th Fundamental Research Symposium*, Oxford, England, September, (1985).

Kerekes, R. J., and Schell, C. J., "Characterization of Fiber Flocculation Regimes by a Crowding Factor," *Journal of Pulp and Paper Science*, 18 (1), J32-J38 (1992).

Kerekes, R. J., "Characterizing Fiber Suspension," *TAPPI 1996 Engineering Conference, Chicago, TAPPI Press*, 21-28 (1996).

Khan, M. A., and Hackam, R., "Loss of Hydrophobicity of High Density Polyethylene," *Conference on Electrical Insulation and Dielectric Phenomena (CEIDP)*, Annual Report, 19 - 22 (1997).

Klein, S. A., Engineering Equation Solver, 6.856-3D, F-Chart Software, 2003

Kluytmans, J. H. J., van Wachem, B. G. M., Kuster, B. M., and Schouten, J. C., "Gas Holdup in a Slurry Bubble Column: Influence of Electrolyte and Carbon Particles," *Industrial & Engineering Chemistry Research*, 40 (23), 5326-5333 (2001).

Kohan, M. I., *Nylon Plastics Handbook*, Hanser/Gardner Publications, Cincinnati, Ohio (1995).

Koide, K., Takazawa, A., Komura, M., and Matsunaga, H., "Gas Holdup and Volumetric Liquid-Phase Mass-Transfer Coefficient in Solid-Suspended Bubble-Columns," *Journal of Chemical Engineering of Japan*, 17 (5), 459-466 (1984).

Krishna, R., Ellenberger, J., and Hennephof, D. E., "Analogous Description of the Hydrodynamics of Gas-Solid Fluidized-Beds and Bubble-Columns," *Chemical Engineering Journal and the Biochemical Engineering Journal*, 53 (1), 89-101 (1993).

Krishna, R., and Ellenberger, J., "Gas Holdup in Bubble Column Reactors Operating in the Churn-Turbulent Flow Regime," *AIChE Journal*, 42 (9), 2627-2634 (1996).

Krishna, R., De Swart, J. W. A., Ellenberger, J., Martina, G. B., and Maretto, C., "Gas Holdup in Slurry Bubble Columns: Effect of Column Diameter and Slurry Concentrations," *AIChE Journal*, 43 (2), 311-316 (1997).

Krishna, R., Ellenberger, J., and Maretto, C., "Flow Regime Transitions in Bubble Columns," *International Communications in Heat and Mass Transfer*, 26 (4), 467-475 (1999a).

Krishna, R., Urseanu, M. I., van Baten, J. M., and Ellenberger, J., "Wall Effects on the Rise of Single Gas Bubbles in Liquids," *International Communications in Heat and Mass Transfer*, 26 (6), 781-790 (1999b).

Krishna, R., "A Scale-up Strategy for a Commercial Scale Bubble Column Slurry Reactor for Fischer-Tropsch Synthesis," *Oil & Gas Science and Technology*, 4 359-393 (2000).

Krishna, R., Urseanu, M. I., and Dreher, A. J., "Gas Hold-up in Bubble Columns: Influence of Alcohol Addition Versus Operation at Elevated Pressures," *Chemical Engineering and Processing*, 39 (4), 371-378 (2000).

Krishna, R., van Baten, J. M., and Urseanu, M. I., "Scale Effects on the Hydrodynamics of Bubble Columns Operating in the Homogeneous Flow Regime," *Chemical Engineering & Technology*, 24 (5), 451-458 (2001).

Kumar, A., Degaleesan, T. E., Laddha, G. S., and Hoelscher, H. E., "Bubble Swarm Characteristics in Bubble-Columns," *The Canadian Journal of Chemical Engineering*, 54 (6), 503-508 (1976).

Kuncova, G., and Zahradnik, J., "Gas Holdup and Bubble Frequency in a Bubble-Column Reactor Containing Viscous Saccharose Solutions," *Chemical Engineering and Processing*, 34 (1), 25-34 (1995).

Lavrenko, P. N., Pogodina, N. V., Ponomarev, I. I., Okatova, O. V., and Evlampieva, N. P., "Stability and Degradation of Poly(Naphthoyleneimidobenzimidazole)," *Polymer Degradation and Stability*, 43 (3), 379-384 (1994).

Li, H., and Prakash, A., "Heat Transfer and Hydrodynamics in a Three-Phase Slurry Bubble Column," *Industrial & Engineering Chemistry Research*, 36 (11), 4688-4694 (1997).

Li, H., and Prakash, A., "Influence of Slurry Concentrations on Bubble Population and Their Rise Velocities on a Three-Phase Slurry Bubble Column," *Powder Technology*, 113 158-167 (2000).

Li, H. A. Z., "Bubbles in Non-Newtonian Fluids: Formation, Interactions and Coalescence," *Chemical Engineering Science*, 54 (13-14), 2247-2254 (1999).

Lin, T. J., Juang, R. C., and Chen, C. C., "Characterizations of Flow Regime Transitions in a High-Pressure Bubble Column by Chaotic Time Series Analysis of Pressure Fluctuation Signals," *Chemical Engineering Science*, 56 (21-22), 6241-6247 (2001).

Lindsay, J. D., Ghiaasiaan, S. M., and Abdel-Khalik, S. I., "Macroscopic Flow Structures in a Bubbling Paper Pulp-Water Slurry," *Industrial & Engineering Chemistry Research*, 34 (10), 3342-3354 (1995).

Maruyama, T., Yoshida, S., and Mizushina, T., "The Flow Transition in a Bubble Column," *Journal of Chemical Engineering of Japan*, 14 (5), 352-357 (1981).

Mason, S. G., "The Flocculation of Pulp Suspensions and the Formation of Paper," *TAPPI Journal*, 33 440-444 (1950).

Mathisen, T., Lewis, M., and Albertsson, A. C., "Hydrolytic Degradation of Nonoriented Poly (Beta-Propiolactone)," *Journal of Applied Polymer Science*, 42 (8), 2365-2370 (1991).

Mersmann, A., "Design and Scale-up of Bubble and Spray Columns," *German Chemical Engineering*, 1 1-11 (1978).

Mikolajewski, E., Swallow, J. E., and Weber, M. W., "Wet Oxidation of Undrawn Nylon 66 and Model Amides," *Journal of Applied Polymer Science*, 8 2067-2093 (1964).

Miyahara, T., Matsuba, Y., and Takahashi, T., "Size of Bubbles Generated from Perforated Plates," *International Chemical Engineering*, 23 517-523 (1983a).

Miyahara, T., Haga, H., and Takahashi, T., "Bubble Formation from an Orifice at High Gas Flow Rates," *International Chemical Engineering*, 23 (3), 524-531 (1983b).

Miyahara, T., and Takahashi, T., "Coalescence Phenomena at the Moment of Bubble Formation at Adjacent Holes," *Chemical Engineering Research & Design*, 64 (4), 320-323 (1986).

Miyahara, T., and Hayashino, T., "Size of Bubbles Generated from Perforated Plates in Non-Newtonian Liquids," *Journal of Chemical Engineering of Japan*, 28 (5), 596-600 (1995).

Muller, F. L., and Davidson, J. F., "Rheology of Shear Thinning Polymer-Solutions," *Industrial & Engineering Chemistry Research*, 33 (10), 2364-2367 (1994).

Nagashiro, W., and Tsunoda, T., "Degradation of Polyacrylamide Molecules in Aqueous Solutions by High-Speed Stirring," *Journal of Applied Polymer Science*, 21, 1149 -153 (1977).

Ohki, Y., and Inoue, H., "Longitudinal Mixing of the Liquid Phase in Bubble Columns," *Chemical Engineering Science*, 25 (1), 1-16 (1970).

Otake, T., Tone, S., Nakao, K., and Mitsuhashi, Y., "Coalescence and Breakup of Bubbles in Liquids," *Chemical Engineering Science*, 32 (4), 377-383 (1977).

Park, Y., Tyler, A. L., and Nevers, N. D., "Chamber Orifice Interaction in Formation of Bubbles," *Chemical Engineering Science*, 32 (8), 907-916 (1977).

Pelton, R., and Piette, R., "Air Bubble Holdup in Quiescent Wood Pulp Suspensions," *The Canadian Journal of Chemical Engineering*, 70 (4), 660-663 (1992).

Petrich, M. P., Koch, D. L., and Cohen, C., "An Experimental Determination of the Stress-Microstructure Relationship in Semi-Concentrated Fiber Suspensions," *Journal of Non-Newtonian Fluid Mechanics*, 95 (2-3), 101-133 (2000).

Philip, J., Proctor, J. M., Niranjan, K., and Davidson, J. F., "Gas Hold-up and Liquid Circulation in Internal Loop Reactors Containing Highly Viscous Newtonian and Non-Newtonian Liquids," *Chemical Engineering Science*, 45 (3), 651-664 (1990).

Ponter, A. B., and Surati, A. I., "Bubble Emissions from Submerged Orifices - a Critical Review," *Chemical Engineering & Technology*, 20 (2), 85-89 (1997).

Prince, M. J., and Blanch, H. W., "Bubble Coalescence and Break-up in Air-Sparged Bubble-Columns," *AIChE Journal*, 36 (10), 1485-1499 (1990).

Racz, G., Koczo, K., and Wasan, D. T., "Mechanisms of Antifoam Deactivation," *Journal of Colloid and Interface Science*, 181 (1), 124-135 (1996).

Reese, J., and Fan, L. S., "Transient Flow Structure in the Entrance Region of a Bubble Column Using Particle Image Velocimetry," *Chemical Engineering Science*, 49 (24B), 5623-5636 (1994).

Reese, J., Jiang, P., and Fan, L. S., "Bubble Characteristics in Three-Phase Systems Used for Pulp and Paper Processing," *Chemical Engineering Science*, 51 (10), 2501-2510 (1996).

Reese, J., Silva, E. M., Tang, S.-T., and Fan, L. S., "Industrial Application of Three-Phase Fluidization Systems," *Fluidization Solids Handling and Processing - Industrial Applications*, Yang, W.-C., Ed., Noyes Publication, Westwood, NJ, 582-682 (1999)

Richardson, J. F., and Zaki, W. N., "Sedimentation and Fluidization: Part 1," *Chemical Engineering Research & Design*, 32 35-53 (1954).

Ruzicka, M., Drahos, J., Zahradnik, J., and Thomas, N. H., "Natural Modes of Multi-Orifice Bubbling from a Common Plenum," *Chemical Engineering Science*, 54 (21), 5223-5229 (1999).

Ruzicka, M., Drahos, J., Zahradnik, J., and Thomas, N. H., "Structure of Gas Pressure Signal at Two-Orifice Bubbling from a Common Plenum," *Chemical Engineering Science*, 55 (2), 421-429 (2000).

Ruzicka, M. C., Zahradnik, J., Drahos, J., and Thomas, N. H., "Homogeneous-Heterogeneous Regime Transition in Bubble Columns," *Chemical Engineering Science*, 56 (15), 4609-4626 (2001a).

Ruzicka, M. C., Drahos, J., Fialova, M., and Thomas, N. H., "Effect of Bubble Column Dimensions on Flow Regime Transition," *Chemical Engineering Science*, 56 (21-22), 6117-6124 (2001b).

Sarrafi, A., Jamialahmadi, M., Muller-Steinhagen, H., and Smith, J. M., "Gas Holdup in Homogeneous and Heterogeneous Gas-Liquid Bubble Column Reactors," *The Canadian Journal of Chemical Engineering*, 77 (1), 11-21 (1999).

Saxena, S. C., Rao, N. S., and Saxena, A. C., "Correlation of Heat-Transfer and Gas Holdup Data from Slurry Bubble-Columns," *International Communications in Heat and Mass Transfer*, 18 (2), 219-228 (1991).

Schafer, R., Merten, C., and Eigenberger, G., "Bubble Size Distributions in a Bubble Column Reactor under Industrial Conditions," *Experimental Thermal and Fluid Science*, 26 (6-7), 595-604 (2002).

Schmid, C. F., Switzer, L. H., and Klingenberg, D. J., "Simulations of Fiber Flocculation: Effects of Fiber Properties and Interfiber Friction," *Journal of Rheology*, 44 (4), 781-809 (2000).

Schulz, T. H., and Heindel, T. J., "A Study of Gas Holdup in Cocurrent Air/Water/Fiber System," *TAPPI Journal*, 83 (6), 58-69 (2000).

Shah, Y. T., Kelkar, B. G., Godbole, S. P., and Deckwer, W. D., "Design Parameters Estimations for Bubble Column Reactors," *AIChE Journal*, 28 (3), 353-379 (1982).

Shah, Y. T., and Deckwer, W. D., "Hydrdynamics of Bubble Columns," *Handbook of Fluids in Motion*, Cheremisinoff, N. P. and Gupta, R., Ed., Ann Arbor Science Publishers, Ann Arbor, MI, 583-633 (1983)

Shamlou, P. A., Rajarajan, J., and Ison, A. P., "Gas Holdup, Liquid Circulation Velocity and Shear Rate in an External Loop Airlift Containing Non-Newtonian Polymer Solutions," *Bioprocess Engineering*, 19 (1998).

Shen, G., and Finch, J. A., "Bubble Swarm Velocity in a Column," *Chemical Engineering Science*, 51 (14), 3665-3674 (1996).

Shnip, A. I., Kolhatkar, R. V., Swamy, D., and Joshi, J. B., "Criteria for the Transition from the Homogeneous to the Heterogeneous Regime in 2-Dimensional Bubble Column Reactors," *International Journal of Multiphase Flow*, 18 (5), 705-726 (1992).

Slade, P. E., and Hild, D. N., "Surface Energies of Nonionic Surfactants Adsorbed onto Nylon Fiber and a Correlation with Their Solubility Parameters," *Textile Research Journal*, 62 (9), 535-546 (1992).

Smook, G. A., *Handbook for Pulp & Paper Technologists*, Angus Wilde Publications, (1992).

Solanki, M. K. S., Mukherjee, A. K., and Das, T. R., "Bubble Formation at Closely Spaced Orifices in Aqueous-Solutions," *Chemical Engineering Journal and the Biochemical Engineering Journal*, 49 (1), 65-71 (1992).

Soszynski, R. M., "The Formation and Properties of Coherent Flocs in Fiber Suspensions," PhD Thesis, University of Bristish Columbia, 1987.

Soszynski, R. M., and Kerekes, R. J., "Elastic Interlocking of Nylon Fibers Suspended in Liquid. Part 1. Nature of Cohesion among Fibers," *Nordic Pulp & Paper Research Journal*, 3 172-179 (1988a).

Soszynski, R. M., and Kerekes, R. J., "Elastic Interlocking of Nylon Fibers Suspended in Liquid. Part 2. Process of Interlocking," *Nordic Pulp & Paper Research Journal*, 3 180-184 (1988b).

Sotelo, J. L., Benitez, F. J., Beltran-Heredia, J., and Rodriguez, C., "Gas Holdup and Mass Transfer Coefficients in Bubble Columns. 1. Porous Glass-Plate Diffusers," *International Chemical Engineering*, 34 (1), (1994).

Su, X., and Heindel, T. J., "Gas Holdup in a Fiber Suspension," *The Canadian Journal of Chemical Engineering*, 81 (3-4), 412-418 (2003).

Su, X., and Heindel, T. J., "Gas Holdup Behavior in Nylon Fiber Suspensions," *Industrial & Engineering Chemistry Research*, 43 (9), 2256-2263 (2004).

Su, X., and Heindel, T. J., "Effect of Perforated Plate Open Area on Gas Holdup in Rayon Fiber Suspensions," *ASME Journal of Fluids Engineering*, Accepted for Publication (2005).

Sundararajakumar, R. R., and Koch, D. L., "Structure and Properties of Sheared Fiber Suspensions with Mechanical Contacts," *Journal of Non-Newtonian Fluid Mechanics*, 73 (3), 205-239 (1997).

Switzer, L. H., and Klingenberg, D. J., "Simulations of Fiber Floc Dispersion in Linear Flow Fields," *Nordic Pulp & Paper Research Journal*, 18 (2), 141-144 (2003).

Switzer, L. H., and Klingenberg, D. J., "Flocculation in Simulations of Sheared Fiber Suspensions," *International Journal of Multiphase Flow*, 30 (1), 67-87 (2004).

Taylor, B. N. and Kuyatt, C. E., Guidelines for Evaluating and Expressing the Uncertainty of NIST Measurement Results, *NIST Technical Note 1297*, National Institute of Standards and Technology, 1994.

Terasaka, K., and Tsuge, H., "Bubble Formation at a Nozzle Submerged in Viscous Liquids Having Yield Stress," *Chemical Engineering Science*, 56 (10), 3237-3245 (2001).

Thalen, N., and Wahren, D., "Shear Modulus and Ultimate Shear Strenght of Some Paper Pulp Fiber Networks," *Svensk. Papperstidn*, 67 (7), 259-264 (1964).

Thanki, P. N., "Photooxidative Degradation and Stabilization of Aliphatic Polyamides in Presence of Blue Dyes," PhD Thesis, University of Pune, India, 1999.

Thorat, B. N., Shevade, A. V., Bhilegaonkar, K. N., Aglawe, R. H., Veera, U. P., Thakre, S. S., Pandit, A. B., Sawant, S. B., and Joshi, J. B., "Effect of Sparger Design and Height to Diameter Ratio on Fractional Gas Hold-up in Bubble Columns," *Chemical Engineering Research & Design*, 76 (A7), 823-834 (1998).

Titomanlio, G., Rizzo, G., and Acierno, D., "Gas Bubble Formation from Submerged Orifices - Simultaneous Bubbling from 2 Orifices," *Chemical Engineering Science*, 31 (5), 403-404 (1976).

Tokoro, T., and Hackam, R., "Effects of Water Salinity, Electric Stress and Temperature on the Hydrophobicity of Nylon," *Conference on Electrical Insulation and Dielectric Phenomena (CEIDP)*, Annual Report, 290-293 (1995).

Tse, K. L., Martin, T., McFarlane, C. M., and Nienow, A. W., "Small Bubble Formation Via a Coalescence Dependent Break-up Mechanism," *Chemical Engineering Science*, 58 (2), 275-286 (2003).

Tsuchiya, K., and Nakanishi, O., "Gas Holdup Behavior in a Tall Bubble Column with Perforated Plate Distributors," *Chemical Engineering Science*, 47 (13-14), 3347-3354 (1992).

Tsuchiya, K., Ohsaki, K., and Taguchi, K., "Large and Small Bubble Interaction Patterns in a Bubble Column," *International Journal of Multiphase Flow*, 22 (1), 121-132 (1996).

Tzeng, J. W., Chen, R. C., and Fan, L. S., "Visualization of Flow Characteristics in a 2-D Bubble Column and Three-Phase Fluidized-Bed," *AIChE Journal*, 39 (5), 733-744 (1993).

Valencia, A., Cordova, M., and Ortega, J., "Numerical Simulation of Gas Bubbles Formation at a Submerged Orifice in a Liquid," *International Communications in Heat and Mass Transfer*, 29 (6), 821-830 (2002).

Van der Zon, A., Hamersma, P. J., Poels, E. K., and Bliek, A., "Coalescence of Freely Moving Bubbles in Water by the Action of Suspended Hydrophobic Particles," *Chemical Engineering Science*, 57 (22-23), 4845-4853 (2002).

Vandu, C. O., and Krishna, R., "Influence of Scale on the Volumetric Mass Transfer Coefficients in Bubble Columns," *Chemical Engineering and Processing*, 43 (4), 575-579 (2004).

Vatai, G., and Tekic, M. N., "Gas Hold-up and Mass-Transfer in Bubble-Columns with Pseudoplastic Liquids," *Chemical Engineering Science*, 44 (10), 2402-2407 (1989).

Veera, U. P., and Joshi, J. B., "Measurement of Gas Hold-up Profiles by Gamma Ray Tomography: Effect of Sparger Design and Height of Dispersion in Bubble Columns," *Chemical Engineering Research & Design*, 77 (A4), 303-317 (1999).

Vial, C., Camarasa, E., Poncin, S., Wild, G., Midoux, N., and Bouillard, J., "Study of Hydrodynamic Behaviour in Bubble Columns and External Loop Airlift Reactors through Analysis of Pressure Fluctuations," *Chemical Engineering Science*, 55 (15), 2957-2973 (2000).

Wallis, G. B., *One Dimensional Two-Phase Flow*, McGraw-Hill, New York (1969).

Walmsley, M. R. W., "Air Bubble Motion in Wood Pulp Fiber Suspension," *APPITA 1992 Proceedings*, 509-515 (1992).

Walter, J. F., and Blanch, H. W., "Bubble Break-up in Gas-Liquid Bioreactors - Break-up in Turbulent Flows," *Chemical Engineering Journal and the Biochemical Engineering Journal*, 32 (1), B7-B17 (1986).

Wang, G., Pelton, R., Hrymak, A., Shawafaty, N., and Heng, Y. M., "On the Role of Hydrophobic Particles and Surfactants in Defoaming," *Langmuir*, 15 (6), 2202-2208 (1999).

Went, J., Jamialahmadi, M., and Muller-Steinhagen, H., "Effect of Wood Pulp Fiber Concentration on Gas Holdup in Bubble Column," *Chemie Ingenieur Technik*, 63 (3), 306-308 (1993).

Wikstrom, T., Defibrator, S., and Rasmuson, A., "Yield Stress of Pulp Suspensions the Influence of Fiber Properties and Processing Conditions," *Nordic Pulp & Paper Research Journal*, 13 (3), 243-250 (1998).

Wilkinson, P. M., "Physical Aspect and Sacle-Up of High Pressure Bubble Column.," PhD Thesis, University of Groningen, 1991.

Wilkinson, P. M., Spek, A. P., and Vandierendonck, L. L., "Design Parameters Estimation for Scale-up of High-Pressure Bubble-Columns," *AIChE Journal*, 38 (4), 544-554 (1992).

Xie, S. Y., and Tan, R. B. H., "Bubble Formation at Multiple Orifices - Bubbling Synchronicity and Frequency," *Chemical Engineering Science*, 58 (20), 4639-4647 (2003).

Xie, T., Ghiaasiaan, S. M., Karrila, S., and McDonough, T., "Flow Regimes and Gas Holdup in Paper Pulp-Water-Gas Three-Phase Slurry Flow," *Chemical Engineering Science*, 58 (8), 1417-1430 (2003).

Yoshida, F., and Akita, K., "Performance of Gas Bubble Columns: Volumetric Liquid-Phase Mass Transfer Coeffficient and Gas Holdup," *AIChE Journal*, 11 (1), 9 (1965).

Zahradnik, J., and Kastanek, F., "Effect of Gas-Distribution on Hydrodynamic Parameters of a Bubble Bed," *Collection of Czechoslovak Chemical Communications*, 43 (1), 216-223 (1978).

Zahradnik, J., and Kastanek, F., "Gas Holdup in Uniformly Aerated Bubble Column Reactors," *Chemical Engineering Communications*, 3 413-429 (1979).

Zahradnik, J., Peter, R., and Kastanek, F., "The Effect of Liquid Phase Properties on Gas Holdup in Bubble Column Reactors," *Collect. Czech. Chem. Commum.*, 52 335-347 (1987).

Zahradnik, J., Fialova, M., Ruzicka, M., Drahos, J., Kastanek, F., and Thomas, N. H., "Duality of the Gas-Liquid Flow Regimes in Bubble Column Reactors," *Chemical Engineering Science*, 52 (21-22), 3811-3826 (1997).

Zahradnik, J., Kuncova, G., and Fialova, M., "The Effect of Surface Active Additives on Bubble Coalescence and Gas Holdup in Viscous Aerated Batches," *Chemical Engineering Science*, 54 (13-14), 2401-2408 (1999).

Zehner, P., "Mehrphasenstromungen in Gas-Flussigkeits-Reaktoren," *Dechema Monogr.*, 114 215-233 (1989).

Zuber, N., and Findlay, J. D., "Average Volumetric Concentration in Two Phase Flow Systems," *ASME Journal of Heat Transfer*, 87 453-468 (1965).

APPENDIX A: EXPERIMENTAL UNCERTAINTY

According to Eq. (3.1), the gas holdup uncertainty is due to pressure measurement error. The superficial gas velocity uncertainty is a result of volumetric gas flow rate measurement error. The effect of bubble column diameter uncertainty on the superficial gas velocity uncertainty is neglected. The gas holdup and superficial gas velocity uncertainties result from: signal fluctuation, calibration errors and instrument limitations. The quantities are calculated following procedures provided in Figliola and Beasley (2000).

The pressure transducer (Parmer, Model 68075) error is 0.25% full scale (34.475 kPa). Figure A.1 shows the pressure signal fluctuation obtained from the middle pressure transducer (see Figure 3.1) for the air-water system at U_g = 2, 9, and 16 cm/s, respectively. It shows that the pressure signal fluctuations increase with increasing superficial gas velocity. The level of pressure signal fluctuation is also affected by fiber mass fraction and pressure transducer location. From Figure A.1, the standard deviation of a single pressure measurement is from 20 Pa ~ 600 Pa. However, the standard deviation of the average pressure of 4000 readings is ±10 Pa, which is much smaller than that of a single pressure measurement. This indicates that with multiple (e.g., 4000) measurements, the resultant average pressure is much more accurate. The pressure transducer calibration error also depends on operation conditions (e.g. superficial gas velocity) and pressure transducer location, and has the same order as the standard deviation of the average pressure.

An uncertainty analysis (Taylor and Kuyatt, 1994) is conducted to estimate the uncertainty in gas holdup using the error propagation approach. An Engineering Equation Solver (EES) (Klein, 2003) program was developed to evaluate the uncertainty in this study.

Gas holdup is given by

$$\varepsilon = 1 - \frac{\Delta P}{\Delta P_o} = 1 - \frac{P_m - P_t}{P_{mo} - P_{to}} \tag{A.1}$$

where P_m and P_t are the pressures measured from middle and top pressure transducers with aeration, respectively; P_{mo} and P_{to} are the corresponding values without aeration.

From Eq. (A.1), the uncertainty of gas holdup can be calculated from the following equation:

$$\begin{aligned} U_\varepsilon^{\,2} &= \left(\frac{\partial \varepsilon}{\partial P_{mo}} U_{pmo}\right)^2 + \left(\frac{\partial \varepsilon}{\partial P_{to}} U_{p_{to}}\right)^2 + \left(\frac{\partial \varepsilon}{\partial P_m} U_{p_m}\right)^2 + \left(\frac{\partial \varepsilon}{\partial P_t} U_{p_t}\right)^2 \\ &= \left(\frac{P_m - P_t}{(P_{mo} - P_{to})^2} U_{p_{mo}}\right)^2 + \left(\frac{P_m - P_t}{(P_{mo} - P_{to})^2} U_{po}\right)^2 + \left(\frac{1}{P_{mo} - P_{to}} U_{po}\right)^2 + \left(\frac{1}{P_{mo} - P_{to}} U_{po}\right)^2 \end{aligned} \tag{A.2}$$

where U represents the combined uncertainty. Using Eq. (A.2), the absolute gas holdup uncertainty is estimated to be ±0.006~0.008%.

Three gas flow meter (Aalborg, Model: GFM 17, 371s, and 571s, respectively) errors are ±2% full scale (15, 50, and 200 l/min, respectively). The relatively standard deviation of the average volumetric gas flow rate of 4000 readings is ±0.1~0.3% of the reading. The superficial gas velocity uncertainty is calculated from

$$U_{U_g}^{\,2} = \left(\frac{U_{\dot{Q}}}{A_c}\right)^2 \tag{A.3}$$

where $\dot{Q}$ is the volumetric gas flow rate and A_c is the column cross-sectional area. The percent uncertainty associated with superficial gas velocity is estimated to be ±2~4%.

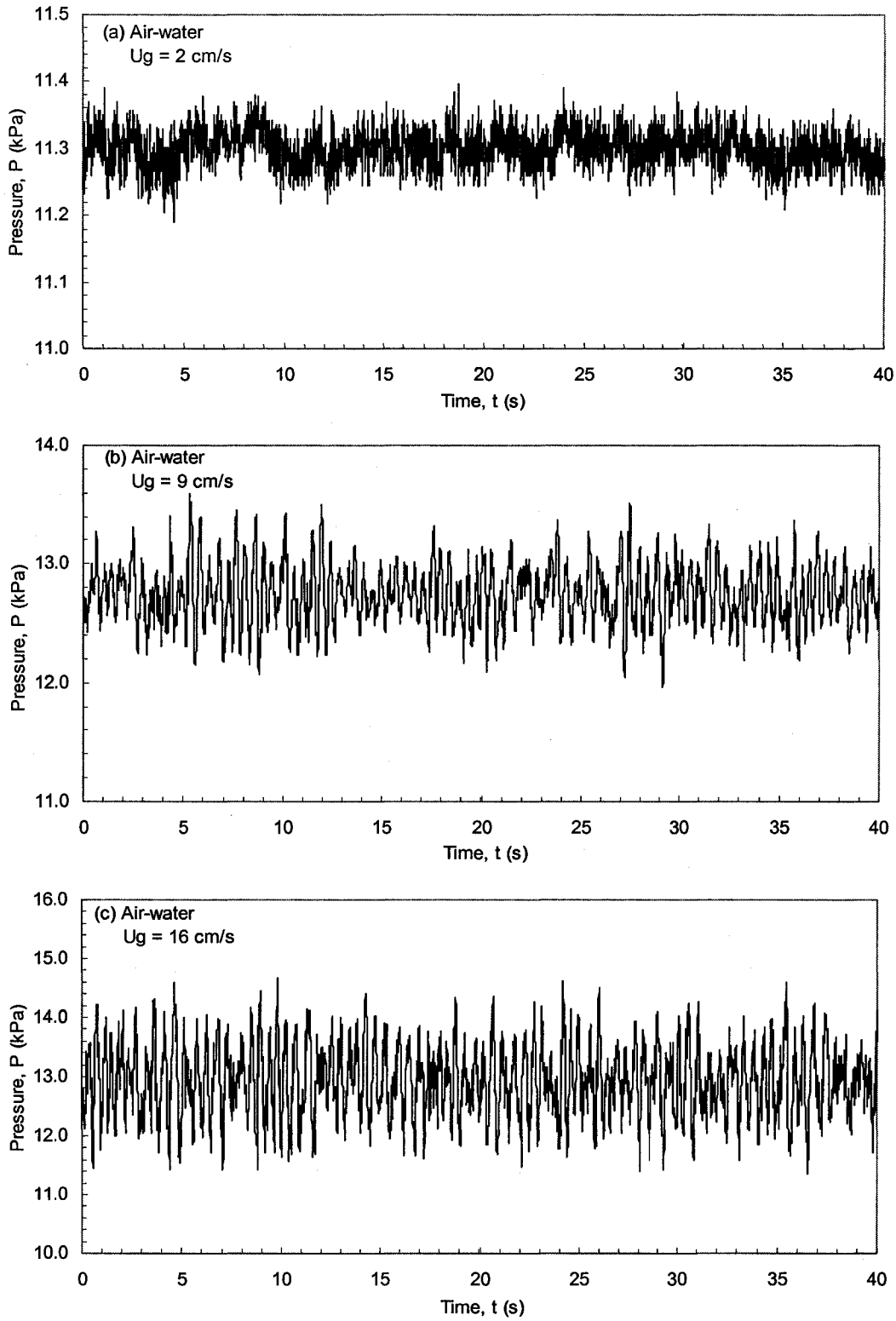

Figure A.1: Pressure fluctuation signals obtained from the middle pressure transducer in an air-water system at (a) $U_g = 2$ cm/s, (b) $U_g = 9$ cm/s, and (c) $U_g = 16$ cm/s.

APPENDIX B: NONDIMENSIONAL ANALYSIS

According to the literature review in Chapter 2 and the present study results in Chapter 4, gas holdup is influenced by the geometry of the bubble column and gas distributor, the physical properties of the gas, liquid, and solid phase, and process related quantities. The parameters influencing gas holdup in a semi-batch gas-liquid-fiber bubble column are listed in Table B1.

Table B1: Parameters influencing gas holdup.

Geometrical Properties	
Bubble Column	• Diameter, D • Initial liquid Height, H
Gas Distributor	• Open area ratio, A • Hole diameter, d_o
Physical Properties	
Gas Phase	• Density, ρ_g • Dynamic viscosity, μ_g
Liquid Phase	• Density, ρ_l • Dynamic viscosity, μ_l
fiber Phase	• Density, ρ_f • Fiber length, L • Fiber diameter, d • Coarseness, ω • Young's Modulus, E • Stiffness, EI • Friction coefficient, f • Fiber number density, N_f
Interface Properties	• Gas-liquid surface tension, σ
Fiber Slurry	• Effective viscosity, μ_{eff}
Process Related	• Superficial gas velocity, U_g • Fiber mass fraction, C • Shear rate, $\dot{\gamma}$ • Gravitational acceleration, g • Density difference between continuous phase and disperse phase, ρ_{eff}-ρ_g • Density difference between liquid and solid phase ρ_l-ρ_f

Hence, gas holdup may be in influenced by:

{**ε**; D, H, A, d_o; ρ_g, υ_g, ρ_l, μ_l, ρ_f, L, d, N_f, ω, E, EI, f; σ_{lg}; U_g, C, $\dot{\gamma}$, g, $g(\rho_{eff}-\rho_g)$, $g(\rho_l-\rho_f)$}

where ε, A, f, and C are already nondimension numbers. Quantities with similar dimensions include (D, H, d_o, L, and d), (ρ_l and ρ_f), ($g(\rho_{eff}-\rho_g)$ and $g(\rho_{eff}-\rho_g)$), and μ_g and μ_l. Thus, only one of the respective quantities with the same units is required for nondimensional analysis. Hence, the quantities involved in this nondimensional analysis are

L, ρ_l, U_g; μ_l, ω, E, EI, σ; $\dot{\gamma}$, g, $g(\rho_{eff}-\rho_g)$, N_f

Selecting L, ρ_l, and U_g as the independent variables, the dimensional matrix method introduced by Zlokarink (2001) is used to create nondimensional numbers:

	L	ρ_l	U_g	ω	μ_l	σ	g	$g(\rho_{eff}-\rho_g)$	E	EI	$\dot{\gamma}$	N_f
Length L	1	-3	1	-1	-1	0	1	-2	-1	3	0	-3
Mass M	0	1	0	1	1	1	0	1	1	1	0	0
Time T	0	0	-1	0	-1	-2	-2	-2	-2	-2	-1	0

Two linear transformations are necessary to obtain the identity matrix,

	L	ρ_l	U_g	ω	μ_l	σ	g	$g(\rho_{eff}-\rho_g)$	E	EI	$\dot{\gamma}$	N_f
L+3M+T	1	0	0	2	1	1	-1	-1	0	4	-1	-3
M	0	1	0	1	1	1	0	1	1	1	0	0
-T	0	0	1	0	1	2	2	2	2	2	1	0

Thus, the dimensionless numbers are:

$$\Pi_1 = \frac{\omega}{L^2\rho_l} \tag{B.1}$$

$$\Pi_2 = \frac{\mu_l}{\rho_l U_g L} \tag{B.2}$$

$$\Pi_3 = \frac{\sigma}{\rho_l L U_g^{\ 2}} \tag{B.3}$$

$$\Pi_4 = \frac{gL}{U_g^{\,2}} \tag{B.4}$$

$$\Pi_5 = \frac{g(\rho_l - \rho_g)L}{\rho_l U_g^{\,2}} \tag{B.5}$$

$$\Pi_6 = \frac{E}{\rho_l U_g^{\,2}} \tag{B.6}$$

$$\Pi_7 = \frac{EI}{\rho_l U_g^{\,2} L^4} \tag{B.7}$$

$$\Pi_8 = \frac{\dot{\gamma} L}{U_g} \tag{B.8}$$

$$\Pi_9 = \frac{1}{N_f L^3} \tag{B.9}$$

Some of the nondimensional numbers shown above can be transformed into new nondimensional numbers by exchanging L with other length quantities. For example, replace L^2 with πd^2 in Π_1 to yield:

$$\Pi_1' = \frac{\rho_f}{\rho_l} \tag{B.10}$$

Exchange L with D in Π_2 to obtain:

$$\Pi_2' = \frac{\mu_l}{\rho U_g D} = Re^{-1} \tag{B.11}$$

Change L with D in Π_3 to obtain produce:

$$\Pi_3' = \frac{\sigma}{\rho_l D U_g^{\,2}} = We^{-1} \tag{B.12}$$

Replace L with D in Π_4 to obtain:

$$\Pi_4' = \frac{gD}{U_g^2} = Fr^{-1} \tag{B.13}$$

Some of the nondiemsional numbers can also be combined:

$$\Pi_5' = \Pi_5 \Pi_2^{-2} = \frac{\rho_l g(\rho_l - \rho_g) D^3}{\mu_l^2} = Ar \text{ (change L with D)} \tag{B.14}$$

$$\Pi_6' = \Pi_6 \Pi_2^{-1} \Pi_8^{-1} = \frac{E}{\rho_l U_g^2} \frac{\rho_l U_g L}{\mu_l} \frac{U_g}{\dot{\gamma} L} = \frac{E}{\mu_l \dot{\gamma}} \tag{B.15}$$

Forgas and Mason (1959) define a bending ratio (BR) according to

$$\Pi_6' \frac{\ln(2\frac{L}{d}) - 1.75}{2(\frac{L}{d})^2} = \frac{E(\ln 2r - 1.75)}{(\mu_l \dot{\gamma}) 2r^4} = BR \tag{B.16}$$

where $r = \frac{L}{d}$. The bending ratio was used by Forgas and Mason (1959) to classify fiber shapes. When BR < 1, fibers are considered as a straight rods, otherwise, fibers tend to bend. Joung et al. (2002) concluded that fiber shape (bending) influences fiber suspension viscosity. Thus, BR may be an important nondimensionalal number to describe gas holdup performance in fiber suspensions.

Switzer and Klingenberg (2003) define an effective fiber stiffness by:

$$\Pi_7' = \Pi_7 (\Pi_2 \Pi_8)^{-1} = \frac{EI}{\rho_l U_g^2 L^4} \left(\frac{\mu_l}{\rho_l U_g L} \frac{\dot{\gamma} L}{U_g} \right)^{-1} = \frac{EI}{\mu_l \dot{\gamma} L^4} = S^{eff} \tag{B.17}$$

The effective fiber stiffness is a nondimensional number representing fiber flexibility. Fiber flexibility has an effect on fiber flocculation and the effective viscosity (Joung et al., 2001; Switzer and Klingenberg, 2004), both of which affect gas holdup.

Other nondimensional numbers that may influence gas holdup include fluid property ratios (i.e., μ_{eff}/μ_l, L/d, H/D, and d_o/D). Thus, a gas holdup model in a gas-liquid-fiber system may be described by:

$$\varepsilon = f(\rho_f/\rho_l, Re, We, Fr, Ar, BR, S^{eff}, f, 1/(N_f L^3), A, C, \mu_{eff}/\mu_l, L/d, d_o/D, H/D) \quad (B.18)$$

For the present study, fiber density is very close to the liquid phase (water), and $\rho_f/\rho_l \approx 1$, hence, it is neglected in the nondimensional analysis. It is assumed that the fibers are well washed and fiber addition does not affect surface tension, so the Weber number (We) can be neglected. The crowding number N (Eq. 2.7) can be formed by combining L/d with C; thus, N is used to replace L/d and C. Joung et al. (2001) proved that the effective viscosity is a function of S^{eff}, thus, the influence of μ_{eff}/μ_l is described by S^{eff}. Overall, gas holdup has been shown to be independent of H/D if H/D > 8 (Bando et al., 2003). In the present study, H/D ≈ 14, hence, H/D can be neglected in this study. Both d_o and D have an effect on gas holdup with d_o affecting the initial bubble diameter (Wilkinson, 1991) and D influencing the column wall effects. However, Zahradnik et al. (1997) reported that gas holdup was independent of hole diameter when $d_o \geq 1.6$mm, which implies the initial bubble diameter does not increase with increasing d_o when d_o is beyond a certain value. Gas holdup has also been shown to be independent of column diameter when D > 15 cm (Zahradnik et al., 1997). Thus, d_o/D may not apply for scale-up.

Therefore, Eq. (B.18) can be reduced into

$$\varepsilon = f(Re, Fr, Ar, BR, S^{eff}, f, N, 1/(N_f L^3), A) \quad (B.19)$$

Note that A can be excluded if scale-up for a specific A is desired.

To determine if Eq. (B.19) is appropriate for gas-liquid-fiber bubble column scale-up, the following work must be done:

1. Gas holdup data must be acquired for different size bubble columns;

2. Gas holdup data using gas distributors with different open area ratios must be recorded for each bubble column. Since it was shown in chapter 4 that gas holdup increases with increasing open area ratio and then decreases when the open area ratio is beyond a certain value, a correlation for open area ratio at which the highest gas holdup is reached is needed.

3. Scale-up requires flow pattern similarity, so appropriate criteria to classify different flow regimes are required. The flow regime in gas-liquid-fiber systems is influenced by open area ratio, bubble diameter, fiber type, mass fraction, and length, and data are required for different bubble column diameters, open area ratios, and fiber types.

4. The influence of shear rate, BR, and S^{eff} on gas holdup is not available in the literature, and new studies in this area are required. However, it is unknown if these parameters can be varied while other fiber properties are held constant.